Invasive Breast Carcinoma of No Special Type, Microinvasive Carcinoma, Tubular Carcinoma, and Cribriform Carcinoma

10

Helena Hwang, Karan Saluja, and Sunati Sahoo

Invasive Breast Carcinoma of No Special Type

Overview

Invasive breast carcinoma of no special type (IBC-NST) is the most common invasive breast carcinoma (IBC). It is a diagnosis of exclusion and considered a "wastebasket" category for tumors that cannot be classified as a special type. In 2012, the World Health Organization (WHO) recommended a change in terminology from invasive ductal carcinoma not otherwise specified (IDC-NOS) to IBC-NST [1]. Invasive breast carcinoma NST comprises 70–80% of all IBC based on Surveillance Epidemiology and End Results (SEER) data and several published series [1–4]. A few studies have reported a lower incidence rate of 47–53%, as these authors segregated tumors showing mixed morphology (invasive carcinoma, NST admixed with some special type IBC) from tumors showing only IBC-NST [5, 6]. In the United States, the median age at diagnosis is 63 with the majority of cases occurring in women in their 50s and 60s [7]. Men in general are at low risk of developing breast cancer, with IBC-NST being the most common type.

Gross and Radiologic Features

Clinically, invasive breast carcinoma NST most commonly presents as a palpable mass. Pain as well as nipple retraction or inversion, skin retraction, or nipple discharge may be present. Rarely, primary breast carcinoma can present in the axilla without any abnormality detected in the breast.

On imaging, breast carcinomas usually present as a mass with some variability in presentation. Broberg et al. described five different groups for invasive carcinomas based on mammographic findings: Group A—presence of spiculated mass with or without calcifications, Group B—increased attenuation or structural variation in the parenchyma such as density or architectural distortion with or without calcifications, Group C—presence of clusters of heterogeneous calcifications without an evident mass, Group D—circumscribed lesions with or without calcifications, and Group E—tumors with no visible abnormality on mammogram [8]. The majority of histologically confirmed IBC are stellate masses without calcifications; some tumors may present as stellate or circumscribed masses with calcifications or as calcifications only (Figs. 10.1 and 10.2). The sensitivity of mammography alone in detecting invasive cancer is highly variable, ranging from 45% to 90%, and depends on a number of factors including age, size of the tumor, breast density, presence of an implant, and prior surgical procedures [9]. One study reported the detection rate to be 50% for tumors less than 10 mm and 88% for tumors greater than 10 mm in diameter [10].

Ultrasonography is not routinely used for screening as it is time consuming and has low sensitivity for calcifications [11, 12]. The sensitivity of ultrasound for mass-forming breast carcinoma is 80–90% [9]. Ultrasound as an adjunct to mammography increases the sensitivity of breast cancer detection in older women and in patients with increased breast density. Ultrasound alone is the recommended first-line breast imaging modality only in young high-risk women (<40 years). Additionally, ultrasound is used routinely to evaluate any suspicious mass found on mammography and to evaluate the axillary lymph nodes.

On ultrasonography, invasive carcinoma commonly presents as an irregular hypoechoic mass with ill-defined margins, sometimes accompanied by spiculation, posterior

H. Hwang · S. Sahoo (✉)
Department of Pathology, UT Southwestern Medical Center, Dallas, TX, USA
e-mail: helena.hwang@utsouthwestern.edu; sunati.sahoo@utsouthwestern.edu

K. Saluja
Department of Pathology, UT Health Science Center at Houston, Houston, TX, USA
e-mail: karan.saluja@uth.tmc.edu

S. J. Shin et al. (eds.), *A Comprehensive Guide to Core Needle Biopsies of the Breast*,
https://doi.org/10.1007/978-3-031-05532-4_10

shadowing, or microlobulation [13] (Fig. 10.3). Other findings that are worrisome for malignancy include "taller than wide" mass as compared to "wider than tall" nodules that tend to be benign. Tall nodules suggest neoplastic growth across the normal tissue plane as the patient is scanned in a supine position [14], whereas benign lesions, such as fibroadenomas, grow along the normal tissue plane resulting in a wide mass [15].

Magnetic resonance imaging (MRI) has been shown to be highly sensitive, but mammography and ultrasound are still the principal imaging modalities to detect breast cancer. Recommendations for annual MRI screening along with mammography are limited to women with a high lifetime risk of breast cancer (20–25% or greater). These include carriers of *BRCA1* or *BRCA2* gene mutations, first-degree relatives with *BRCA1* or *BRCA2* gene mutations, patients who had radiation therapy to the chest between the ages of 10 and 30, and patients with either Li-Fraumeni or Cowden syndrome or who have first-degree relatives with these syndromes [16].

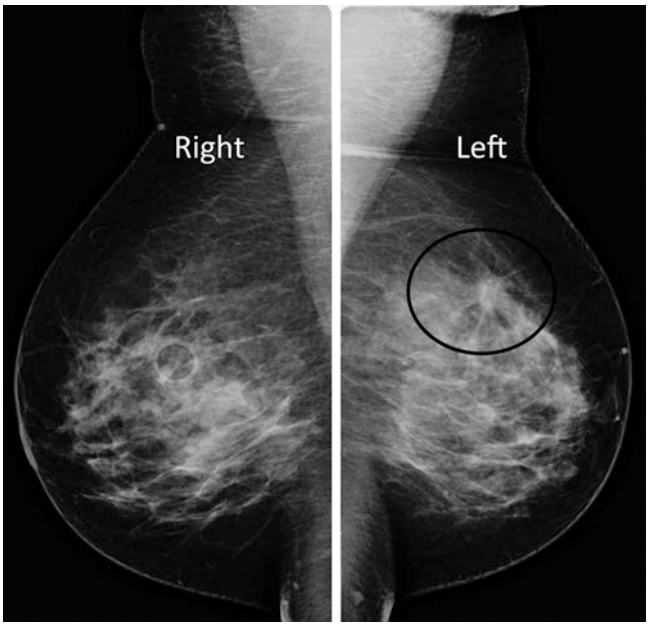

Fig. 10.1 Invasive breast carcinoma NST. Mammography demonstrates a 1.8 cm spiculated mass with associated architectural distortion in the middle depth of the left breast. (Courtesy of Stephen Seiler. Used with permission)

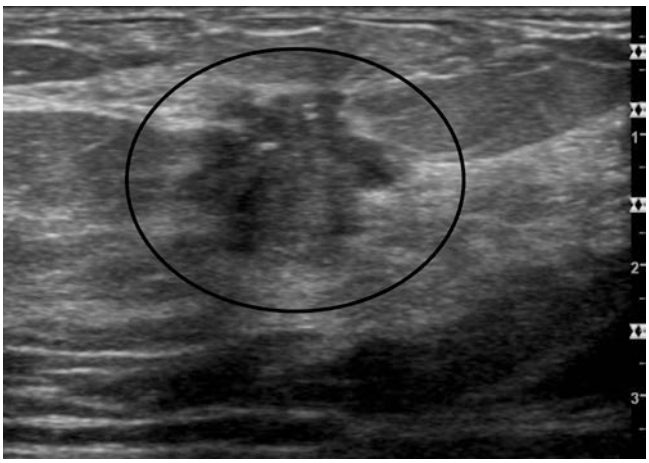

Fig. 10.3 Invasive breast carcinoma NST. Ultrasound shows an irregular hypoechoic mass with indistinct and angular margins (*circled*). (Courtesy of Stephen Seiler. Used with permission)

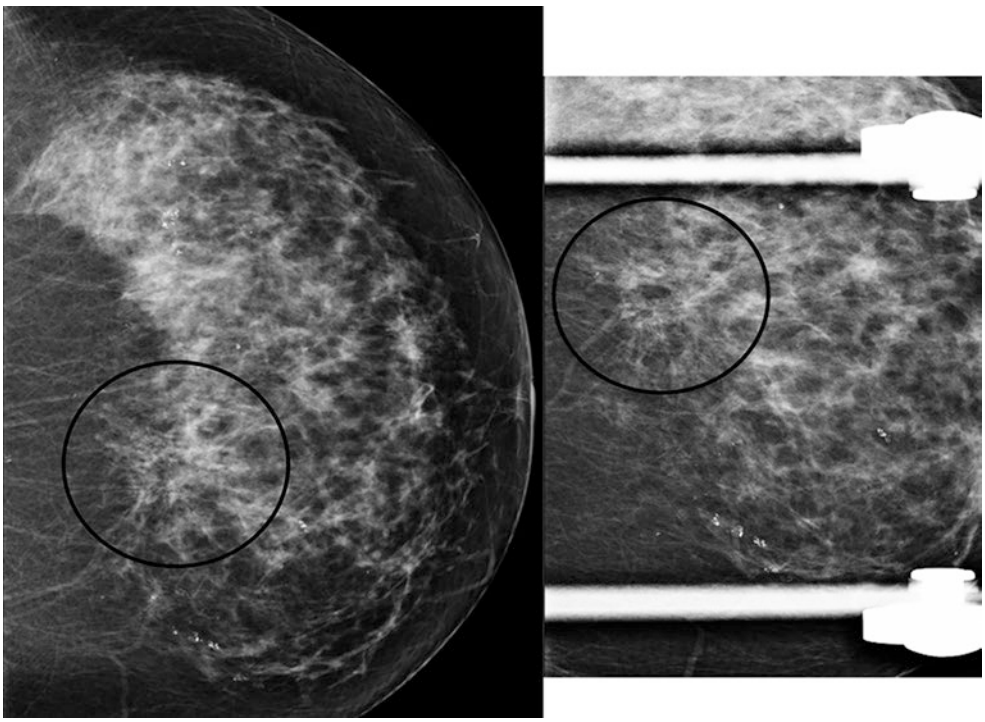

Fig. 10.2 Invasive breast carcinoma NST. Mammography demonstrates subtle architectural distortion in the middle to posterior depth of the medial left breast. This distortion persists on subsequent spot compression imaging (*circled*). (Courtesy of Stephen Seiler. Used with permission)

MRI is also commonly used to determine the extent of disease and detect additional tumors in newly diagnosed breast cancer patients. The tumor size obtained from MRI corresponds more closely to pathologic tumor size than measurements by mammography, ultrasound, or clinical assessment [9]. MRI has also proven to be the most accurate method for assessing treatment response and measuring residual tumor in patients who undergo neoadjuvant chemotherapy [17]. Although MRI is highly sensitive, the specificity for detecting carcinoma is low [18, 19]. Some of the benign lesions that can present as an enhancing lesion on MRI include inflammatory lesions and benign lesions such as fibroadenoma, sclerosing adenosis, intraductal papilloma, and apocrine metaplasia [18, 19].

On MRI, image morphology and contrast enhancement kinetics are used to determine how suspicious a lesion is. Lesions that are irregular and enhance rapidly on injection of the MR contrast agent Gadolinium, sometimes with ring enhancement, tend to be malignant, due to increased vascularity in malignant lesions. In contrast, benign lesions generally show slow and less avid enhancement. Lesions that show rapid contrast enhancement followed by rapid washout are highly predictive of malignancy (Fig. 10.4). Similarly, lesions that do not show any enhancement have a high negative predictive value for a malignant process. Schnall et al. reported a negative predictive value of 94% for invasive carcinoma and 88% for any malignant process. Of the non-enhancing lesions, 16% turned out to be ductal carcinoma in situ (DCIS) and 3% were invasive carcinoma on final pathologic assessment [20].

Digital breast tomosynthesis (DBT) is a newer imaging technology that is essentially "three-dimensional" mammography. While the benefits of DBT are currently being actively studied, it appears to increase the cancer detection rate and reduce recall rates. Tomosynthesis is particularly useful in assessing asymmetries and architectural distortions as it allows better assessment of the shape and margins of masses [21].

Grossly, IBC-NST appears as a white-tan to yellow-tan, firm-to-hard, stellate mass (Fig. 10.5). Close inspection may reveal white fibrous streaks extending into the surrounding fibroadipose tissue. A chalky-white appearance within the tumor is indicative of either necrosis or calcifications. About one-third of tumors can have somewhat circumscribed borders with a soft fleshy texture, although this feature is mostly seen with special types of mammary carcinoma such as mucinous, solid papillary, and basal-like triple-negative breast carcinoma (Fig. 10.6). Most IDCs induce fibroblastic stromal reaction (desmoplasia) and hence was described as scirrhous carcinoma in the past [22]. The consistency of an IDC depends primarily on the amount of desmoplastic or fibroblastic stroma present in the tumor.

Invasive breast carcinoma is most often identified in the upper outer quadrant (40–50%) irrespective of laterality,

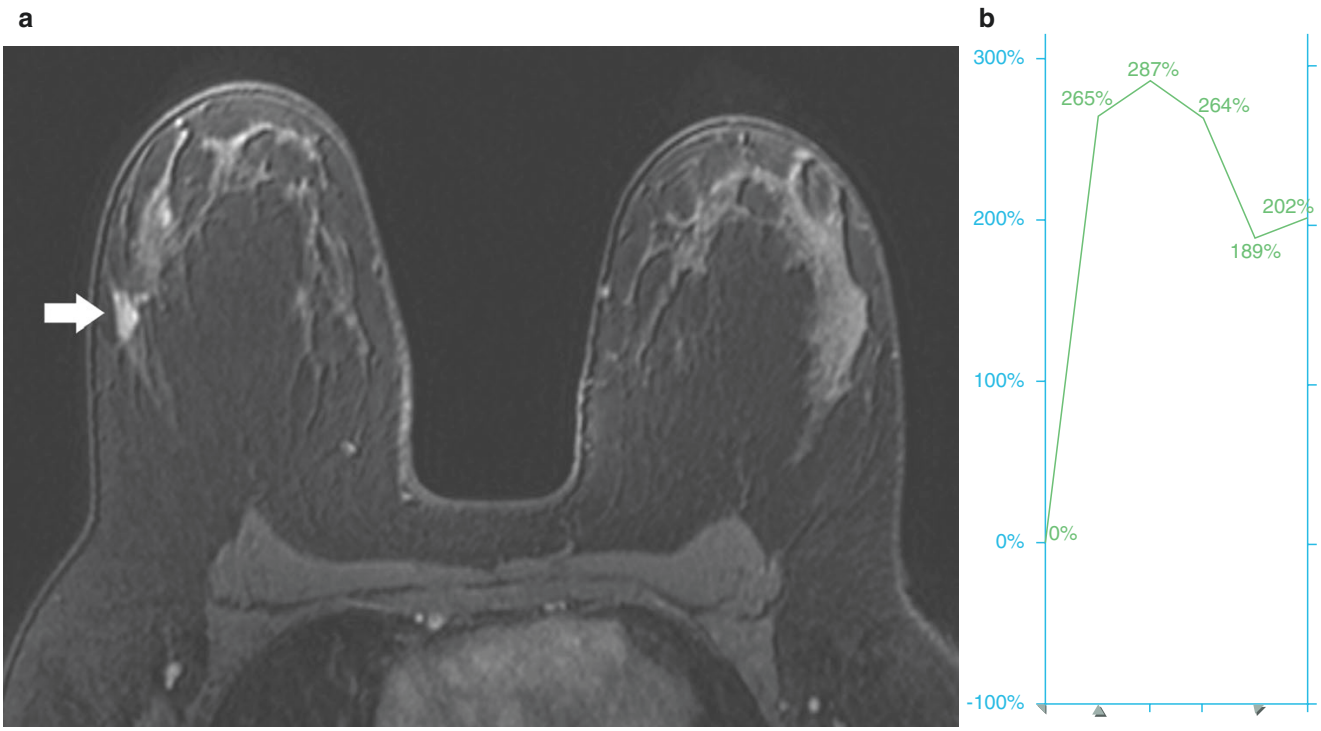

Fig. 10.4 Invasive breast carcinoma NST. MRI was performed for high-risk screening in this patient with a known *BRCA2* mutation. (**a**) An irregular heterogeneously enhancing mass is seen in the lateral right breast (*arrow*). (**b**) Time–intensity curve (kinetics) shows a rapid uptake and rapid wash out, a pattern typically seen with malignancy. (Courtesy of Stephen Seiler. Used with permission)

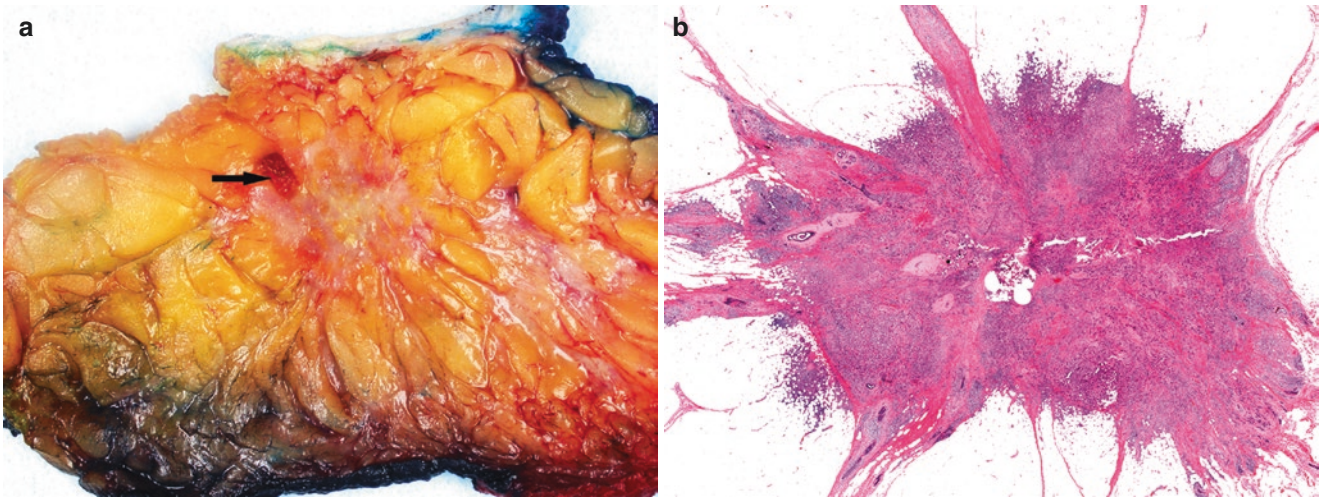

Fig. 10.5 Invasive breast carcinoma NST. (**a**) Gross appearance of a stellate mass with infiltrating margin and pink gelatinous material (hydrogel) indicative of the prior core biopsy site (*arrow*). (**b**) Scanning view depicts the stellate appearance of the tumor on histology

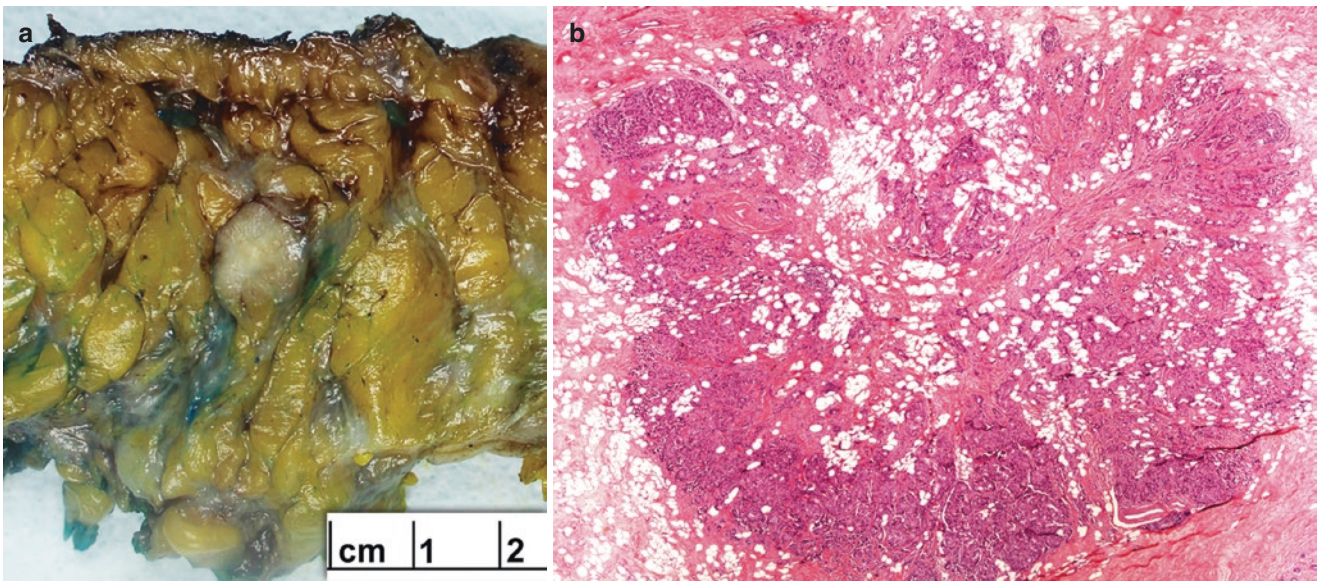

Fig. 10.6 Invasive breast carcinoma NST. A 7 mm IBC with relatively circumscribed borders, (**a**) gross appearance and (**b**) scanning view shows relatively well-delineated border on histology

followed by central breast, upper inner, lower outer and lower inner quadrants. The frequency corresponds with the amount of breast parenchyma present in the respective quadrants [2].

Microscopic Features

WHO defines pure IBC-NST as tumors showing less than 10% of a special subtype such as invasive lobular carcinoma (ILC). When a tumor shows a component of a special type such as tubular or lobular carcinoma, WHO recommends that the term "mixed IBC-NST and special subtype carcinoma" be used with the percentage of the special subtype given [1].

The morphology of IBC-NST is highly heterogeneous. The majority of tumors show a highly infiltrative border appreciated on scanning power, recapitulating the stellate appearance seen grossly (Fig. 10.7). The tumor may grow as cords, trabeculae, diffuse sheets, or a mixture of these patterns in addition to showing gland or tubule formation (Figs. 10.8, 10.9, and 10.10). Occasionally, tumors may exhibit single cell infiltration or a targetoid configuration entrapping benign ducts or lobules that resemble ILC at low-power examination but lacks the dyscohesion of lobular carcinoma (Fig. 10.11). Arps et al. termed IDC with prominent single cell infiltration as IDC with lobular features and reported that these tumors showed more aggressive behavior than ILC and IDC that did not show lobular features [23] (Fig. 10.12). Rarely, small foci of squamous or sebaceous

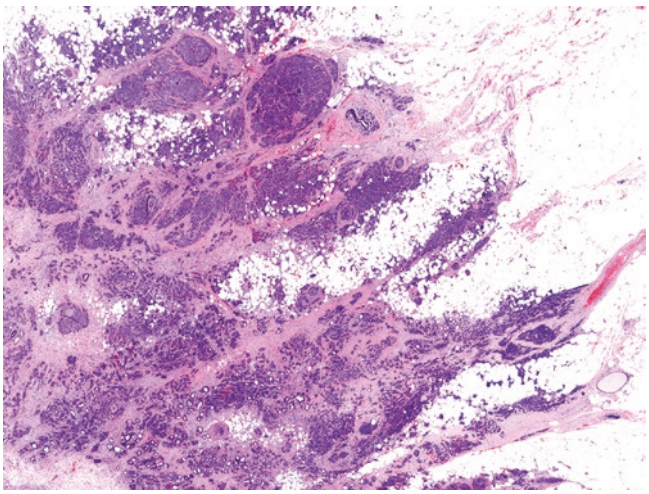

Fig. 10.7 Invasive breast carcinoma NST. Low power depicts the stellate appearance of the tumor due to infiltration of the fibrous bands by tumor cells with associated desmoplasia

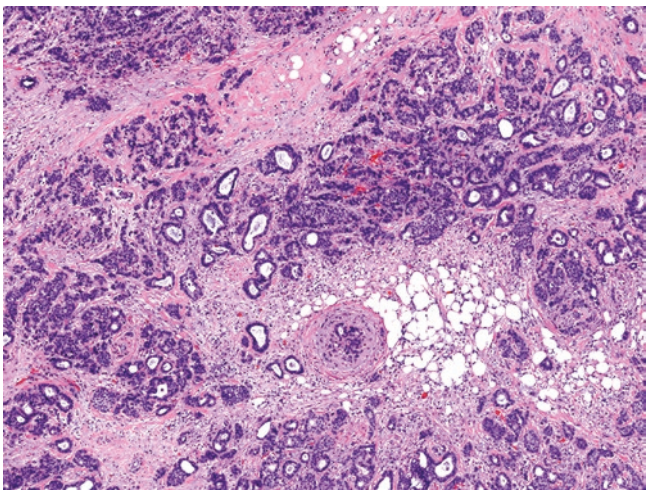

Fig. 10.8 Invasive breast carcinoma NST. Low power of the tumor displays varying architectural patterns comprising glands and solid nests

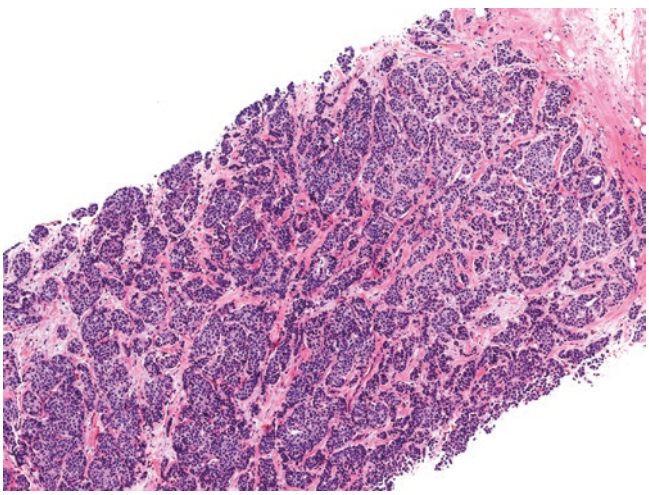

Fig. 10.9 Invasive breast carcinoma NST, with prominent nesting pattern and well-delineated border

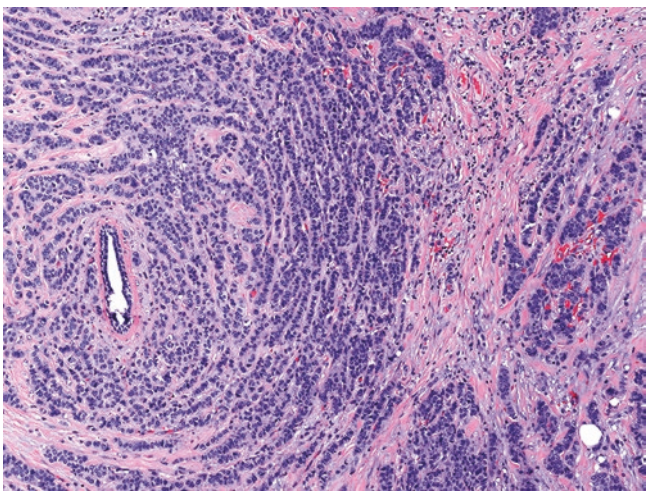

Fig. 10.11 Invasive breast carcinoma NST, with targetoid growth pattern around a benign duct (*left*)

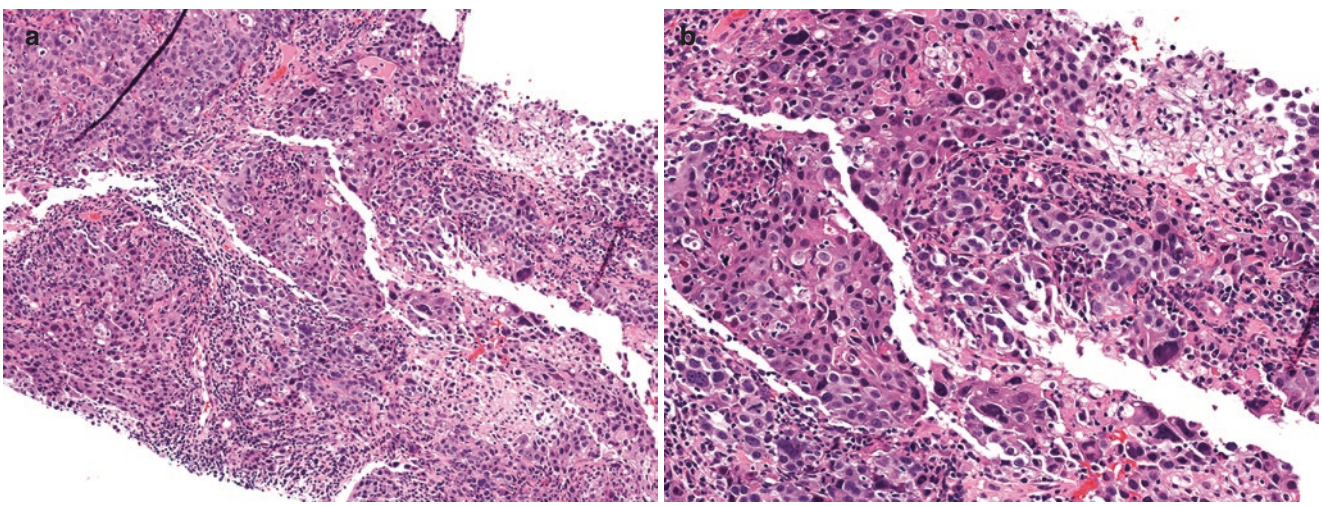

Fig. 10.10 Invasive breast carcinoma NST, poorly differentiated with highly pleomorphic tumor cells, (**a**) low-power and (**b**) high-power magnifications

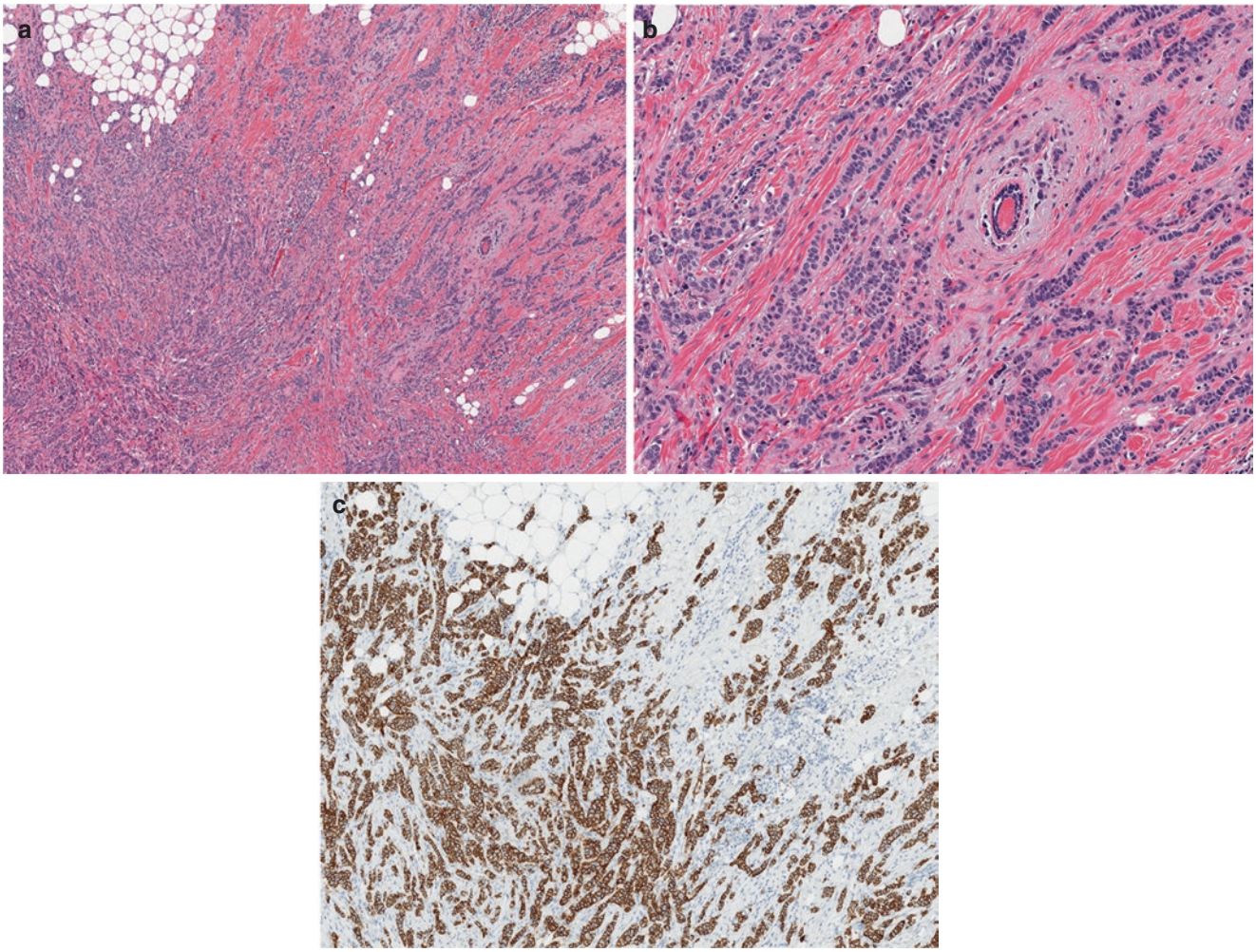

Fig. 10.12 Invasive breast carcinoma with lobular features. (**a**) Low-power view shows diffuse infiltration by single cells and thin cords of tumor, (**b**) high-power view shows invasive carcinoma cells with minimal nuclear pleomorphism, and (**c**) E-cadherin shows positive membrane staining in the tumor

differentiation can be seen, particularly in high-grade IBC NST (Figs. 10.13 and 10.14).

The stroma of IBC NST can be highly variable, ranging from pauci-cellular and edematous to showing marked desmoplasia, dense sclerosis, or hyalinization. It can also appear to be highly cellular due to an admixed lymphoplasmacytic infiltrate (Fig. 10.15). Some tumors may show a large central area of sclerosis (Fig. 10.16). Necrosis may be present, either as single cell necrosis/apoptosis or focal to extensive.

Histologic Grading

Histologic grading in IBC has been shown to be a reliable prognostic indicator, even though it can be subjective [24–27]. The Nottingham grading system, a modification of the original Scarff-Bloom-Richardson grading system, is used for histologic grading of breast carcinomas [25, 28, 29]. The Nottingham grade along with lymph node status and tumor size is collectively required for calculation of the Nottingham Prognostic Index (NPI) [30]. The higher the NPI score, the worse the prognosis. Patients are stratified into good, moderate, or poor prognostic groups using the NPI score [31].

Histologic grading requires assessment of three components of tumor morphology, each of which is given a score from 1 to 3. The final grade is calculated by adding the three scores. The three components are tubule/acinar/glandular formation, nuclear atypia/pleomorphism, and mitotic rate. Glandular formation is generally assessed at low-power examination and a score is given based on the percentage of tubule formation. A score of 1 is given when more than 75% of the tumor shows tubule formation, a score of 2 is for 10–75% tubule formation, and a score of 3 is for less than 10% gland formation. Tumor clusters with reverse polarization of tumor cells as seen in micropapillary carcinoma, solid tumor clusters floating in mucin pools as seen in mucinous carcinoma, and solid tumor nodules with a pushing border as seen in some invasive (solid) papillary carcinomas are by default scored as 3. Pure cribriform architecture is scored as 1.

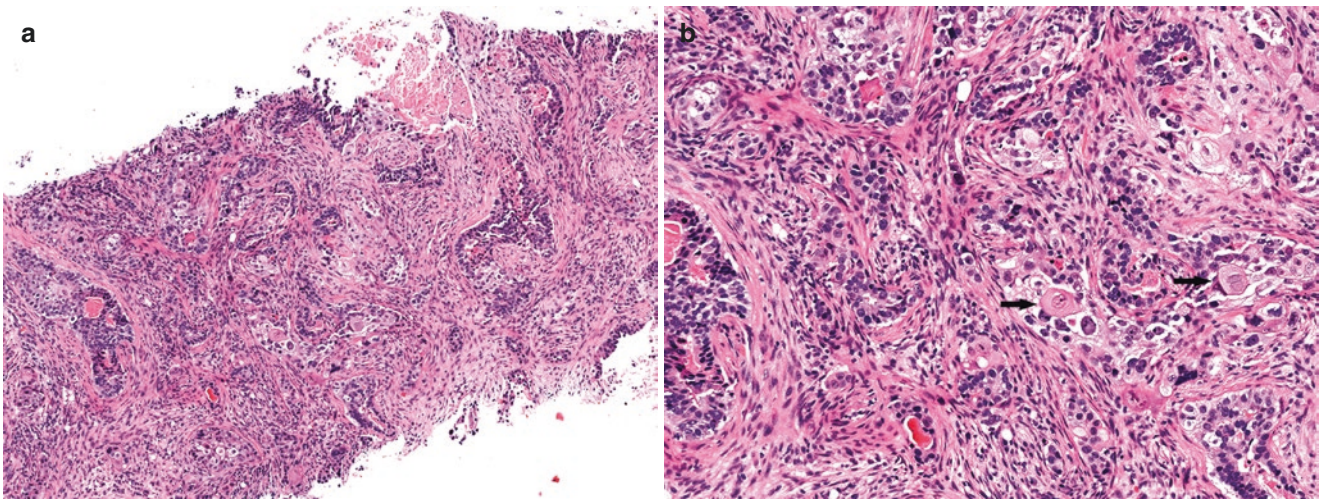

Fig. 10.13 Invasive breast carcinoma NST, poorly differentiated with focal squamous differentiation (*arrow*), (**a**) low-power and (**b**) high-power magnifications

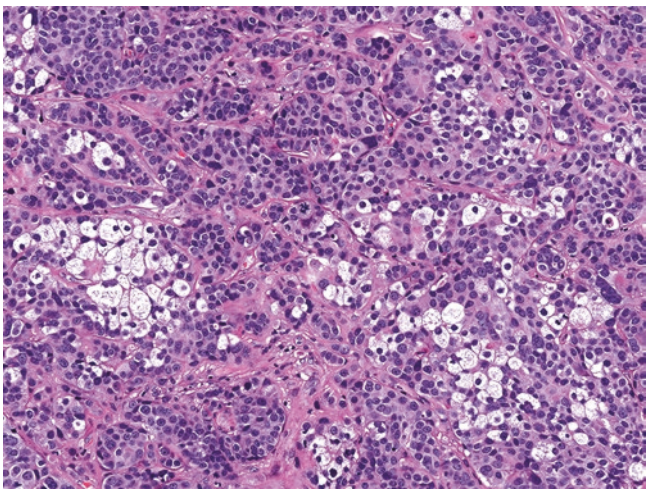

Fig. 10.14 Invasive breast carcinoma NST, moderately differentiated with focal sebaceous differentiation

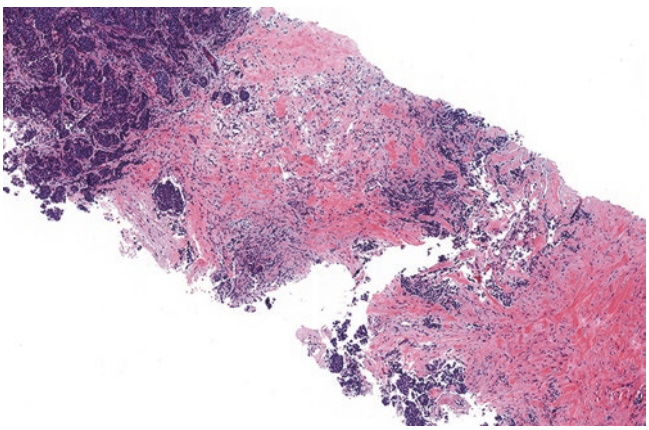

Fig. 10.16 Invasive breast carcinoma NST. Low power displays an IBC with a central zone of sclerosis

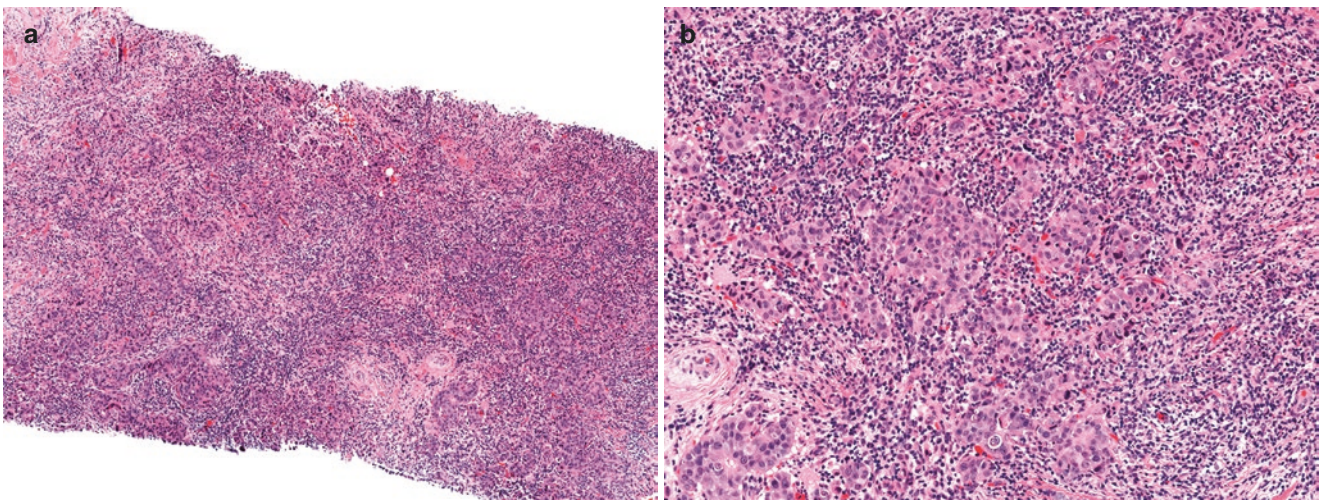

Fig. 10.15 Invasive breast carcinoma NST, high grade with prominent inflammatory cell infiltration, (**a**) low-power and (**b**) high-power magnifications

Nuclear pleomorphism refers to an amalgamation of variation in tumor nuclear size, chromatin characteristics, and the presence of nucleoli. Of the three components used for grading, nuclear grade is the most subjective. For nuclear size estimation, comparison with the adjacent or entrapped benign breast ductal epithelial cells should be used. If there are no benign breast epithelial cells nearby, stromal lymphocytes can be used as a reference. Tumors with small and regular nuclei with evenly dispersed chromatin and indistinct nucleoli, similar or slightly larger (up to 1.5 times) than the size of the adjacent normal breast epithelial cells is given a score of 1. Tumors with moderate variation in nuclear shape and size (1.5–2 times) than normal epithelial cells, occasional bigger nuclei among most tumor cells, uneven distribution of chromatin, vesicular nuclei with chromatin dispersed more peripherally towards the nuclear membrane and small visible nucleoli are given a score of 2. A score of 3 is reserved for tumors with marked nuclear size variation, frequent bizarre nuclei, nuclei with a predominant vesicular chromatin pattern and prominent to macro nucleoli. Some high-grade tumors with markedly enlarged nuclei with frequent mitoses may not show variation in nuclear size but should be scored as 3.

Strict criteria for the mitotic count should be adhered to, as the mitotic index is a reflection of the proliferative potential of the tumor and perhaps the most important semiquantitative component of the histologic grading system with prognostic implications. The current recommendation is to count mitotic figures on routine H&E stain. Immunohistochemistry/immunohistochemical (IHC) stains such as anti-phosphohistone H3 (pHH3) can highlight mitotic figures but at present is not recommended to assess mitotic count [32]. Only unequivocal mitotic figures should be counted. Care should be taken to distinguish apoptotic cells (characterized by dense pink eosinophilic cytoplasm and dark pyknotic nuclei often noted in higher grade tumors) and intratumoral lymphocytes from mitoses. The count should be performed at high-power field (400×), and the total number of mitoses per ten adjacent high-power fields should be used to estimate the mitotic score. In an excisional specimen, the area with the most mitotic activity should be counted; this generally corresponds to the leading edge or the periphery of the tumor. One should avoid counting mitosis in the center of the tumor, which often has sclerosis or low cellularity. The same rule also applies in core needle biopsy (CNB) samples, although it is highly dependent on sampling, i.e., the area and amount of tumor sampled. Additionally, crush artifact resulting from the biopsy procedure may impact mitosis count and nuclear grading in CNB samples (Fig. 10.17).

The size of a high-power field is variable and may differ up to sixfold from one microscope to another (Table 10.1).

Other factors that may affect mitotic count are the type of fixative and fixation time. Start et al. found that a delay in tissue fixation for up to 6 h reduced the number of visible mitoses by a mean of 53% without any effect on nuclear pleomorphism or tubule formation [33]. Robbins et al. reported that tissues fixed in B5 fixative rather than in buffered formalin/formaldehyde tend to show increased nuclear pleomorphism/size and higher mitotic count, though that difference was not statistically significant [34]. Therefore, the current recommendation is to use 10% neutral phosphate-buffered formalin at pH 7.0 with an optimal formalin-to-tissue ratio of 10:1. The tissue should be fixed in formalin as soon as possible. It is recommended that the time interval between tissue removed from the patient to its placement in formalin (cold ischemia time) be less than 1 h [35]. This is easily achievable in core needle biopsy (CNB) samples. However, for excision specimens, one needs to be mindful of ischemia time as inking and sectioning takes time. Minimizing the tissue ischemia time to less than 1 h is also important for biomarker studies.

Once the three components have been assessed, the scores are added to determine the histologic grade (Table 10.1). Tumors with a score of 3–5 are well differentiated (grade 1), score 6–7 are moderately differentiated (grade 2), and score 8–9 are poorly differentiated (grade 3) (Figs. 10.18, 10.19, and 10.20). The concordance rate for histologic grade between CNB and excision is reported to be 59–91% [36–39], with the majority of cases (30–40%) upgraded on excision by one level [40]. An upgrade rate of two levels, i.e., from grade 1 to grade 3, is very rare (0–2%) [41–43]. The discordance in tumor grade is mainly due to underestimation of mitotic count, followed by nuclear pleomorphism and tubule formation [41, 43]. One study reported better correlation between anti-pHH3 and MIB-1 staining with that of mitotic figures obtained from excision specimens than on CNBs [44]. The underestimation of mitotic activity in CNBs can be problematic, particularly when the difference in scoring results in an upgrade of the overall histologic grade on excision. Clinicians find this seemingly discordant histologic grade reported between the CNB and the subsequent excision specimen disconcerting and confusing. Hence, if such a scenario is foreseen, it is suggested that the histologic grade in the CNB be reported as "well to moderately differentiated (Grade 1–2)" so that both "options" are available to the pathologist who will be reporting the final histologic grade on the excision specimen. Alternatively, a statement such as "Final histologic grade should be based on the excision specimen" could be included in the comment of the pathology report.

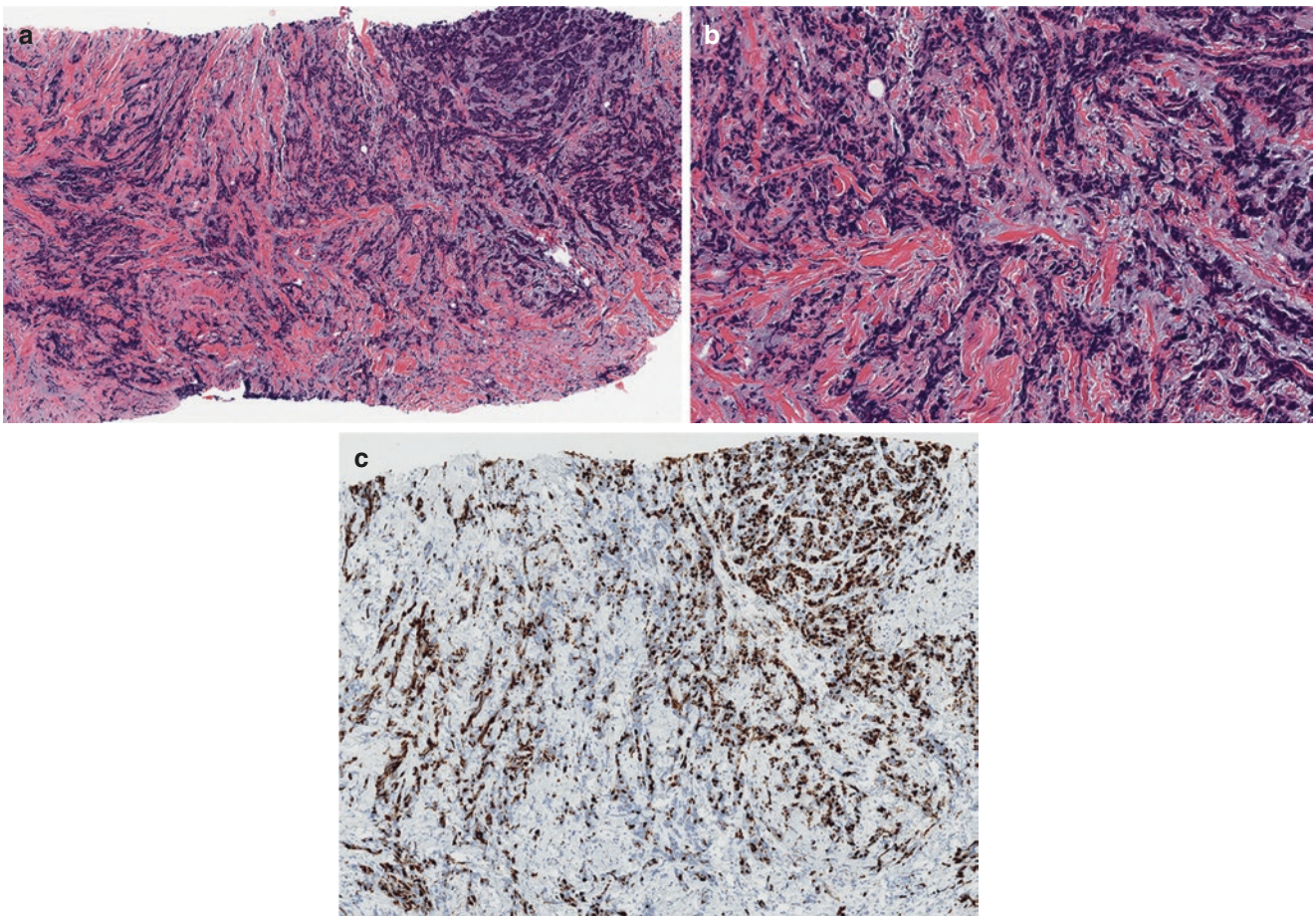

Fig. 10.17 Invasive breast carcinoma NST, with marked crush artifact that interferes with histologic grading, specifically nuclear pleomorphism and mitotic count, (**a**) low-power and (**b**) high-power magnifications, (**c**) Ki-67 stain shows high proliferation rate

Table 10.1 Nottingham scoring system to evaluate histologic grade for invasive breast carcinoma

	Score		
Parameters	1	2	3
Tubule/gland formation			
	>75%	10–75%	<10%
Nuclear pleomorphism/size			
	Small/regular nuclei with evenly dispersed chromatin and indistinct nucleoli; size 1.5× normal breast epithelial nuclei	Moderate variation in nuclear shape with uneven distribution of chromatin, vesicular nuclei, and occasional small visible nucleoli; size 1.5–2× normal breast epithelial nuclei	Marked nuclear size variation, frequently bizarre nuclei with a predominant vesicular chromatin pattern and prominent to macro nucleoli; size >2–2.5× normal breast epithelial nuclei
Mitotic count[a]			
Field diameter (mm)			
0.4	≤4	5–9	≥10
0.45	≤5	6–11	≥12
0.5	≤7	8–14	≥15
0.55	≤8	9–17	≥18
0.6	≤10	11–20	≥21
0.65	≤12	13–24	≥25

Reproduced from Elston, C.W. and Ellis, I.O. (1991), Pathological prognostic factors in breast cancer. I. The value of histological grade in breast cancer: experience from a large study with long-term follow-up. Histopathology, 19: 403–410. https://doi.org/10.1111/j.1365-2559.1991.tb00229.x, with permission of John Wiley and Sons

Final grade (addition of scores of each component): Grade 1: total score, 3–5. Grade 2: total score, 6 and 7. Grade 3: total score, 8 and 9. Based on Elston and Ellis modification of the original Scarff-Bloom-Richardson grading system [27]

[a] Mitotic count varies according to the field diameter and field area at high-power magnification (400×)

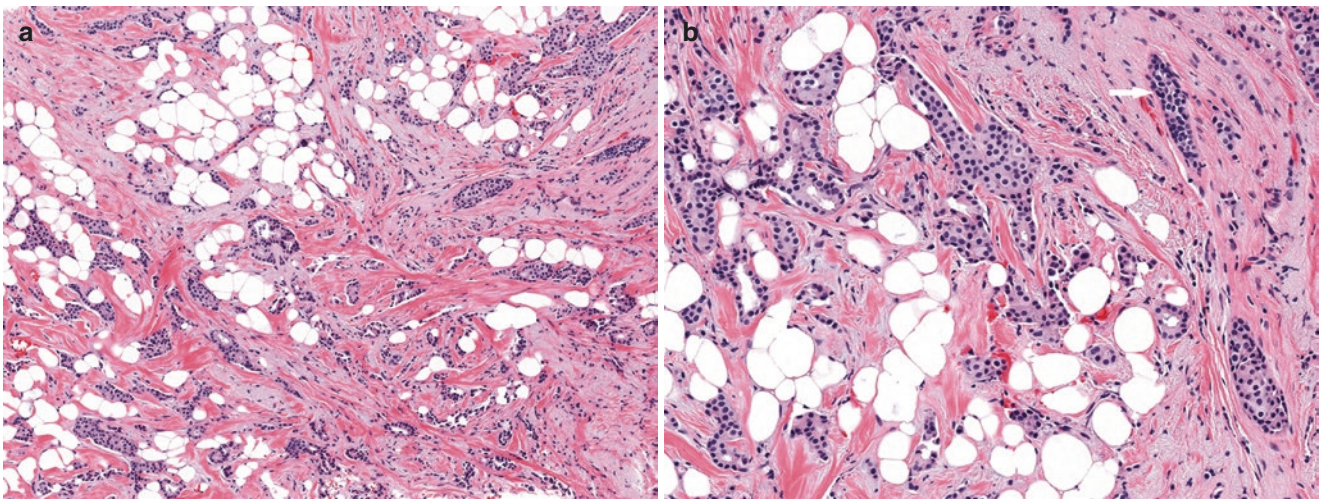

Fig. 10.18 Invasive breast carcinoma NST, grade 1, (**a**) low-power and (**b**) high-power magnifications (arrow indicates normal duct for comparison)

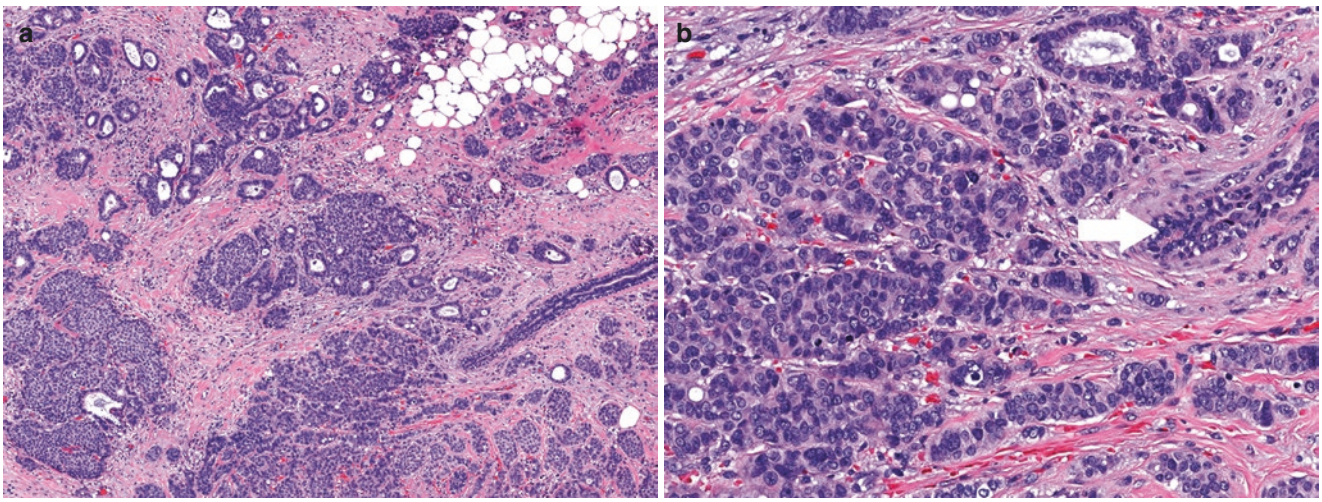

Fig. 10.19 Invasive breast carcinoma NST, grade 2, (**a**) low-power and (**b**) high-power magnifications (arrow indicates normal duct for comparison)

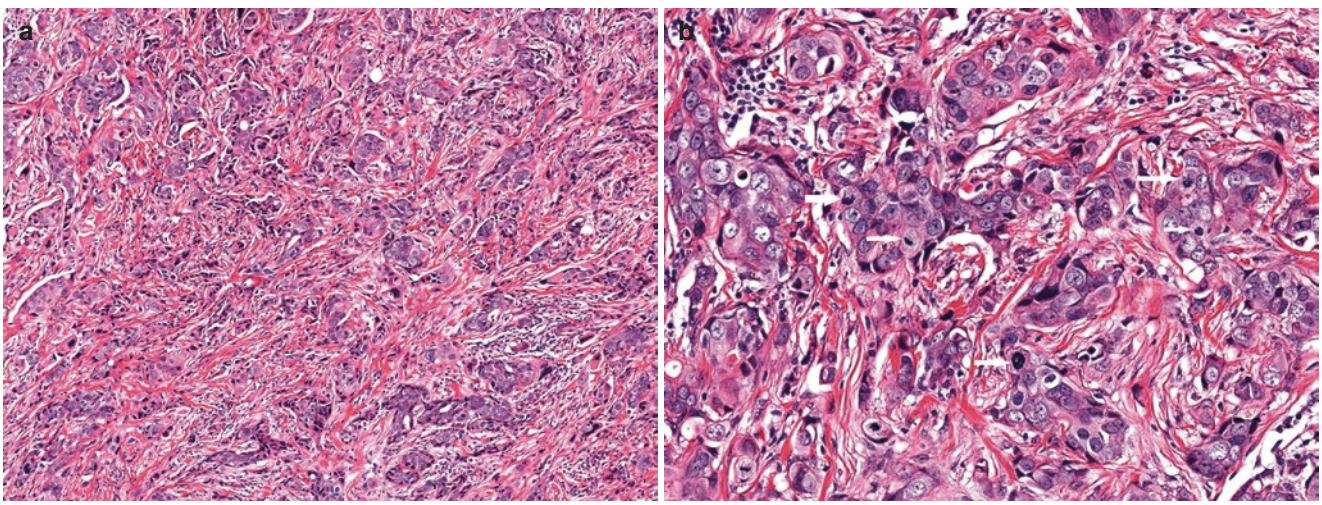

Fig. 10.20 Invasive breast carcinoma NST, grade 3, (**a**) low-power and (**b**) high-power magnifications (arrows indicating mitosis)

Reporting Core Needle Biopsy

A correct pathologic diagnosis of invasive carcinoma in a CNB is paramount as it not only guides further treatment but also provides important information for prognostic and predictive factors. In patients who undergo neoadjuvant therapy and have complete pathologic response, the CNB will be the only available tumor tissue for diagnosis and biomarker studies. As sampling is limited on a CNB, utmost vigilance should be taken not to overdiagnose invasive carcinoma. Several studies have reported high concordance rates ranging from 91% to 100% between CNB and the subsequent excision for a malignant diagnosis [45–47]. The sensitivity and specificity of diagnosing invasive carcinoma in CNB ranges from 85 to 100% and 96 to 100%, respectively [48–50].

Once the diagnosis of malignancy is established, every effort should be made to report tumor type, histologic grade, tumor size, the presence or absence of coexistent in situ carcinoma, lymphovascular invasion, the presence and extent of necrosis and tumor infiltrating lymphocytes (TILs). If coexistent DCIS is identified, its extent, architectural type, and nuclear grade should be reported. Recording the number of cores containing tumor and the largest linear extent of the tumor in core biopsies becomes important in certain instances: small tumors can be entirely removed with no residual tumor left in the excision specimen, the size of the tumor on the CNB can be larger than in the excision, and to ensure that there is more than minimal invasive component (at least more than 2 mm and ideally 5 mm of tumor tissue) available to perform and assess tumor biomarkers. The latter is extremely important in cases where neoadjuvant chemotherapy is planned. Routinely performing ER, PR, and HER2 on CNB samples rather than the excision is preferred as there is less variation in cold ischemia time and duration of fixation; the hormone receptor (HR) and HER2 status also dictate possible pre-surgical systemic therapy.

Differential Diagnosis

The differential diagnosis of IBC-NST includes both malignant and benign lesions. The main invasive carcinoma in the differential is ILC, particularly ILC variants, e.g., pleomorphic type, as they can show similar architecture and high-grade morphology (discussed in Chap. 15) (Fig. 10.21). Distinction between IBC NST and ILC is recommended because their clinical behavior and outcome are different [51, 52].

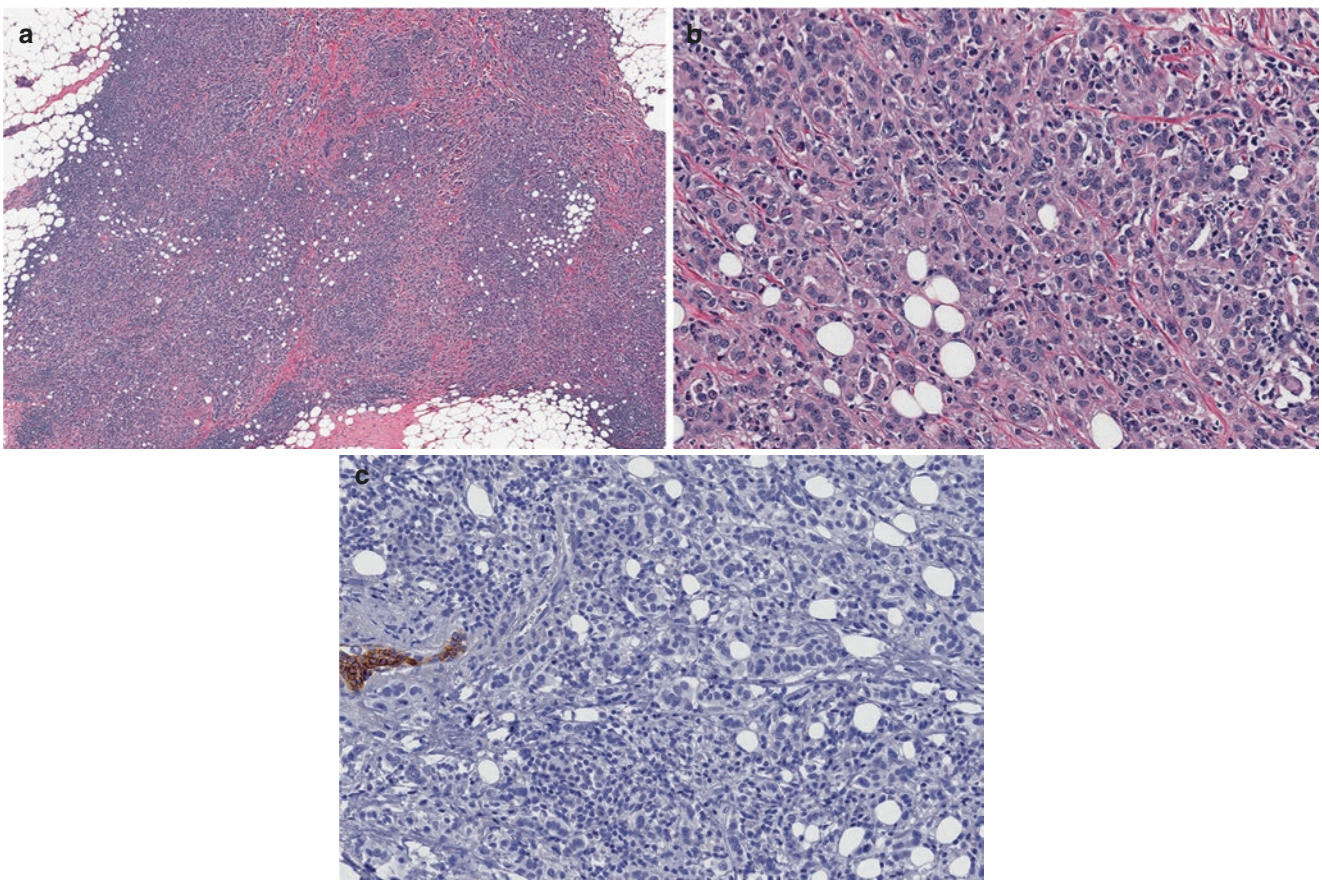

Fig. 10.21 Invasive lobular carcinoma mimicking ductal carcinoma, (**a**) low-power view shows a diffuse infiltration of tumor cells admixed with inflammatory infiltrate, (**b**) high-power view shows highly pleomorphic tumor cells growing in a trabecular pattern, and (**c**) E-cadherin shows negative staining in the tumor cells but positive staining of a normal duct on the left

Benign and in situ lesions that may mimic IBC-NST include nipple adenoma, sclerosing adenosis alone or secondarily involved by DCIS/lobular carcinoma in situ (LCIS), radial scar with epithelial hyperplasia, and complex sclerosing lesions involved by epithelial hyperplasia, DCIS or LCIS (Figs. 10.22, 10.23, 10.24, 10.25, and 10.26). Histological

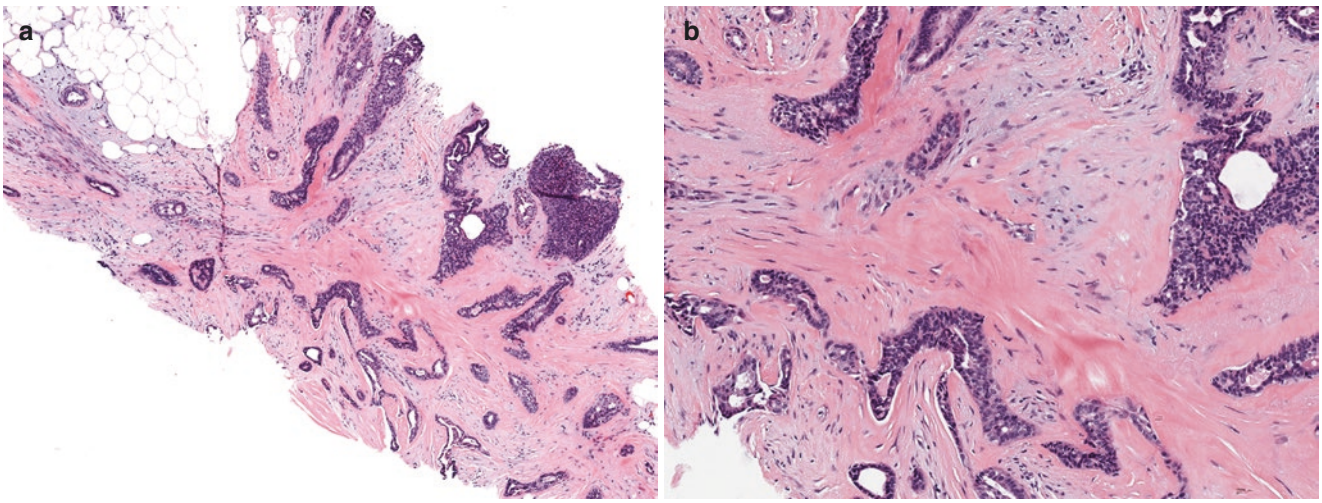

Fig. 10.22 Radial scar mimicking IBC-NST and DCIS. (**a**) Low-power and (**b**) high-power magnifications

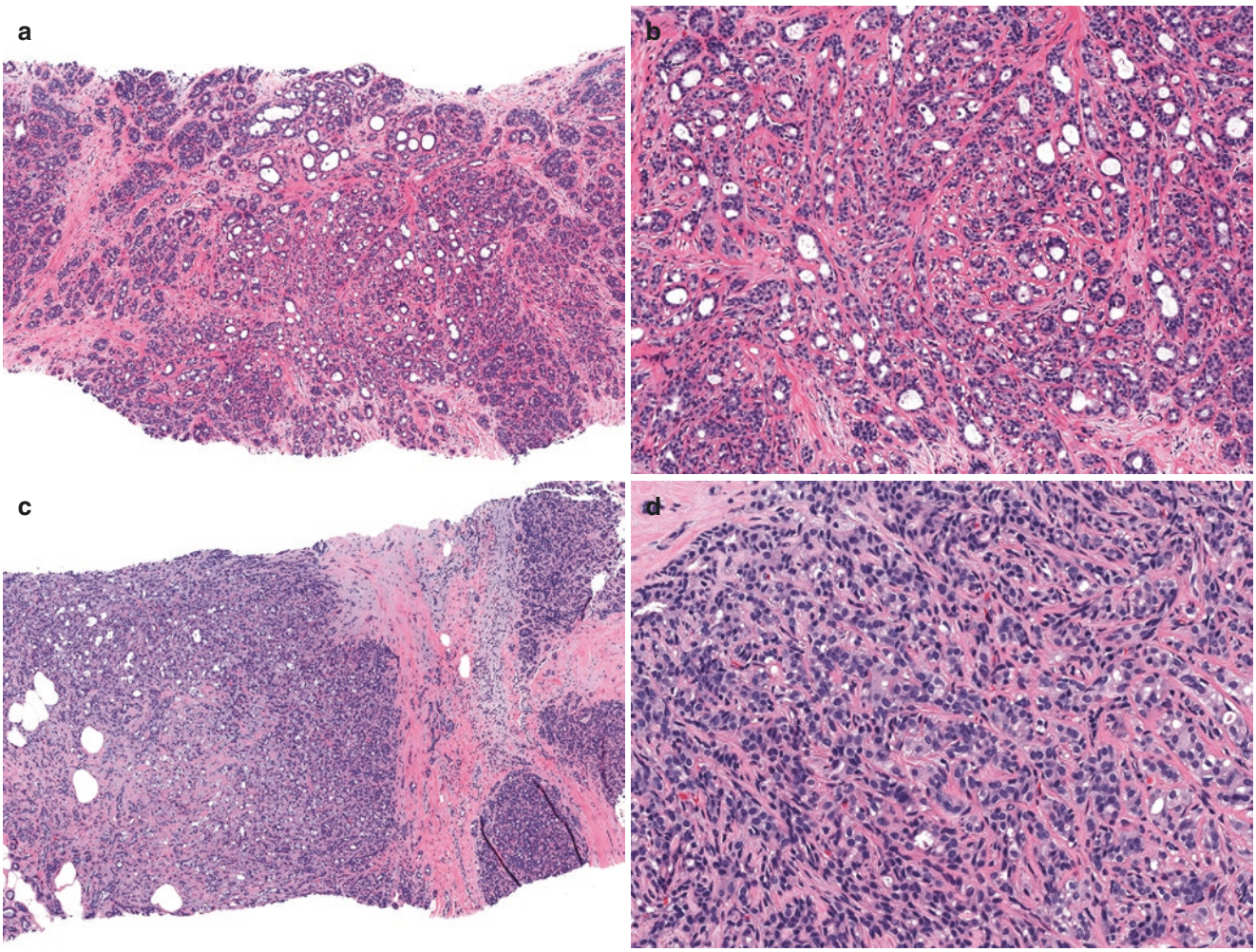

Fig. 10.23 Extensive mass-forming sclerosing adenosis. Example 1 (**a**, **b**). The distorted lobules and sclerosis mimic invasive carcinoma. Example 2 (**c**, **d**). The distorted lobules and areas of stromal sclerosis can easily be mistaken for invasive carcinoma

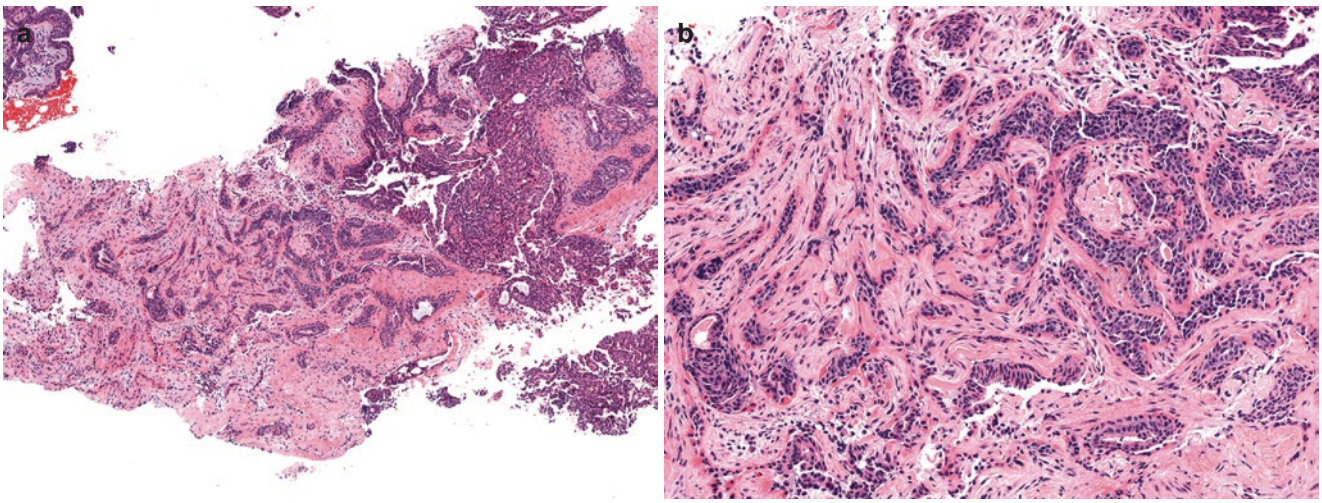

Fig. 10.24 Sclerosing papilloma. (**a**) Entrapped glands and sclerosis in an intraductal papilloma can be mistaken for invasive breast carcinoma NST. (**b**) High-power magnification reveals smooth outline of the entrapped glands by pink basement membrane

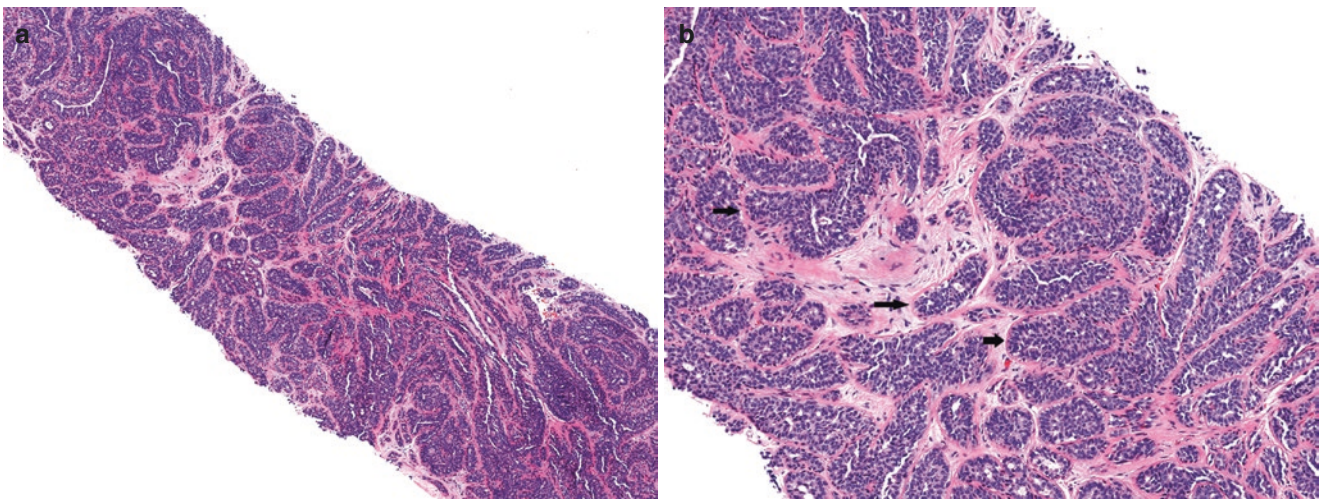

Fig. 10.25 Complex sclerosing lesion with epithelial hyperplasia. (**a**) Epithelial hyperplasia in the benign entrapped glands in a fibrotic stroma mimics invasive carcinoma. (**b**) High-power view shows benign epithelial cells and pink basement membrane (*arrows*)

features that can help to identify a lesion as benign include circumscribed or lobular configuration at low-power examination and most importantly identification of myoepithelial cells beneath the hyperplastic epithelium and the smooth outline of the distorted epithelial cells conferred by an intact basement membrane. Immunostains for myoepithelial cells such as smooth muscle myosin heavy chain (SMM), p63, or calponin can be extremely helpful in these cases. In cases where the nature of the lesion remains equivocal and the diagnosis cannot be made with confidence, it is preferable to request a repeat CNB or state that final classification will be performed after the evaluation of the excision specimen, rather than commit to a questionable diagnosis.

The majority of IBC-NST exhibits infiltrative margins but at times may show a circumscribed border with a pushing front. When necrosis is present in the center of large expansile solid nests of tumor cells that are high grade, it can resemble comedo-type DCIS. These high histologic grade circumscribed lesions are commonly "triple-negative" breast carcinoma or "IBC with medullary pattern" (Fig. 10.27). Careful assessment of the intervening stroma that usually reveals desmoplasia should prompt one to consider the diagnosis of invasive carcinoma, which can be further confirmed by myoepithelial stains. When low-to-intermediate grade IBC-NST with circumscribed/pushing edge is encountered, solid papillary carcinoma should be included in the differen-

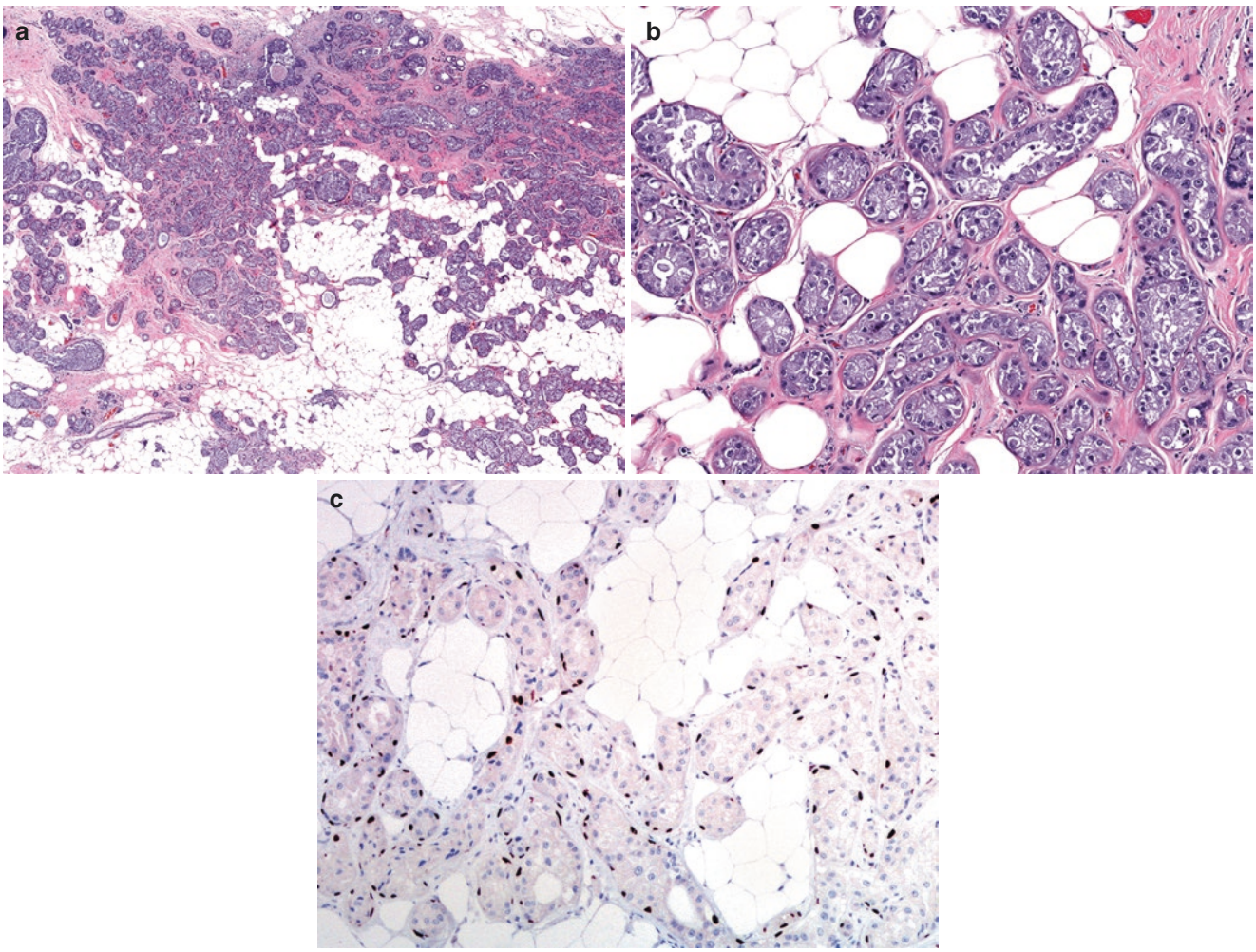

Fig. 10.26 DCIS involving sclerosing adenosis mimics invasive carcinoma. (**a**) Low-power and (**b**) high-power magnifications. (**c**) p63 stain shows intact myoepithelial cells around glands

tial diagnosis, especially in older women who tend to have these tumors. Occasionally, low-grade IBC-NST may show prominent large nests of tumor cells embedded in fibrotic stroma resembling DCIS (Fig. 10.28).

Lymphomas of the breast, whether primary or secondary, are rare. High-grade lymphoma can mimic high-grade IBC-NST with an inflammatory infiltrate [53, 54]. The most common primary breast lymphoma in most series is diffuse large B cell lymphoma (DLBCL), with frequency ranging from 49% to 64% [55, 56]. The next most common lymphomas encountered are extranodal marginal zone lymphoma of mucosa-associated lymphoid tissue (MALT) type (19–23%) and follicular lymphomas (14–19%) [55, 56]. Lymphoma usually presents as a mass lesion in the breast. High-grade lymphoma should be suspected when the lesion is diffuse, grows as sheets, and shows intimate mixture of neoplastic cells and other chronic inflammatory cells (Fig. 10.29).

Lastly, IBC-NST must be differentiated from metastases to the breast from extramammary sites. Although uncommon, metastases to the breast accounts for up to 3% of all breast masses [57]. Fortunately, most patients who present with metastases to the breast already have an earlier diagnosis of the primary tumor. The tumors that metastasize to the breast include melanoma and carcinomas from ovary, lung, thyroid, kidney, and liver [58–60]. Breast involvement by metastatic carcinoma may be a sign of rapid widespread dissemination with a survival rate of only 10.9 months [61]. Certain features that may be indicative of metastasis are absence of microcalcifications, lack of spiculations on imaging, or lack of skin involvement clinically, but none of these

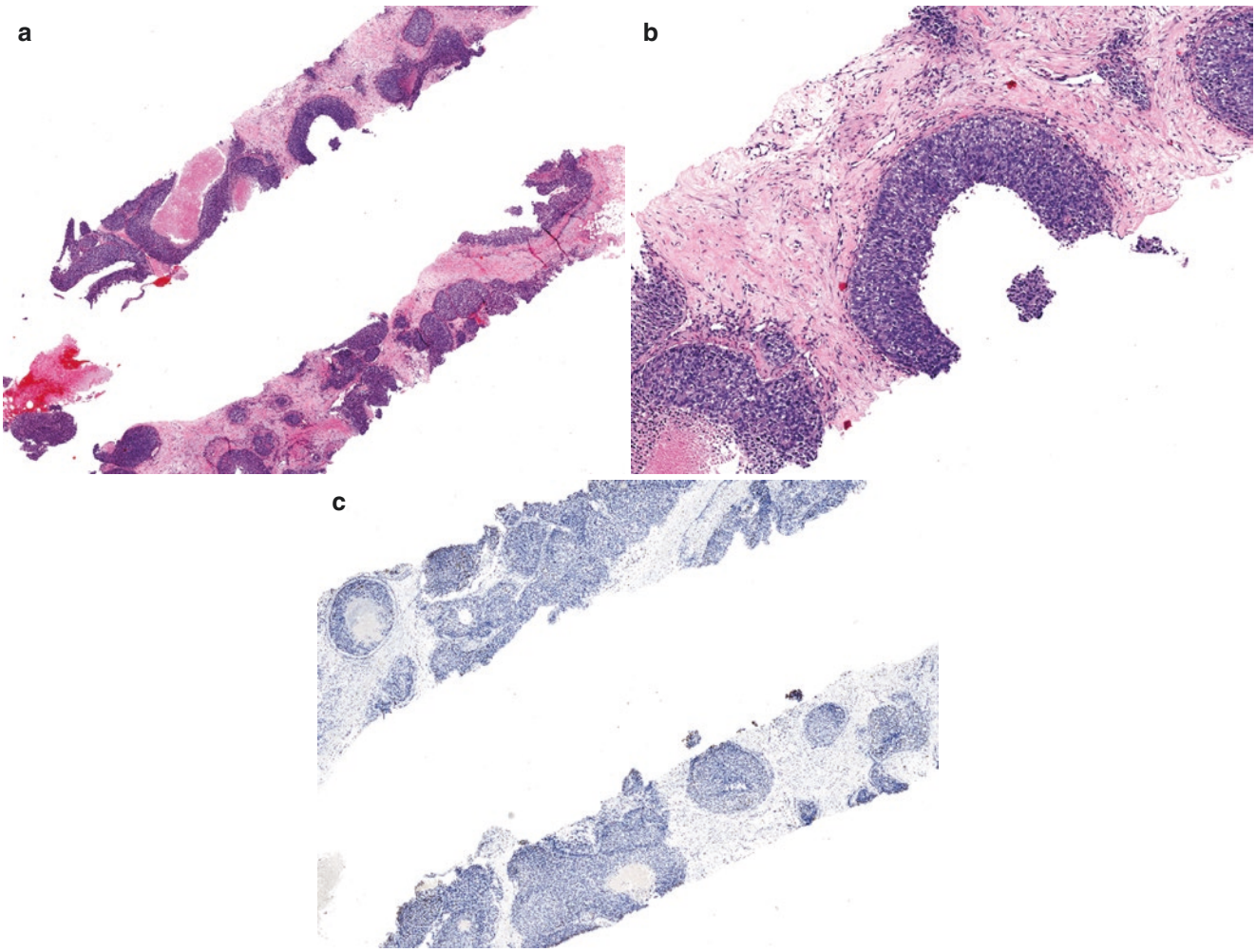

Fig. 10.27 Invasive breast carcinoma NST masquerading as DCIS. (**a**) A 2 cm mass that shows large solid nests of tumor with round borders and central necrosis resembling DCIS. (**b**) High-power view shows altered desmoplastic stroma between the nests distinct from normal breast stroma. (**c**) Immunostain for p63 shows lack of myoepithelial cells in the entire lesion

features are specific for metastatic disease. In a CNB, metastatic tumor to breast should be suspected when a malignant tumor with unusual morphology is encountered or when a tumor believed to be breast primary shows an unusual staining pattern with prognostic markers (Figs. 10.30 and 10.31). The presence of in situ carcinoma favors tumor of breast origin, although incidental DCIS can be present adjacent to metastatic tumor. In some cases, metastatic tumors may not display any of the above features. What is crucial in these cases is having a detailed clinical history. On the rare occasion when metastasis to the breast is the first manifestation of the tumor, a detailed discussion with clinicians is required to determine the primary site. A panel of immunostains may help determine the primary site, keeping in mind that no stain is pathognomonic for a site of origin. TTF1, for example, can be positive in breast carcinomas [62] and focal expression of WT1 in IBC with mucinous differentiation has been reported [63].

Immunohistochemistry

Invasive breast carcinomas tend to be CK7 positive and CK20 negative, consistent with most tumors found above the diaphragm. Immunostains that can help identify breast as the site of origin include ER, GATA3, GCDFP-15, and mammaglobin. ER is expressed in approximately 80% of IBC [64]. Strong, diffuse ER expression may be sufficient to ren-

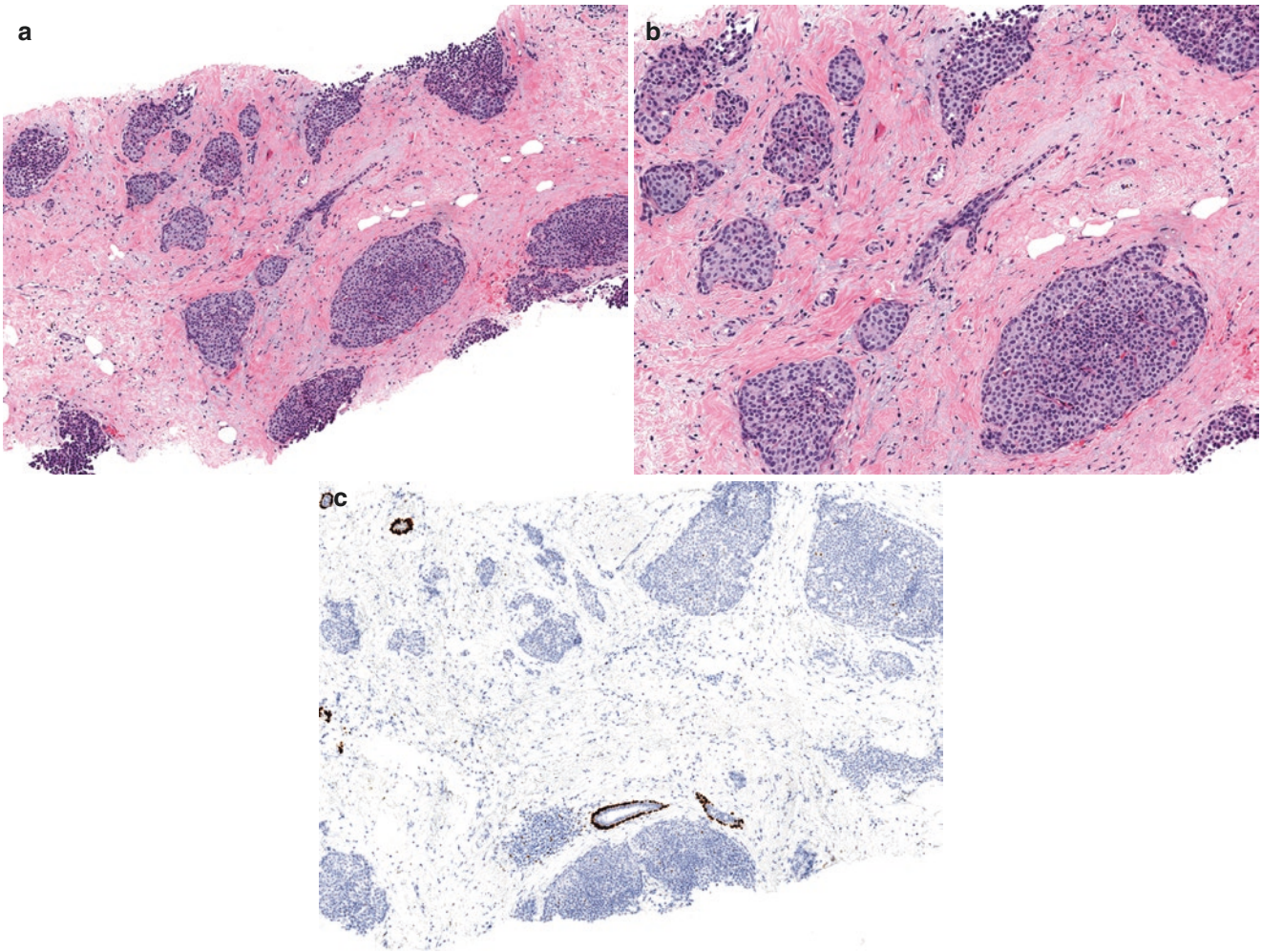

Fig. 10.28 Invasive breast carcinoma NST, moderately differentiated mimicking DCIS. (**a**) Low-power view shows solid nests of low nuclear grade cells with round to oval borders, (**b**) high-power view, and (**c**) SMM immunostain shows absence of staining around the nests confirming the tumor's invasive nature

der a diagnosis of metastatic breast carcinoma in the appropriate clinical setting. ER however is not specific and can be expressed in skin adnexal, salivary gland, and gynecologic tumors. Mammaglobin and GCDFP-15 are highly specific (both have >90% specificity) but have low sensitivity for IBC (mammaglobin 50%, GCDFP-15 20–50%) [65–68]. Staining for both markers also tends to be patchy. Similar to ER, other tumors that are likely to express both these markers are skin adnexal, salivary gland, and gynecologic tumors [66, 69]. GCDFP-15 is a marker of apocrine differentiation and accordingly is more sensitive in cases of apocrine carcinoma (75%) or IBC with apocrine differentiation (55%) compared to carcinoma without apocrine differentiation (23%) [70].

GATA3, a member of a zinc finger transcription factor family, is expressed in 70–90% of breast carcinomas [71, 72]. Of greater utility however, GATA3 is expressed in up to 70% of triple-negative breast carcinomas (TNBC) [73]. GATA3 is also expressed in a majority of skin adnexal, skin squamous cell, and urothelial carcinomas [72].

While well-differentiated metastatic IBC will usually express ER and GATA3, TNBC may not show expression of these markers which can make diagnosing metastatic TNBC challenging in some cases. One stain that may help in such a setting is SOX10. SOX10 is an immunostain that is primarily associated with nerve sheath tumors and melanoma but has also been shown to be expressed in up to 70% of TNBC [74].

Pathogenesis

Seminal papers by Wellings and colleagues demonstrated that both ductal and lobular neoplasia arise from the terminal

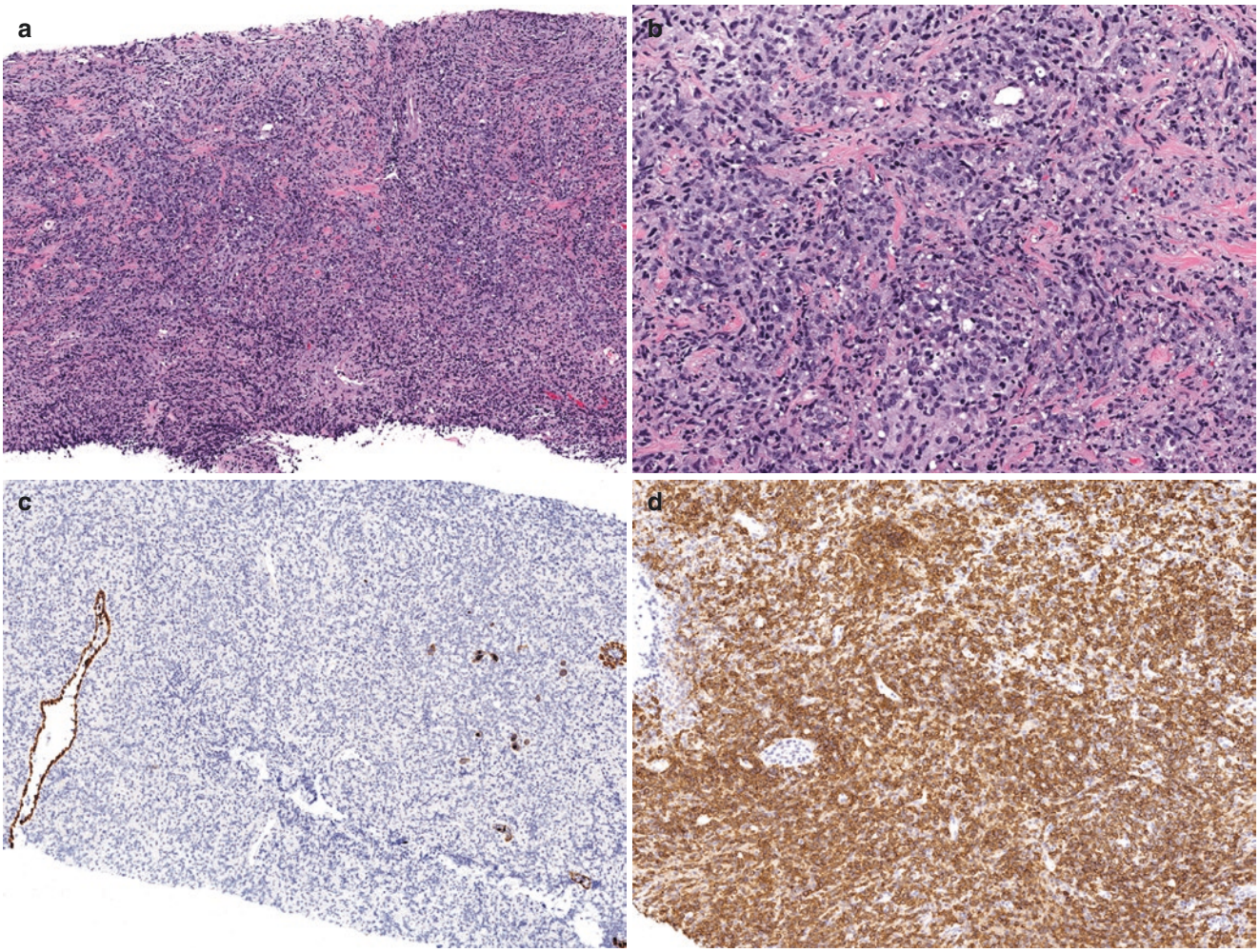

Fig. 10.29 Primary lymphoma of breast. (**a**) Core needle biopsy reveals a diffuse infiltrate with aggregates of neoplastic cells mimicking IBC-NST with inflammatory infiltrates. (**b**) High-power view shows larger neoplastic cells intimately admixed with inflammatory cells. (**c**) Cytokeratin stain shows complete lack of staining in neoplastic cells while (**d**) immunostain for CD20 is diffusely positive

duct lobular unit (TDLU) [75, 76], in contrast to the conventional thought at that time that lobular tumors arise from lobules and ductal tumors arise from ducts. Just as lobular neoplasia (atypical lobular hyperplasia and LCIS) is a non-obligate precursor to ILC [77–79], flat epithelial atypia (FEA), atypical ductal hyperplasia (ADH), and DCIS are considered non-obligate precursors to IBC-NST [75, 76, 80, 81]. Contrary to the historical belief that a tumor progresses from a precursor lesion to low-grade invasive carcinoma to high-grade invasive carcinoma, genetic and gene expression studies have supported two different pathways: a low-grade pathway and a high-grade pathway.

High-grade DCIS and poorly differentiated IBC share common genetic alterations whereas low-grade lesions, such as ADH, low-grade DCIS, and well-differentiated invasive carcinoma, exhibit similar genomic changes, providing little support for a transition from a low-grade carcinoma to a high-grade carcinoma. Comparative genomic hybridization (CGH) studies have revealed that the low-grade evolutionary pathway is characterized by frequent loss of chromosome 16q, gain of chromosome 1q, and infrequent amplification of 17q12 [82–84]. Similarly, various loss-of-heterozygosity (LOH) and CGH-based studies have demonstrated similar genetic alterations (16q loss and 1q gain) in FEA and ADH [82, 85, 86]. On the other hand, loss of chromosome 16q is infrequent in high-grade lesions further supporting segregation of low- and high-grade lesions [83, 84]. Furthermore, high-grade carcinomas (both in situ and invasive) demonstrate complex karyotypes such as loss of 8p, 11q, 13q, and 14q, gains of 1q, 5p, 8q, and 17q, and amplification of 17q12 and 11q13 [84, 87]. However, some studies have suggested, albeit in a small subset of tumors,

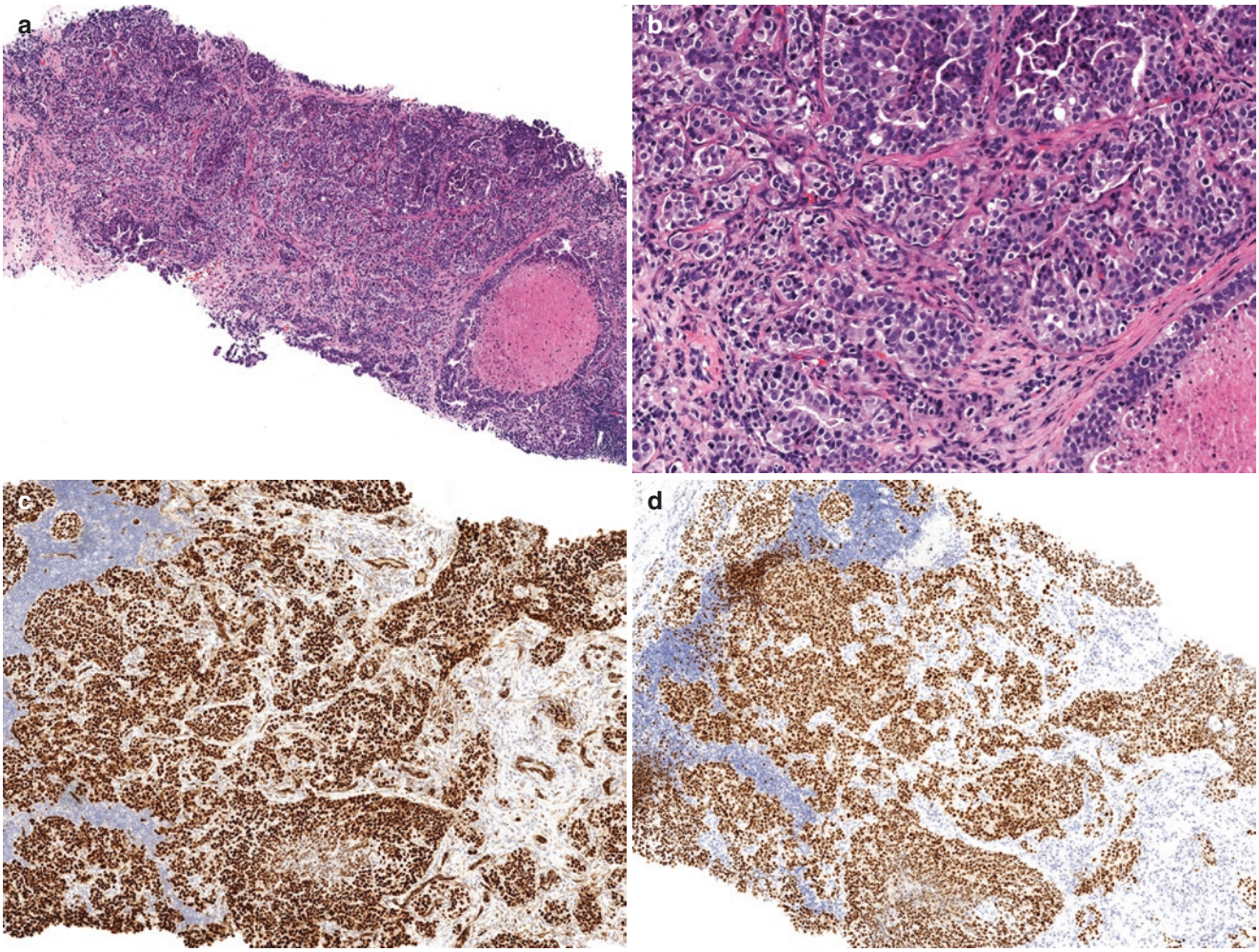

Fig. 10.30 Serous carcinoma of the ovary metastatic to breast. (**a**) Low-power magnification shows a high-grade invasive tumor with areas of necrosis mimicking in situ carcinoma, (**b**) high-power magnification, (**c**) WT1 and (**d**) PAX8 show diffuse nuclear staining in tumor cells confirming its Mullerian origin

that there might be a pathway leading from low-grade to high-grade as they demonstrated loss of 16q in high-grade lesions [88, 89]. Natrajan et al. noted 16q loss is more frequent in high-grade luminal subtype carcinomas compared to other high-grade carcinomas such as HER2 only or basal-like phenotypes [88].

Invasive breast carcinoma NST is a heterogenous disease, varying in histologic grades, HR/HER2 biomarker status, gene expression profiles, and genetic alterations. By gene expression profiling, IBCs-NST encompass all five intrinsic molecular subtypes: luminal A, luminal B, HER2-enriched, basal-like, and normal breast-like. Luminal A tumors (overall corresponding to low-grade, ER/PR-positive, HER2-negative IBC-NST with low Ki-67 proliferation rate) are enriched in *PIK3CA* mutations (~50%), whereas basal-like tumors (in general as high-grade ER/PR/HER2 triple-negative IBC-NST) have a high prevalence of *TP53* mutations (~85–90%). Studies from patients with genetic tumor syndromes have identified multiple genes that when altered are associated with an increased susceptibility to breast cancer. These breast cancer-predisposing genes include *BRCA1*, *BRCA2*, *PTEN* (Cowden syndrome), *TP53* (Li-Fraumeni syndrome), *ATM*, *PALB2*, and *CHEK2*, among others. Many of these genes are involved in DNA repair. Breast cancers occurring in these genetic tumor syndromes are mostly IBC-NST; however, tumors with mutations in select genes, either germline or somatically acquired, tend to show specific pathologic features. For example, most IBC with germline and/or somatic *BRCA1* mutations appear well-demarcated, have prominent lymphoplasmacytic infiltrate and are high grade with high mitotic activity. Breast cancers from Li-Fraumeni patients are most likely to be grade 3 IBC-NST

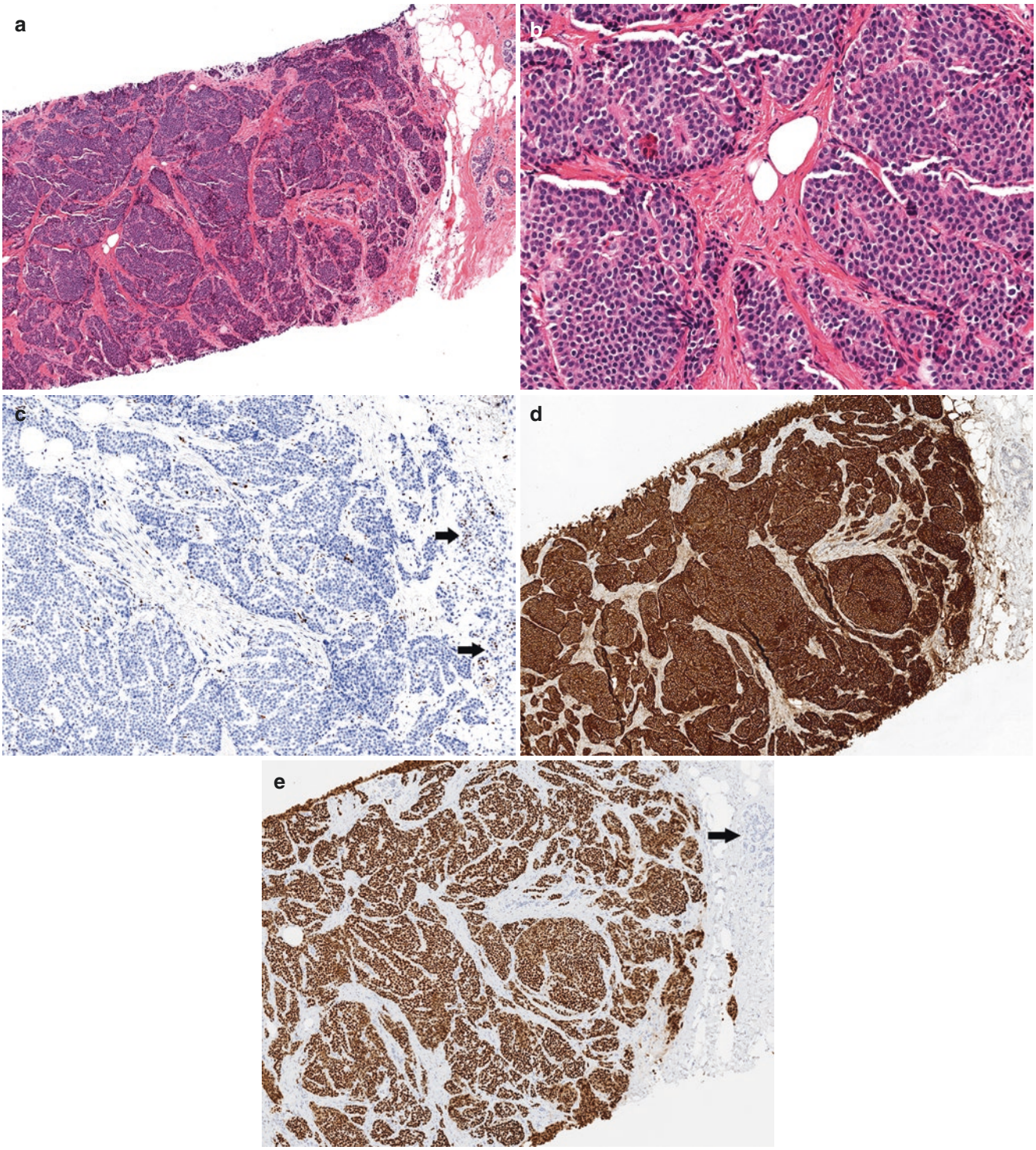

Fig. 10.31 Neuroendocrine tumor of ileum metastatic to breast. (**a**) Low-power view shows infiltrative growth pattern mimicking moderately differentiated IBC-NST. (**b**) High-power view shows prominent nesting and fine powdery chromatin of tumor cells. (**c**) Negative hormone receptor (ER/PR) staining (estrogen receptor stain shows compressed normal lobules with focal positive staining (*arrows*)) prompted further IHC investigation. (**d**) Chromogranin and (**e**) CDX2 show diffuse staining in tumor cells and no staining in normal lobule (*arrow*) (all breast-specific markers were negative, not shown)

with frequent HER2 overexpression/amplification (~60%), while apocrine differentiation is common in breast cancers from patients with germline *PTEN* mutations. Please refer to Chap. 23 for comprehensive discussion in molecular profiling of breast cancer.

Prognosis

The prognosis of IBC-NST depends on a number of factors. These include age, tumor size, histologic grade, lymph node status, hormone receptor (HR) status, and HER2 status. HR and HER2 status are also significant predictive factors for endocrine and anti-HER2 therapy, respectively (Fig. 10.32). Tumor infiltrating lymphocytes have recently been found to be a prognostic factor in TNBC and HER2-positive breast cancer [90]. Other factors that have been studied but found to be of uncertain significance include the presence of angioinvasion, perineural invasion, tumor necrosis, and DCIS (and its extent), among others [90]. Prognostic and predictive factors, including panel-based gene expression signatures (such as OncotypeDx®, MammaPrint®, Prosigna® and EndoPredict®), are further discussed in Chaps. 22 and 23.

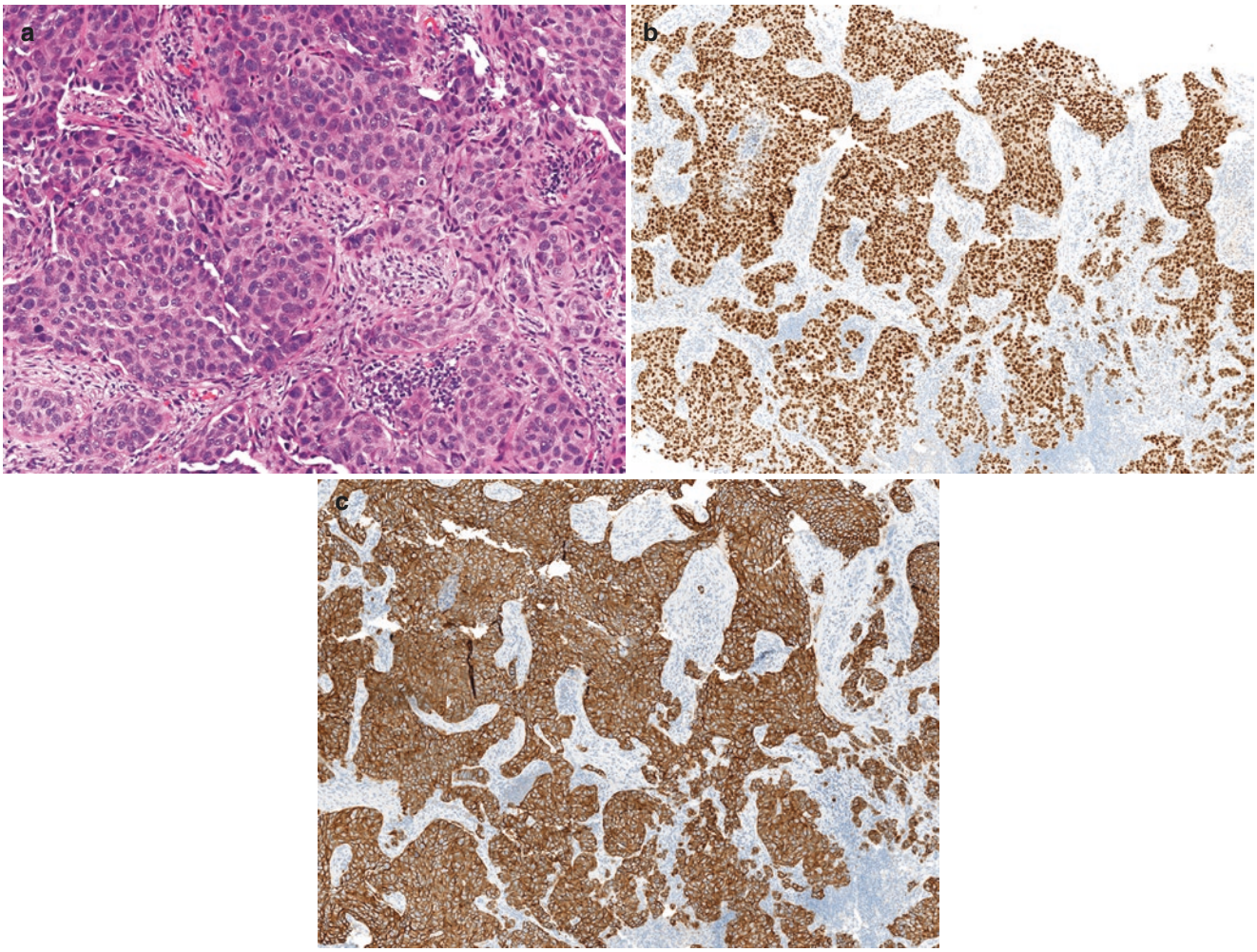

Fig. 10.32 Invasive breast carcinoma NST. (**a**) Low-power magnification, (**b**) diffuse strong nuclear staining with estrogen receptor, and (**c**) strong complete membranous staining with HER2

Microinvasive Breast Carcinoma

Overview

Microinvasive carcinoma (MIC) of the breast is defined as invasive carcinoma not exceeding 1 mm in greatest dimension [91]. MIC is uncommon and accounts for 0.68–2.4% of all IBCs [92–94]. It is usually associated with carcinoma in situ (CIS) and has been found in 9.5–13% of all DCIS cases [95, 96].

Microinvasion has been defined in various ways in the past. Some of the initial studies describing lymph node involvement in patients with MIC defined it as DCIS with stromal invasion without defining the size of invasion [97, 98]. Other definitions used previously include "DCIS with focal stromal invasion in less than or equal to 10% of the surface of histological section examined" [99], "more than single collection of cells outside the lobular unit or immediate periductal area" [100], "maximal extent of invasion…not more than 2 mm or comprising <10% of the tumor with 90% of DCIS" [101], "a single focus of invasive carcinoma ≤2 mm or up to three foci of invasion each not more than 1 mm in greatest dimension" [102], and "infiltration of neoplastic cells beyond the specialized lobular or intralobular stroma" [103]. In 1982, Lagios et al. defined microinvasion as invasive carcinoma less than 1 mm [104]. In 1996, the *American Joint Committee on Cancer* (AJCC) formally recognized MIC as invasive carcinoma measuring 1 mm or less, the definition of which has remained unchanged in subsequent editions of the *Cancer Staging Manual* [91].

Gross and Radiologic Features

MIC is a microscopic finding and does not have any specific clinical, radiological, or gross correlate that would distinguish it from "pure" DCIS of similar size and grade. However, certain radiologic features have been identified that are predictive of microinvasion or small invasive carcinoma. Large size DCIS (>5 cm), cases where the main mammographic feature is a mass, distortion, or asymmetry versus calcifications, and correspondingly patients who had ultrasound-guided CNB rather than a stereotactic CNB have been found to be associated with an upgrade to MIC when only DCIS was diagnosed on CNB [105–107]. Vieira et al. reviewed the ultrasound findings of 11 of 21 patients with MIC and found 10 manifested as a solid hypoechoic mass, supporting the association of microinvasion with mass-forming DCIS [105].

Microscopic Features

MIC is typically identified in association with high-grade DCIS (Fig. 10.33). It is unusual in the setting of low-grade DCIS (Fig. 10.34). Besides high-grade DCIS, MIC may be seen with LCIS, either classic or pleomorphic types [108] (Figs. 10.35 and 10.36). Histologic clues for microinvasion include high-grade DCIS, presence of periductal chronic inflammation, stromal edema, and stromal desmoplasia around DCIS (Fig. 10.37). The presence of excessive microcalcifications or comedonecrosis in high-grade DCIS is also associated with greater chance of finding MIC [95, 102, 109], but none of the above features are specific for microinvasion as they are often present in DCIS cases without invasion. If one is unable to follow the smooth outline around the branching ducts, lobules or other benign sclerosing lesions replaced by DCIS, MIC should be strongly suspected. The cells in microinvasive foci are cytologically identical to the adjacent in situ component and usually appear as single cells or small angulated clusters, often within the stroma immediately adjacent to the in situ component. Due to the limited amount of invasive tumor, assigning a combined histologic grade is not feasible. Therefore, it is recommended to specify only the nuclear grade for MIC or, if reasonable, the degree of differentiation based on tubular formation and nuclear grade. The presence of stromal retraction around the neoplastic nests, a finding often noted in frankly invasive carcinoma, is another helpful clue in the diagnosis of MIC (Figs. 10.38 and 10.39). Invasive foci may be multifocal in MIC and therefore a thorough sampling and search for additional (possibly larger) foci should be conducted when a single focus of MIC is identified in cases with extensive DCIS [109]. While the size of individual foci of MIC should not be added together to yield a single cumulative size of tumor, there are otherwise no standard guidelines dictating the minimum distance between foci to designate one as an individual focus.

Conversely, one should be careful not to overdiagnose MIC, a common pitfall highlighted by one retrospective review. This study found only 19.3% cases with an initial

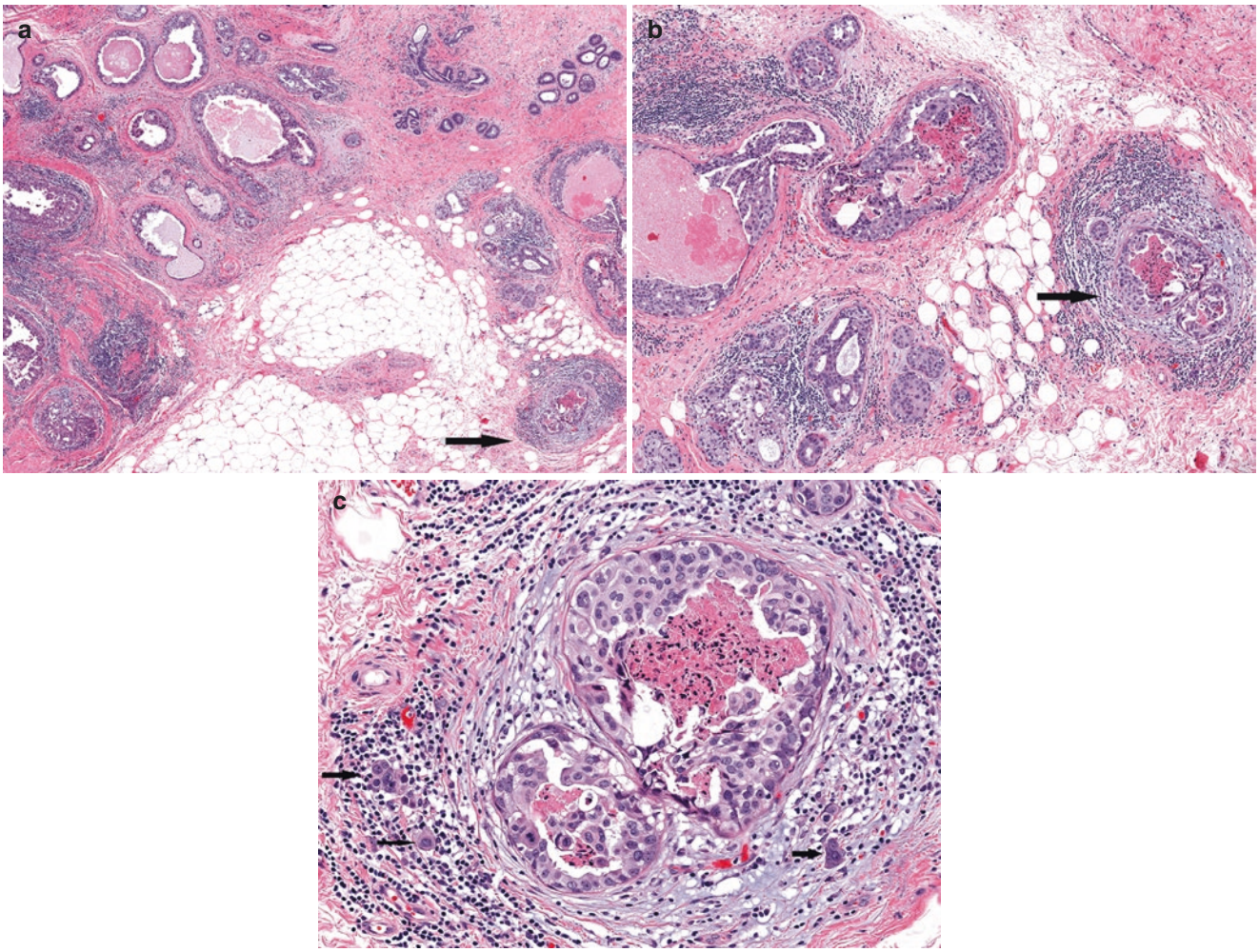

Fig. 10.33 High-grade DCIS with microinvasion. (**a**) Low-power view shows multiple ducts involved by high-grade DCIS with central necrosis and periductal fibrosis. (**b**) Medium power view reveals a focus of DCIS with prominent periductal fibrosis and inflammation (*arrow*). (**c**) Few single cells and small clusters of neoplastic cells in the intralobular stroma around DCIS are seen (*arrows*)

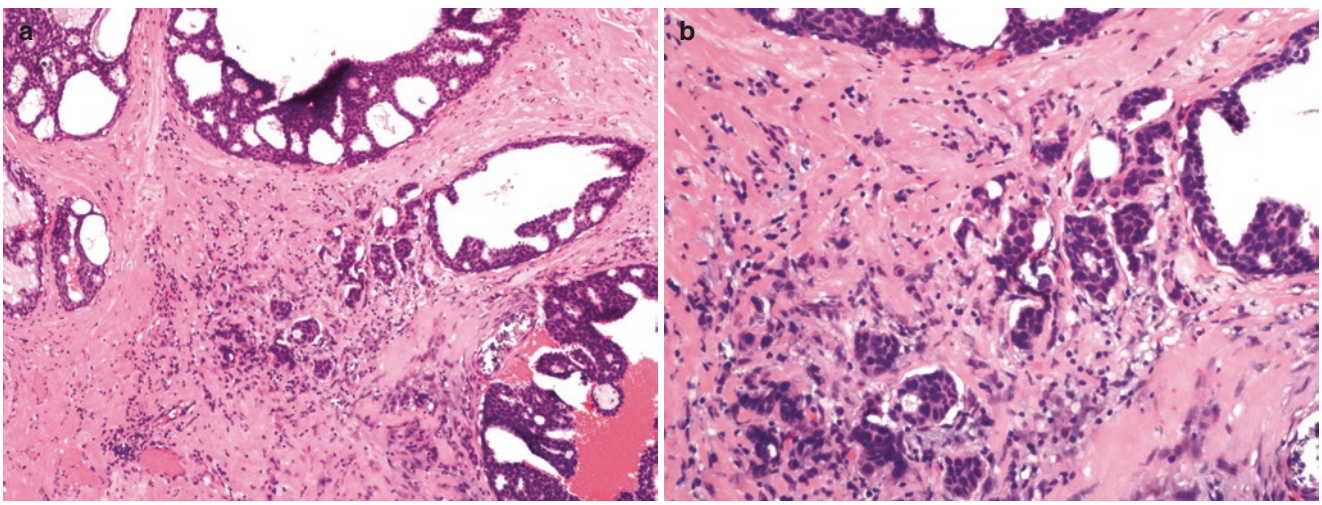

Fig. 10.34 Low-grade DCIS with microinvasion, (**a**) low-power and (**b**) high-power magnifications

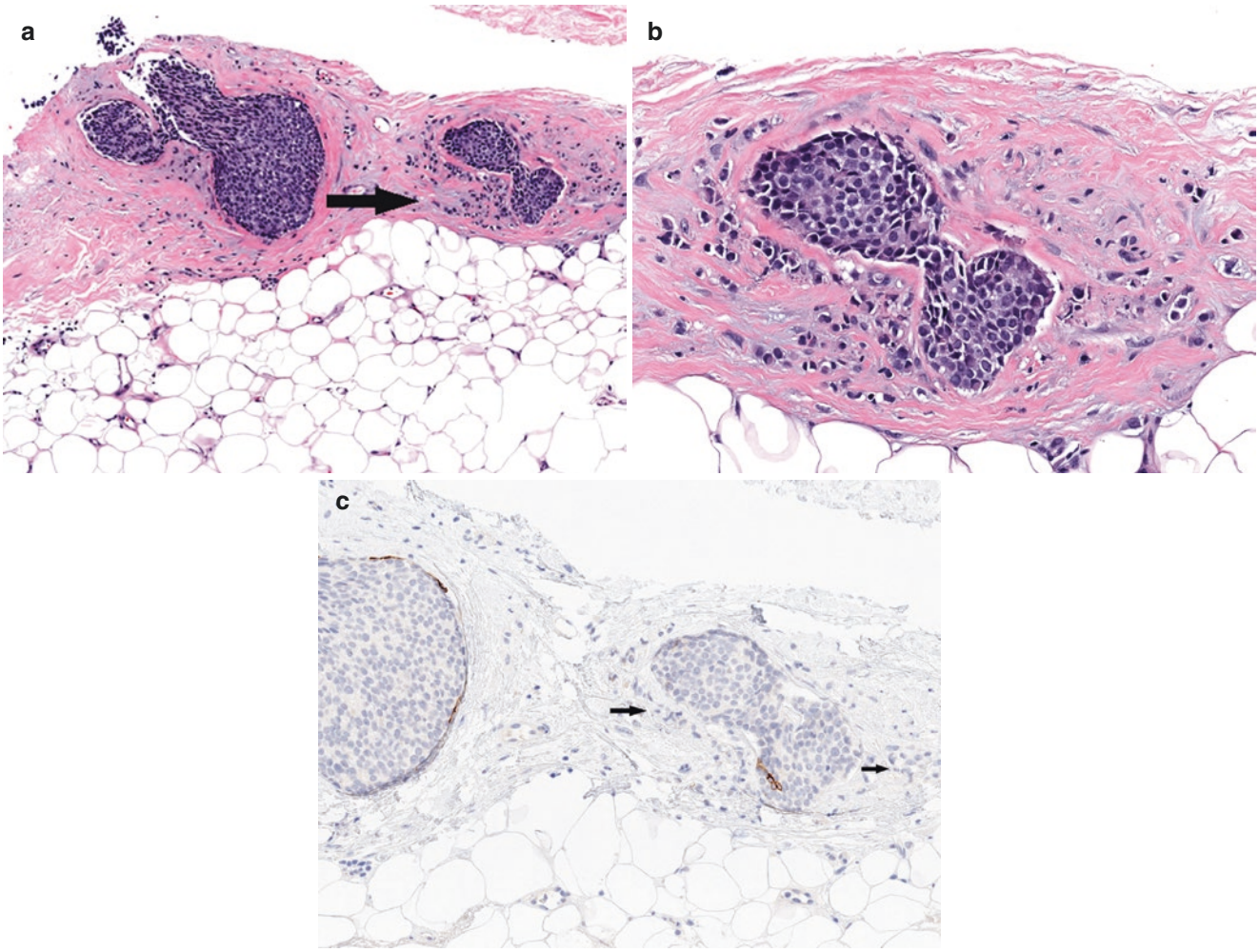

Fig. 10.35 Microinvasive lobular carcinoma associated with classic LCIS. (**a**) Low-power view shows microinvasive lobular carcinoma (*arrow*). (**b**) High-power view highlights linear infiltration by single tumor cells scattered around LCIS. (**c**) E-cadherin immunostain shows lack of staining in both in situ and invasive components (*arrow*) while focal weak positivity is retained in myoepithelium investing LCIS

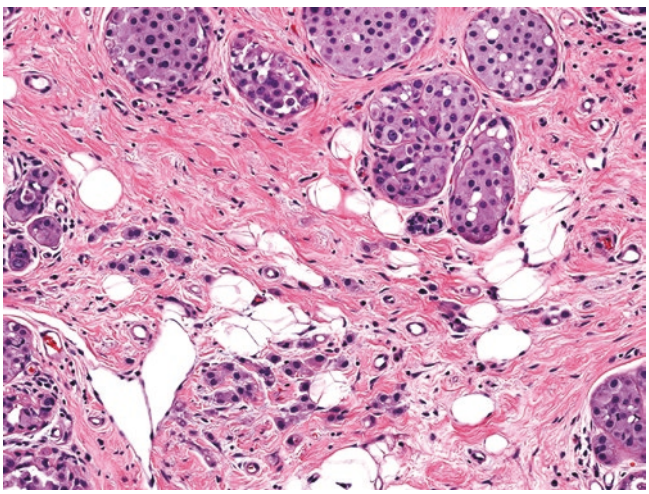

Fig. 10.36 Microinvasive lobular carcinoma (*center left*) associated with pleomorphic LCIS

diagnosis of MIC or suspicious for microinvasion were truly MIC [110]. Diagnosing MIC on CNB is of particular importance because of the implications for further management (discussed in the section "Prognosis").

Differential Diagnosis

Lesions that can mimic MIC or small invasive carcinoma in a CNB include lobular involvement by DCIS (cancerization of lobules), branching or budding ducts of DCIS distorted by fibrosclerosis, and sclerosing lesions including adenosis or radial scar involved by DCIS (Figs. 10.40, 10.41, 10.42, 10.43, and 10.44). This can be particularly challenging in a CNB where the underlying lesion, e.g., sclerosing adenosis, may not be present or apparent due to limited material. MIC should be cautiously diagnosed in limited samples unless it

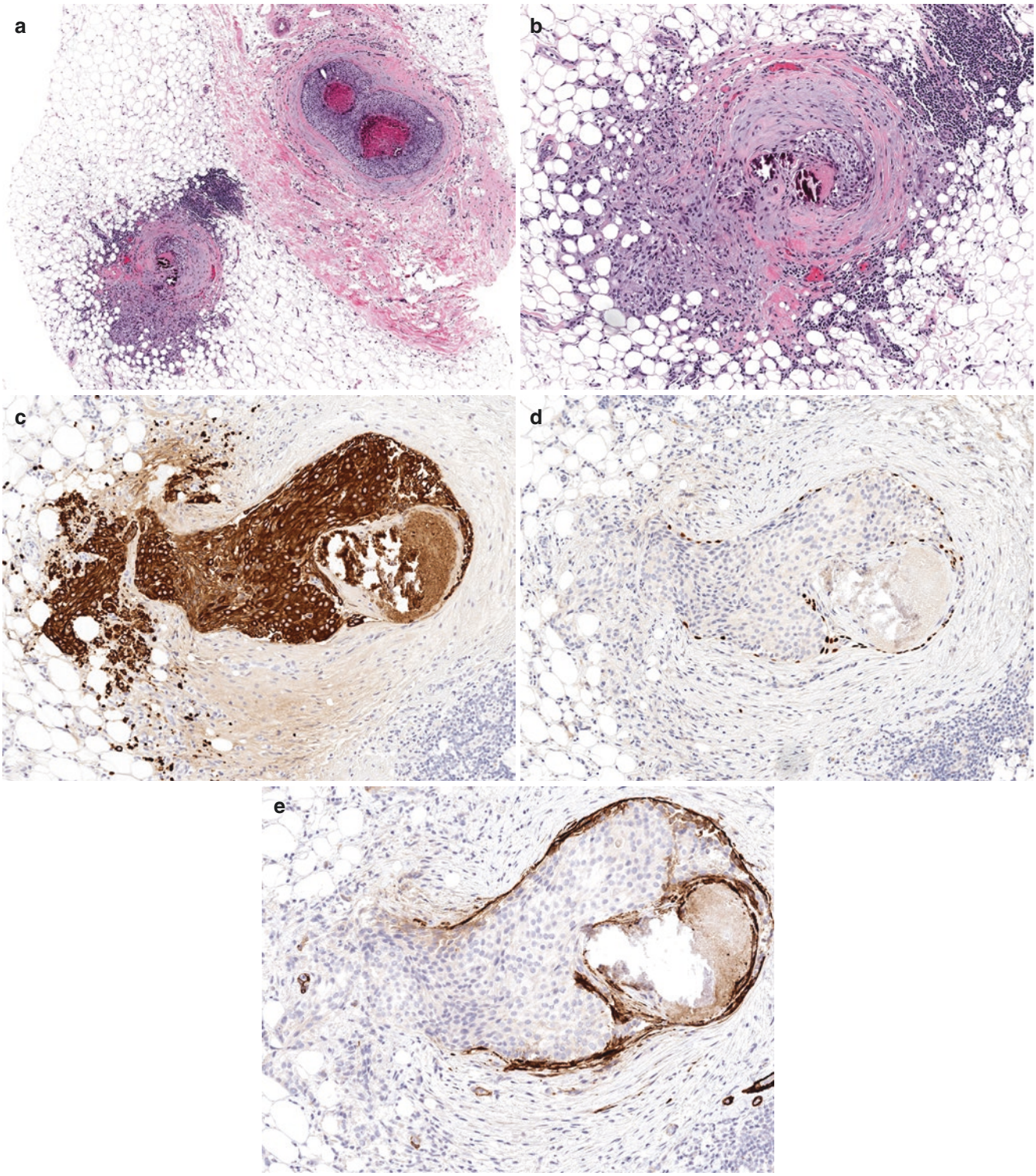

Fig. 10.37 DCIS with microinvasion. (**a**) Low-power view shows DCIS associated with marked periductal fibrosis and inflammation extending into the fat (*lower left*). (**b**) Higher power view shows the duct with disrupted wall but the presence of microinvasive carcinoma is difficult to discern. (**c**) Cytokeratin stain highlights the single cells dispersed in the fibrotic and inflammatory stroma. (**d**) Immunostain for p63 shows myoepithelial cells surrounding portion of the DCIS but absent in microinvasive carcinoma. (**e**) SMM shows similar pattern with loss of myoepithelial cells in the microinvasive focus

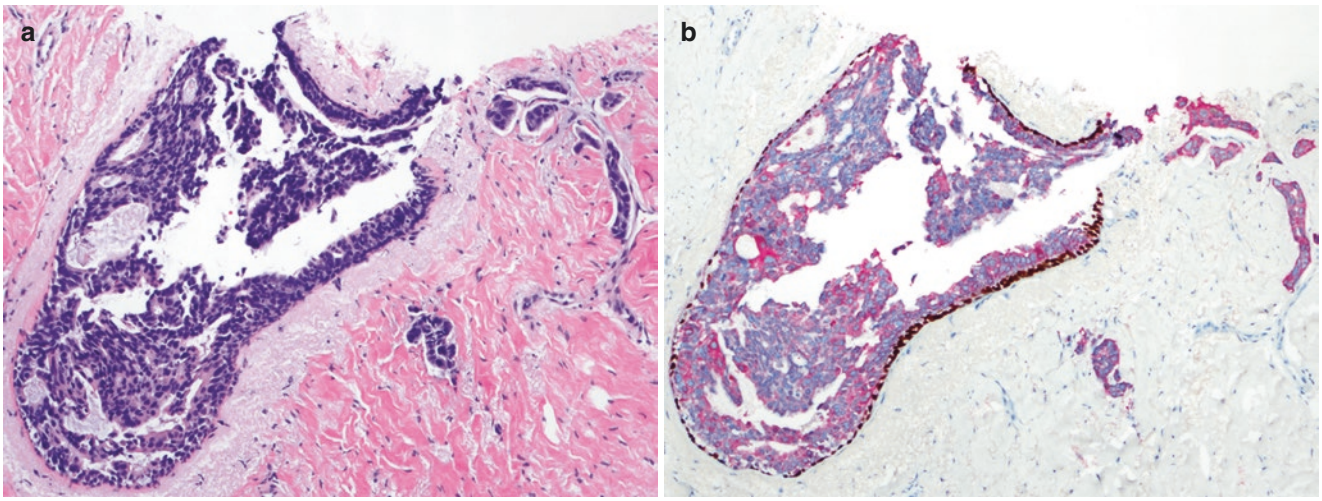

Fig. 10.38 Microinvasive carcinoma in a core needle biopsy adjacent to DCIS. (**a**) H&E section demonstrates stromal retraction around the invasive tumor nests. (**b**) Double IHC stain for p63 (brown chromogen) and cytokeratin (red chromogen) shows complete lack of myoepithelial staining around MIC

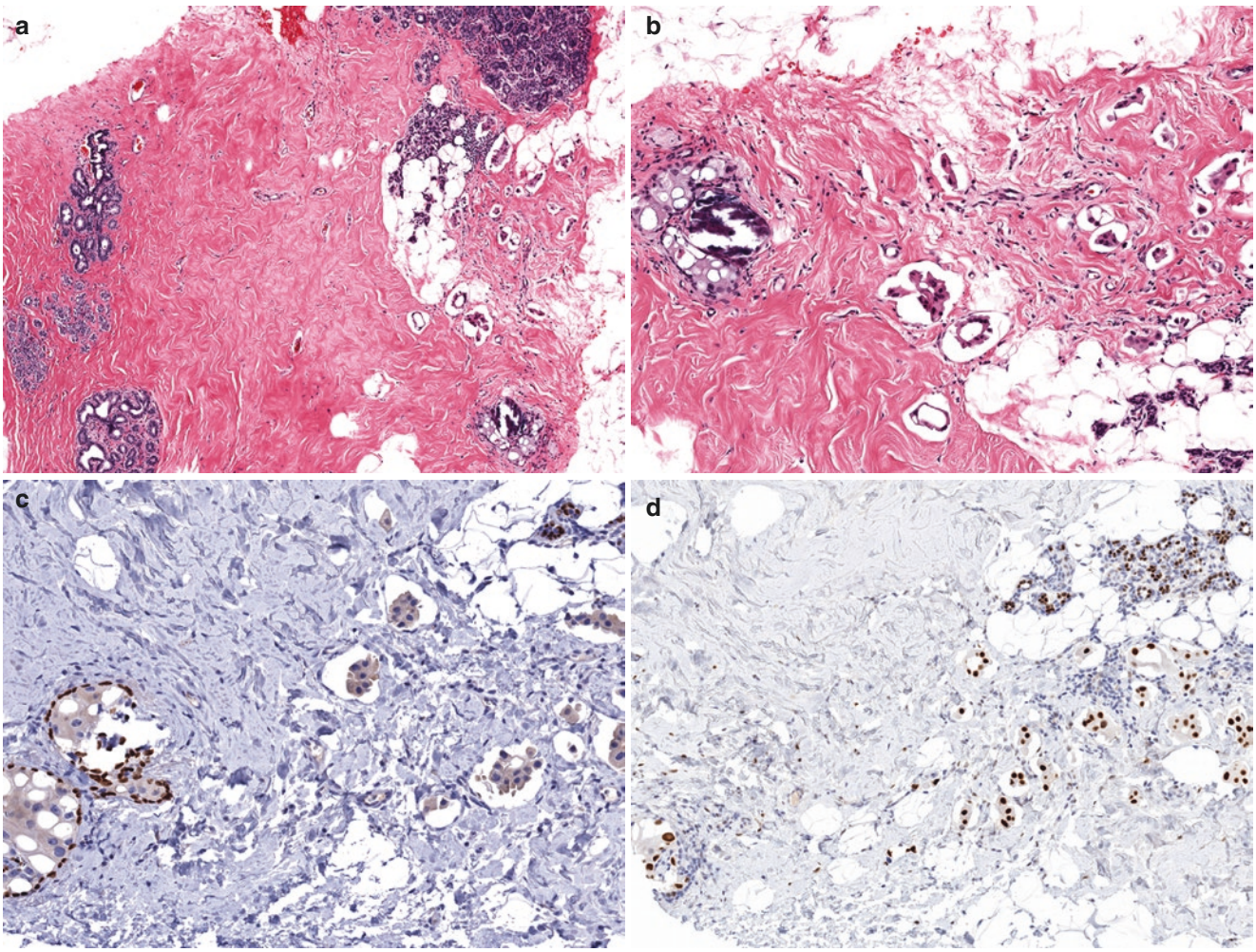

Fig. 10.39 Microinvasive carcinoma with marked retraction artifact. (**a**) Core needle biopsy with microinvasion and a small focus of DCIS with associated calcification. (**b**) High-power view highlights stromal retraction around the invasive tumor nests. (**c**) Immunostain for p63 shows lack of myoepithelial cells in microinvasive focus (*right*) while DCIS retains positivity (*left*). (**d**) Microinvasive carcinoma as well as DCIS are positive for estrogen receptor immunostain

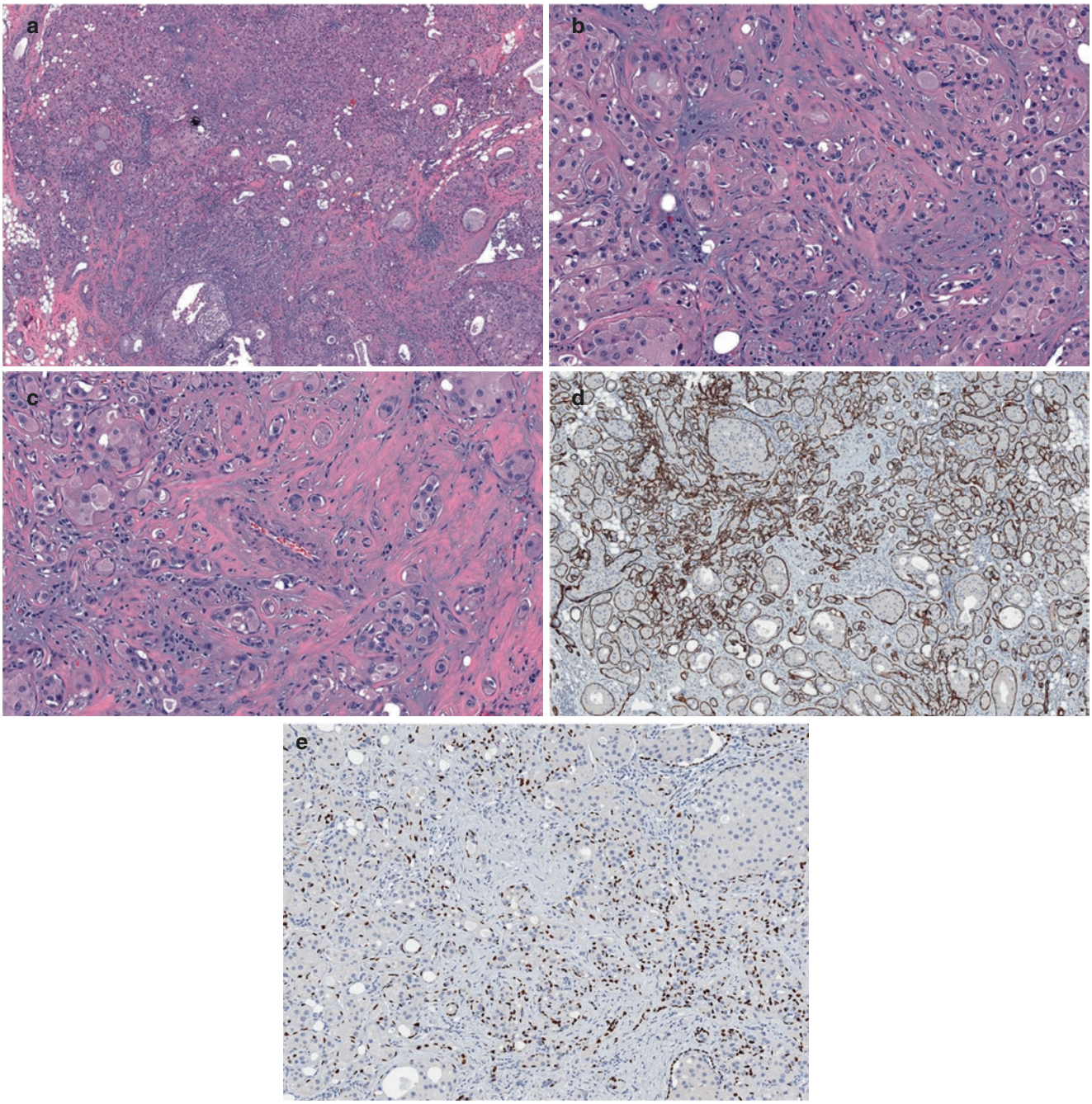

Fig. 10.40 Mass-forming DCIS. (**a**) Low-power and (**b**, **c**) high-power magnifications of different areas of the tumor consisting of sclerosis and entrapped cancerized lobules mimicking invasive carcinoma. (**d**) Immunostains for SMM and (**e**) p63 highlight intact myoepithelial cells throughout the lesion including sclerosing areas

is unequivocal. If the suspected microinvasive focus is depleted on myoepithelial immunostains or the immunostains are inconclusive, a diagnosis of "DCIS, suspicious for microinvasion" with an explanatory note is recommended.

One pitfall unique to excision specimens is the artifactual displacement of epithelial cells into the stroma, introduced at the time of a CNB or fine-needle aspiration. These embedded epithelial clusters can mimic MIC, particularly if the displaced cells are neoplastic (Fig. 10.45). Displaced epithelium can occur after a CNB for DCIS where neoplastic cells are easily dislodged [111, 112]. Microscopic clues including associated reparative fibrosis, fat necrosis, recent hemor-

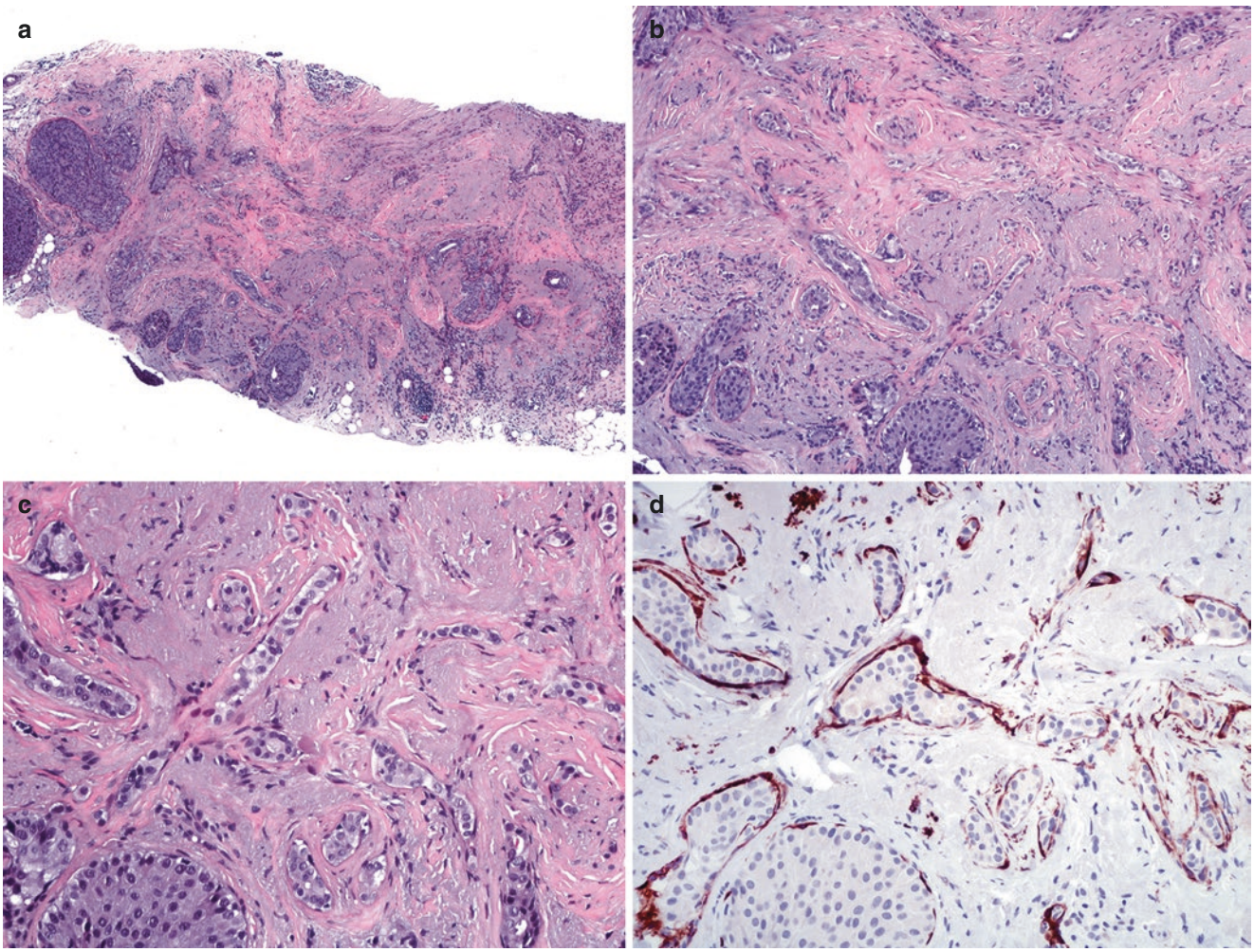

Fig. 10.41 Radial scar involved by DCIS. (**a**) Low-power view of CNB containing a sclerosing lesion, (**b**) center of the radial scar with elastosis and entrapped ducts and lobules involved by neoplastic cells. (**c**) Medium power view shows elongated entrapped neoplastic ductules. (**d**) SMM immunostain shows intact myoepithelial cells around entrapped ductules

rhage, or hemosiderin-laden macrophages in a previous core biopsy tract should make the pathologist to consider a diagnosis of epithelial displacement rather than invasive carcinoma [112]. Immunohistochemical stains for myoepithelial cells are only helpful in rare cases of displaced non-high-grade DCIS or benign entity where myoepithelium is still retained in the epithelial clusters. The absence of myoepithelium evidenced by negative staining, however, does not exclude the possibility of displaced epithelium.

Immunohistochemistry

As with any IBC, the most useful immunostains to confirm a diagnosis of MIC are those for myoepithelial cells. In addition, cytokeratin can be helpful, particularly in cases of DCIS with marked lymphocytic infiltrate, as it highlights single cells and small epithelial clusters of MIC (Fig. 10.37). Ideally, MIC is easier to confirm if double IHC staining for myoepithelial cells and cytokeratin is available (Fig. 10.38). Immunostains for basement membrane such as collagen type IV and laminin are not necessary and further can be difficult to interpret.

Due to the small size of MIC, residual MIC may not be present on subsequent stains for ER/PR/HER2 analysis. In many cases, however, the adjacent DCIS shows identical expression of these markers, and some may use this as a surrogate [113]. Cases of high-grade DCIS with MIC are often ER/PR negative and HER2 positive (Fig. 10.46).

The limited amount of invasive tumor available for IHC assessment underscores the importance of anticipating the stains needed and proceeding accordingly. When MIC is sus-

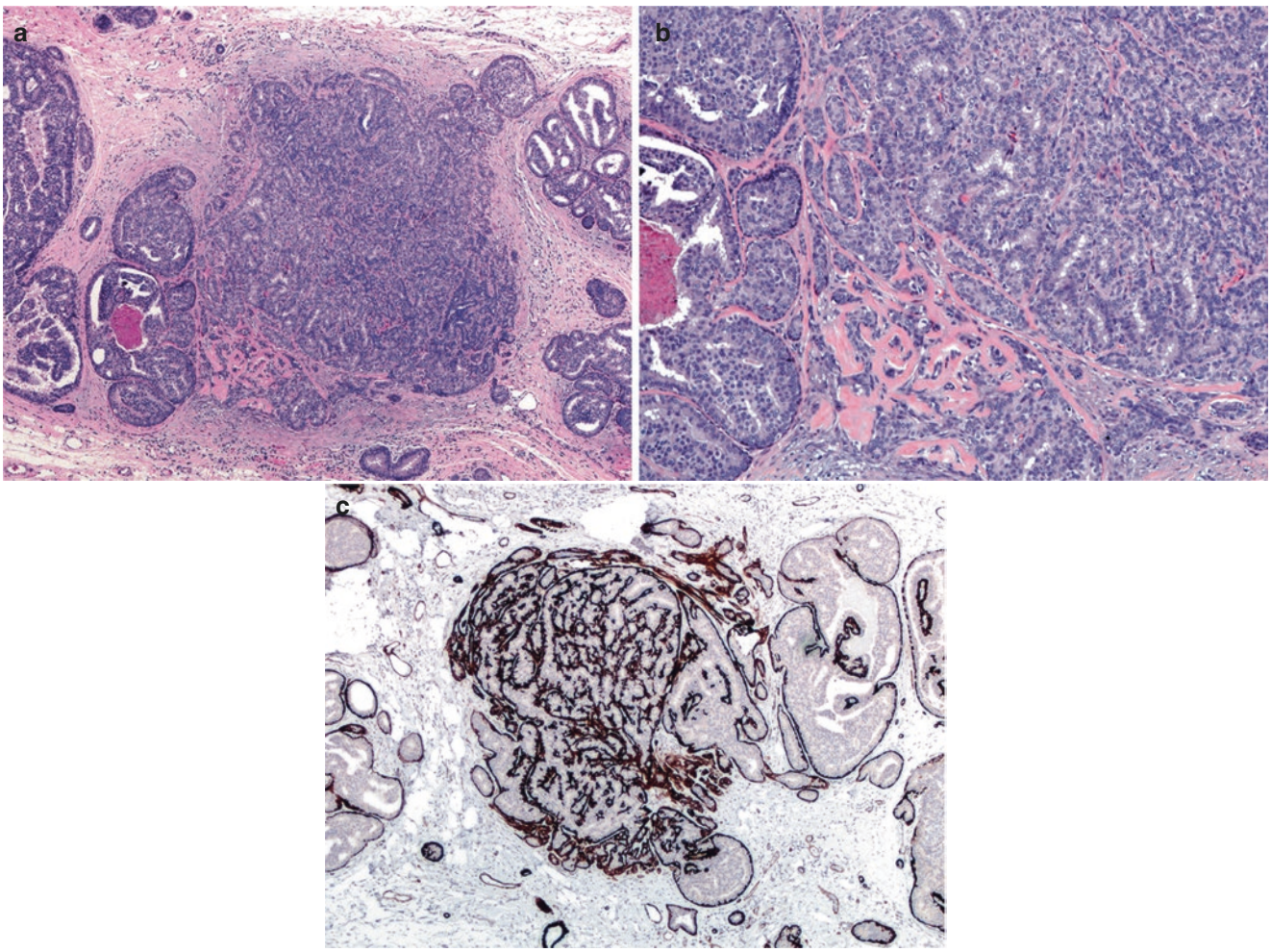

Fig. 10.42 Low-grade DCIS involving sclerosing adenosis. (**a**) Low-power and (**b**) high-power magnifications. (**c**) SMM immunostain shows intact myoepithelium

pected in a background of DCIS, performing at least two myoepithelial stains, a cytokeratin stain, ER, PR, and preparing at least three unstained slides for possible subsequent HER2 immunostain and HER2 FISH, with instructions that they all be cut from the paraffin block in one sitting is recommended. Implementing a breast MIC stain protocol may be prudent.

Prognosis

Few studies have addressed the upgrade of DCIS diagnosed on CNB to microinvasive or frankly invasive carcinoma. In one study, 13 of 93 patients (14%) with DCIS diagnosed on CNB also had microinvasion and another 31 (33%) had invasive carcinoma on excision [107]. Another study of 192 patients diagnosed as DCIS on vacuum-assisted CNB reported 10% and 29% upgrade to microinvasion and invasive carcinoma, respectively [114]. In the United Kingdom, 3% of DCIS cases diagnosed on CNB were upgraded to microinvasion and 18% to invasive carcinoma [115].

The incidence of sentinel lymph node metastasis in MIC is less than 5%. One meta-analysis that included 968 patients from 24 studies reported 3.2% macrometastasis (95% confidence interval (CI) 2.1–4.6%), 4% micrometastasis (95% CI 2.7–5.5%), and 2.9% isolated tumor cells (95% CI 1.6–4.6%) in MIC [116]. In addition, patients with MIC have a 0.95% risk of metastasis to non-sentinel lymph nodes as reported in one study [116]. Several studies have reported excellent prognosis in MIC irrespective of lymph node involvement [117, 118]. Disease-free survival and overall survival for patients with MIC closely resembles that of pure DCIS of equivalent size and grade [119]. The risk of distant metastasis is extremely low, ranging from 0% to 2% with a median follow-up of 4–9 years [117, 118, 120]. Another study however found the prognosis of microinvasive carcinoma to

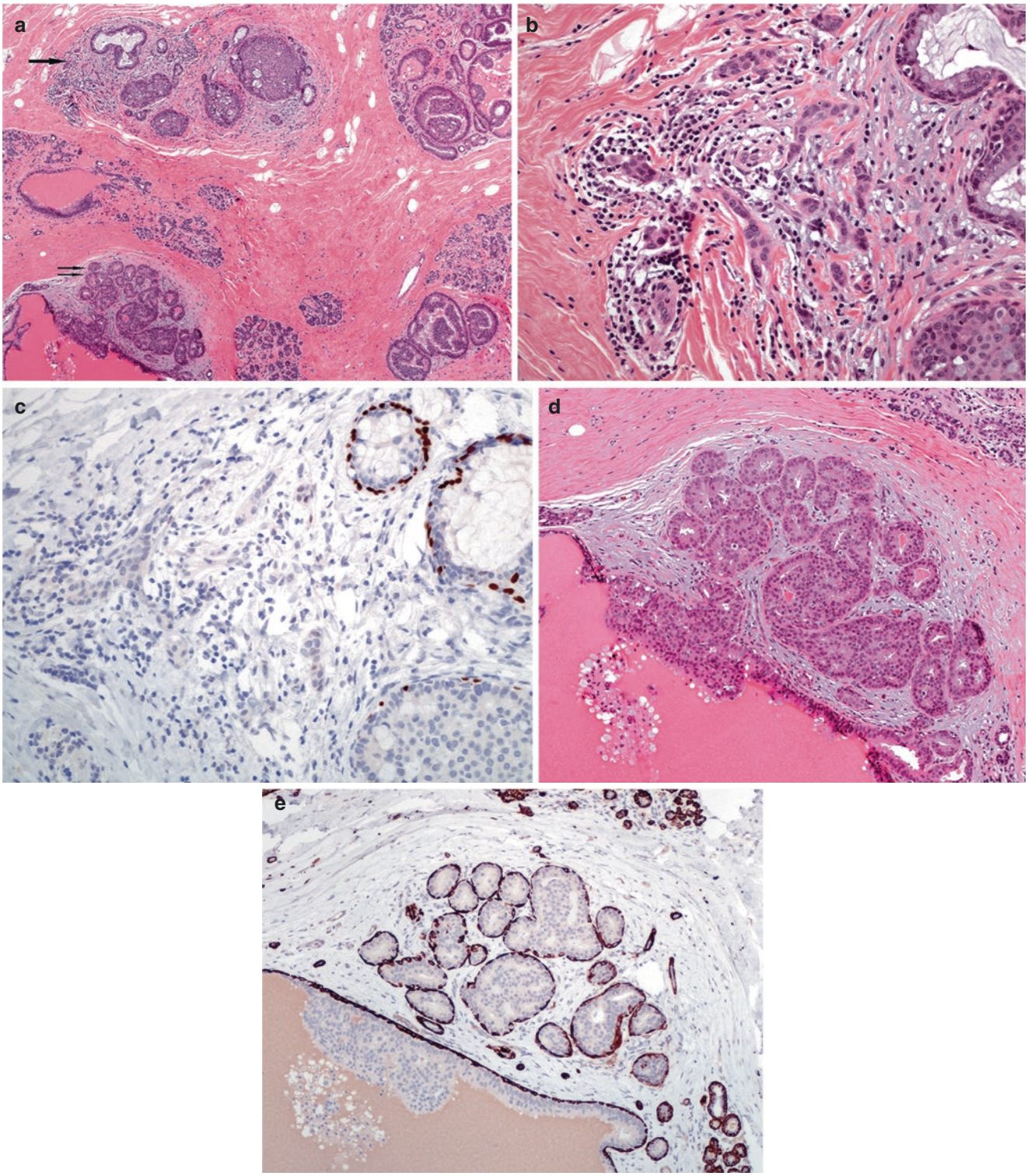

Fig. 10.43 Low-grade DCIS. Microinvasion vs cancerized lobules. (**a**) Low-power view shows microinvasion (*single arrow*) and cancerized lobules (*two arrows*). (**b**) High-power view of microinvasion. (**c**) p63 stain shows lack of staining in microinvasive carcinoma. (**d**) High-power view of cancerized lobules. (**e**) SMM immunostain shows intact myoepithelial cells around cancerized lobules

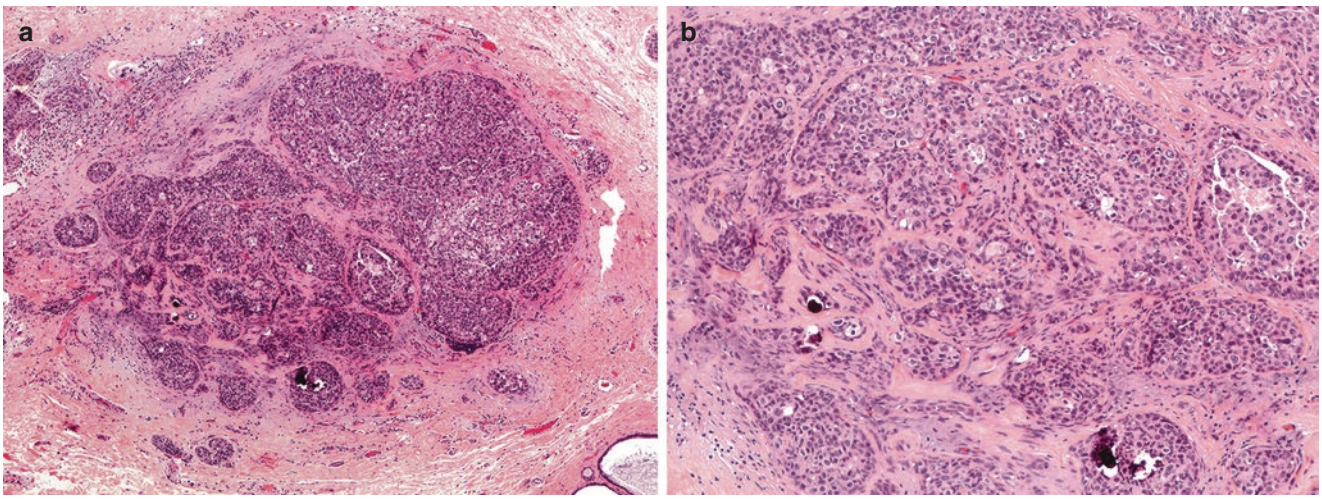

Fig. 10.44 High-grade DCIS with sclerosis. (**a**) Low-power view, (**b**) high-power view reveals the smooth outline of pink basement membrane around the distorted lobules which can be helpful if present

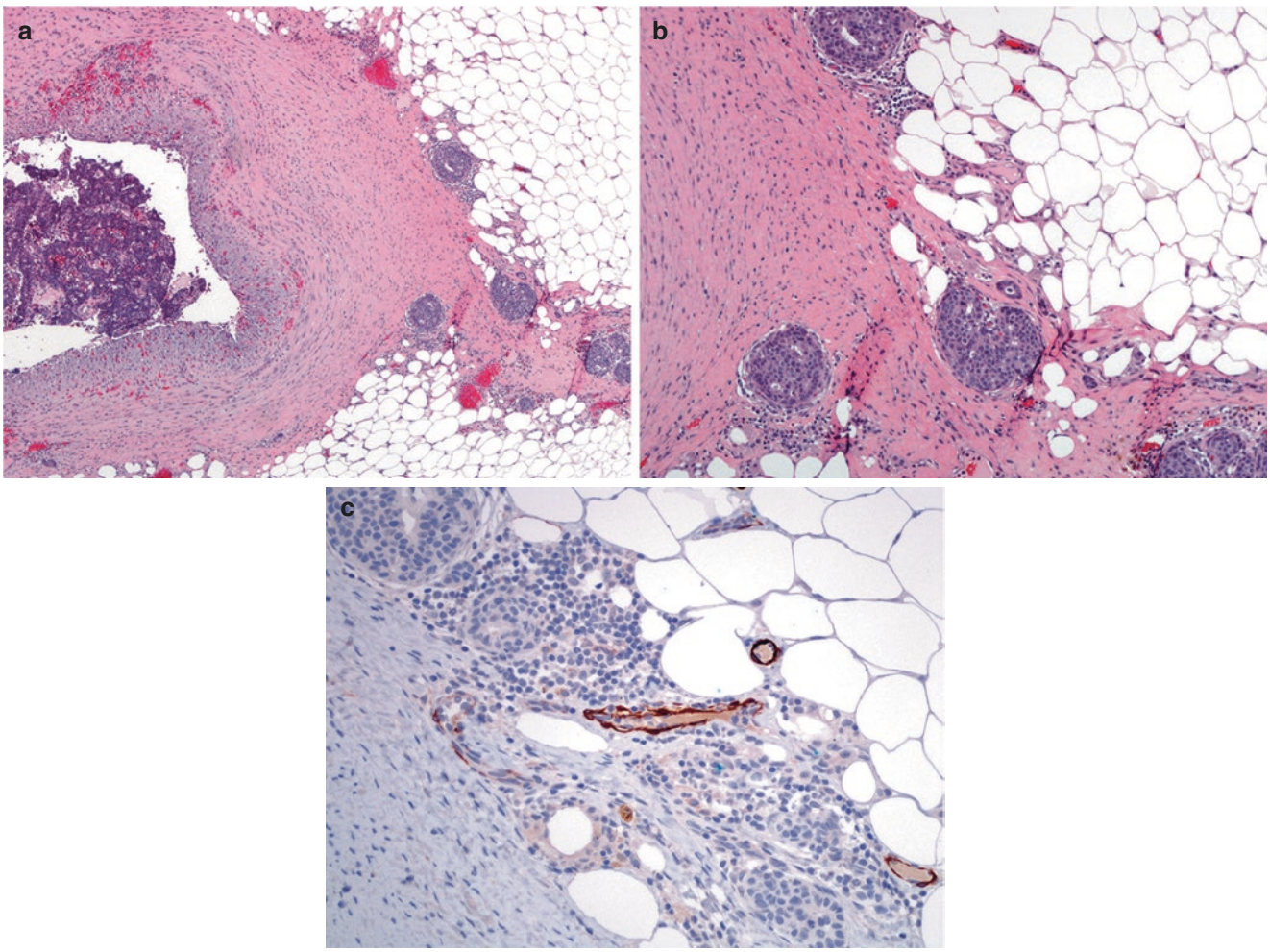

Fig. 10.45 Displaced neoplastic cells from a prior core biopsy of an encapsulated papillary carcinoma. (**a**) Low-power magnification shows the encapsulated papillary carcinoma and the needle tract with displaced neoplastic cells embedded in scar tissue. (**b**) High-power magnification reveals nests of neoplastic cells with associated fat necrosis. (**c**) Immunostain for SMM demonstrates lack of myoepithelial cells around the displaced nests

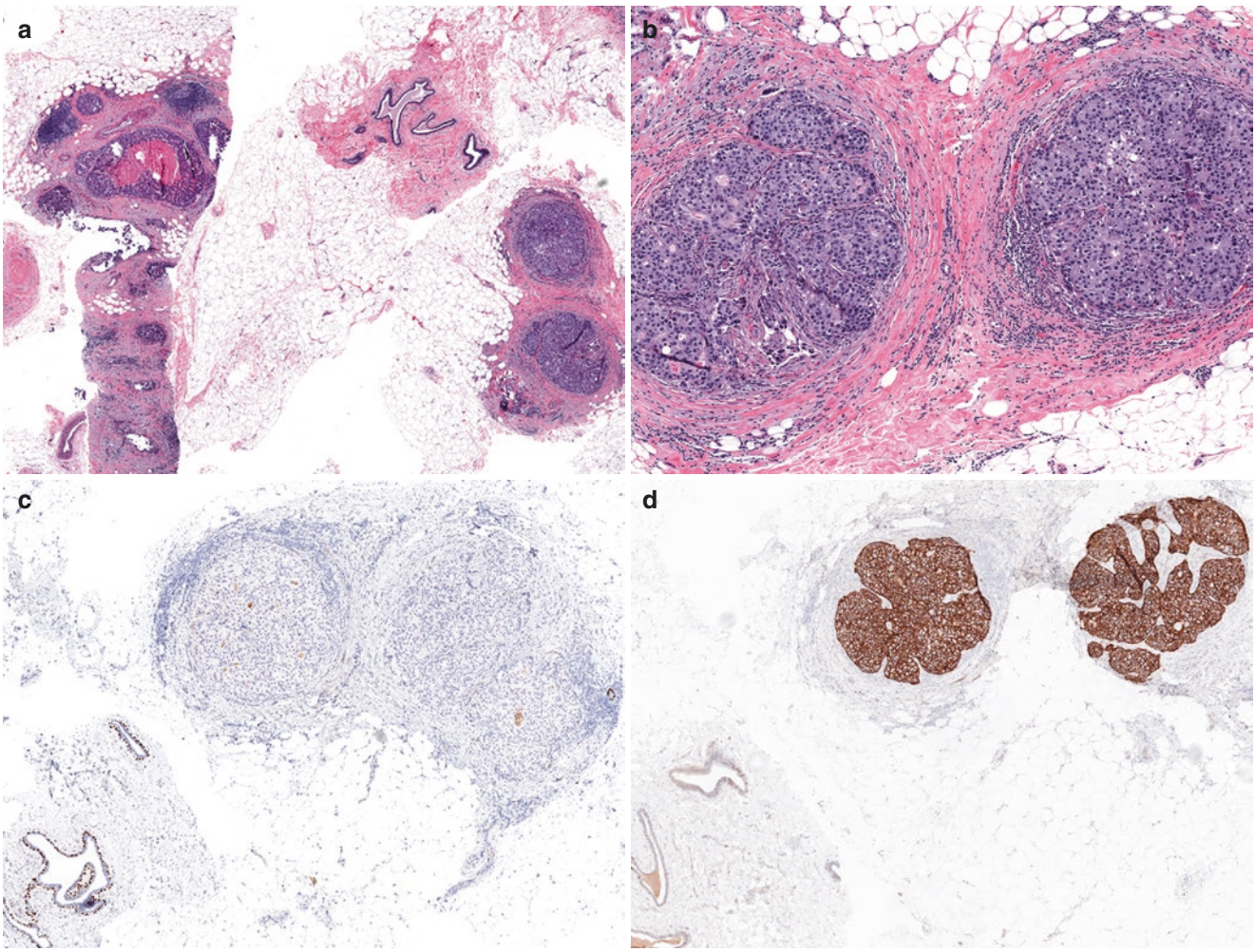

Fig. 10.46 Microinvasive carcinoma masquerading as DCIS. (**a**) Low-power view, (**b**) high-power view shows round contour in the invasive foci that can be misconstrued as in situ carcinoma. (**c**) Immunostain for SMM shows complete lack of staining in those foci. (**d**) HER2 stain shows strong positive membranous staining (3+) in MIC (both DCIS and MIC were negative for ER and PR, not shown)

resemble invasive carcinomas less than 1 cm in size while a SEER analysis found an increased mortality rate for microinvasive carcinoma versus DCIS [121, 122].

Whether sentinel lymph node biopsy (SLNB) is performed in patients diagnosed with pure DCIS or DCIS with microinvasion depends not only on whether the patient is undergoing breast-conserving surgery or total mastectomy but also on the clinical presentation and imaging findings. The 2014 *American Society of Clinical Oncology* (ASCO) guidelines recommend that SLNB be performed in cases of DCIS or DCIS with microinvasion diagnosed on CNB if mastectomy is planned as it obviates the need for subsequent axillary dissection if invasive carcinoma is found [120]. In patients undergoing breast-conserving surgery, this issue is more controversial. Some support routine SLNB because there is a 10–20% chance of an upgrade from DCIS with or without microinvasion to frank invasive carcinoma, especially when DCIS is large (≥5 cm), DCIS presents as a mass lesion by imaging and/or on physical examination, or high-grade DCIS is associated with comedonecrosis [123, 124].

Tubular Carcinoma

Overview

Tubular carcinoma is a well-differentiated invasive carcinoma with distinct morphologic features and an excellent prognosis. It is rare, often reported to comprise less than 2% of all IBC [125–128]. Most women are diagnosed in their late 50s or early 60s [127, 129–131]. SEER data shows that the majority of tubular carcinomas occur in non-Hispanic white women (90%), followed by African-American (3.6%), Asian/Pacific Islanders (3.5%), Hispanic white (2.3%), and American Indian/Alaska Native (0.5%) women [132]. Tubular carcinoma is also rare in men [133]. Tubular carci-

noma can be multifocal with one study finding 10 of 103 patients with pure tubular carcinomas having multiple foci ranging from 2 to 5 in number [134].

Gross and Radiologic Features

On mammogram, tubular carcinoma appears as a round, oval or lobulated, dense mass with irregular or spiculated margins, occasionally accompanied by microcalcifications [135, 136] (Fig. 10.47). Imaging findings are nonspecific and can overlap with patterns seen in sclerosing adenosis, radial scar, or IBC-NST [137, 138] (Fig. 10.48). Widespread mammographic screening has led to an increased incidence of tubular carcinomas as it detects non-palpable tumors (1 cm or less in size); small, incidental tumors are also found in biopsies performed for unrelated reasons [139–141]. Ultrasonography has been reported to be more helpful than mammography in detecting smaller-sized lesions [142] (Fig. 10.49).

Tubular carcinomas that are grossly identifiable are indistinguishable from other IBC-NST, appearing as tan-white to gray, ill-defined, firm to hard, stellate lesions. The stellate appearance is due to extensive elastosis and desmoplasia that often accompanies this tumor. The majority of tubular carcinomas are 1 cm or less, but larger tumors have been described [129, 131, 143]. The largest tubular carcinoma reported in the literature is 12 cm [144]. Larger tumors however are more likely to be mixed type with an IBC-NST component, rather than pure tubular carcinomas.

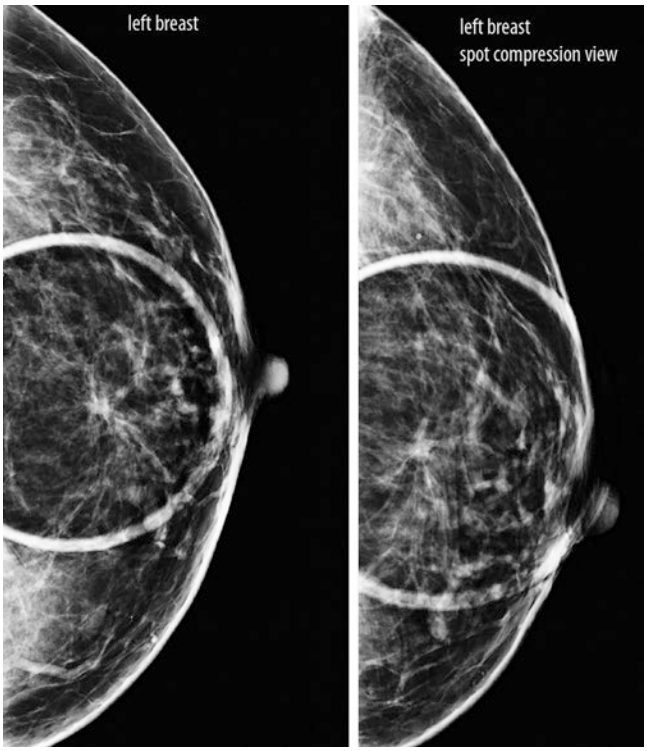

Fig. 10.47 Tubular carcinoma. Mammographic appearance of a 7 mm irregular mass with spiculated margins and associated architectural distortion seen at the 12 o'clock region that persists on spot compression view

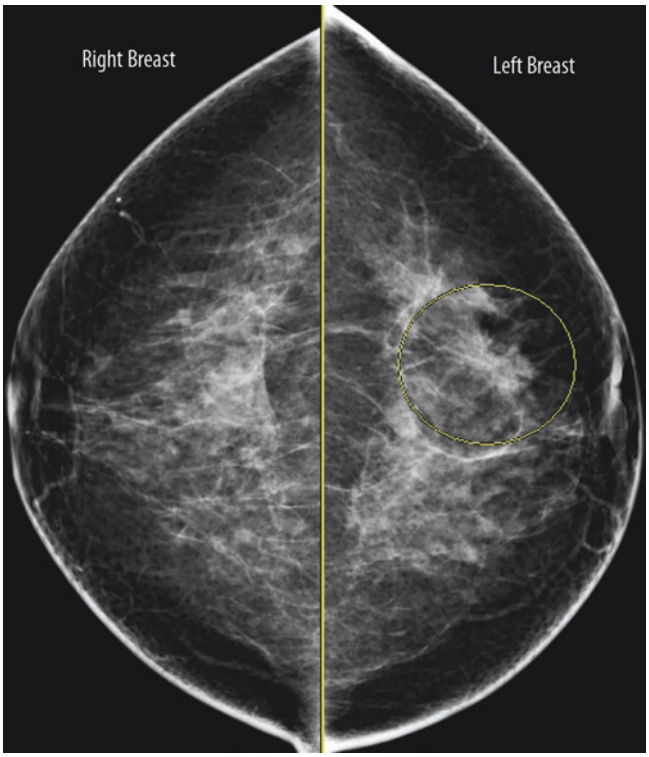

Fig. 10.48 Radial scar. Mammographic appearance of a 2.5 cm focal asymmetry (*circled*) that was interpreted as BIRADS 5, suspicious for invasive carcinoma

Fig. 10.49 Tubular carcinoma. Ultrasound of the tumor in Fig. 10.47 shows an oval hypoechoic mass

Microscopic Features

Tubular carcinoma is characterized by glands or tubules with open lumens lined by a single layer of neoplastic epithelium. In the majority of cases, the lesion is easily recognizable at low power because of the pale blue tincture of the stroma that appears different from the surrounding normal breast. The tubules are arranged in a haphazard manner, often embedded within a dense sclerotic and elastotic stroma, imparting a stellate appearance to the tumor (Figs. 10.50, 10.51, 10.52, 10.53, and 10.54). The tubules are round to oval, often angulated, lined by monotonous cuboidal to low columnar cells with eosinophilic to amphophilic cytoplasm and apical snouts (Fig. 10.55). Myoepithelial cells are absent around these tubules. The nuclei lining the tubules are low-grade, basally oriented, with evenly dispersed chromatin and inconspicuous nucleoli. Mitoses are rare. Microcalcifications are often identified in tubular carcinomas, either in the stroma, with associated benign lesions (discussed later), in associated DCIS, or in the neoplastic tubules. Lymphovascular invasion is extremely rare and necrosis is virtually non-existent.

In the past, the proportion of tubules required to classify a tumor as tubular carcinoma ranged from 75% to 100% [127,

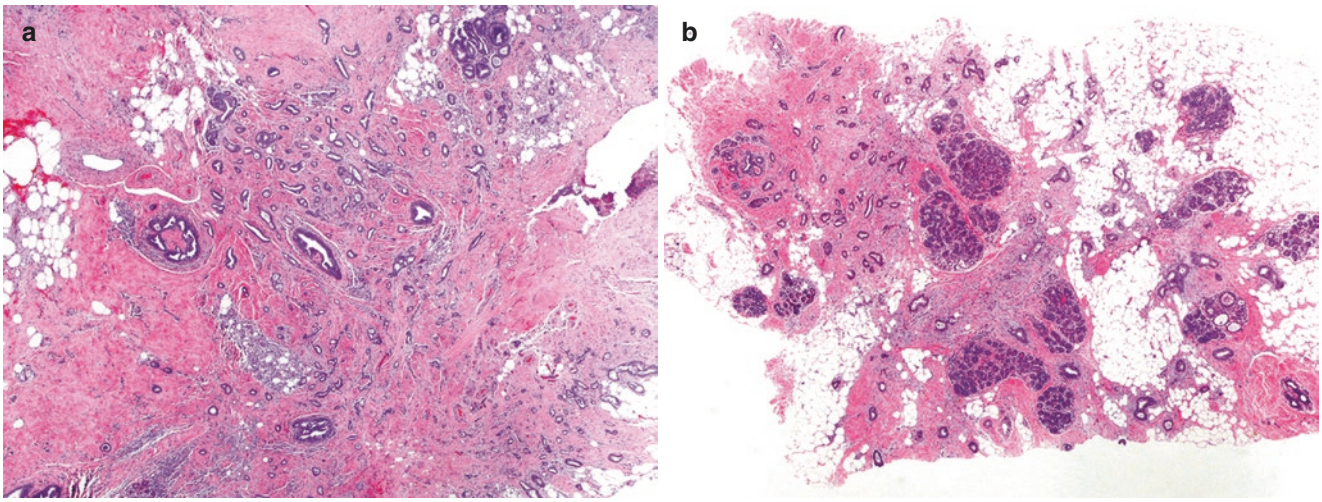

Fig. 10.50 Tubular carcinoma. (**a**) The haphazard arrangement of the tubules in a dense stroma contributes to the stellate appearance of the tumor. (**b**) Low-power view of a tubular carcinoma with pale appearing stroma

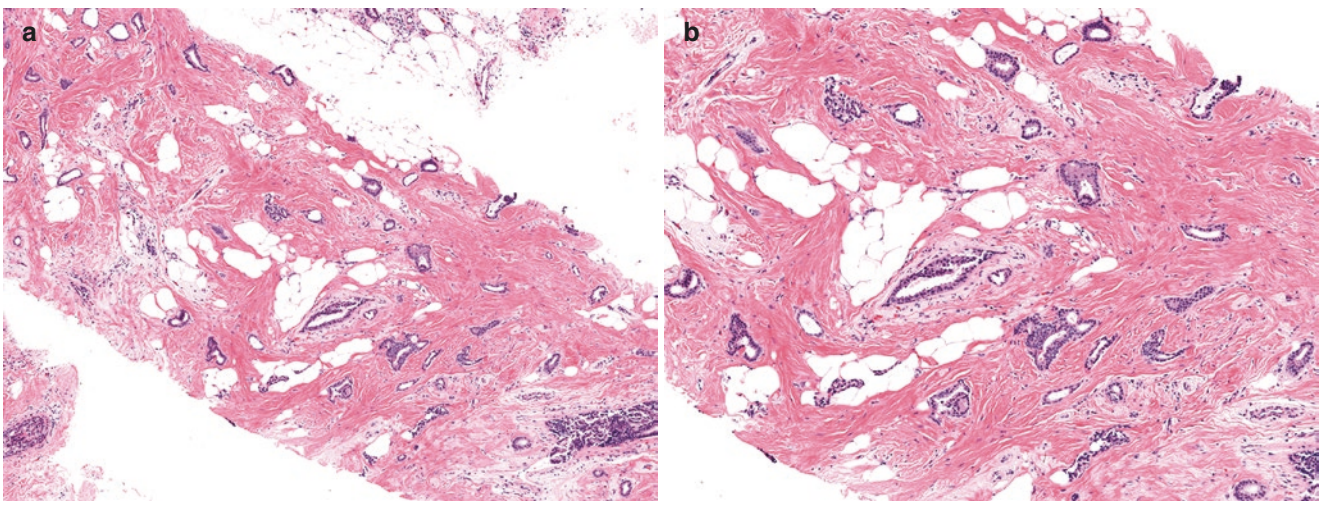

Fig. 10.51 Tubular carcinoma. (**a**) Low-power view shows the haphazard arrangement of tubules in dense stroma with focal elastosis. (**b**) High-power view shows angulated glands

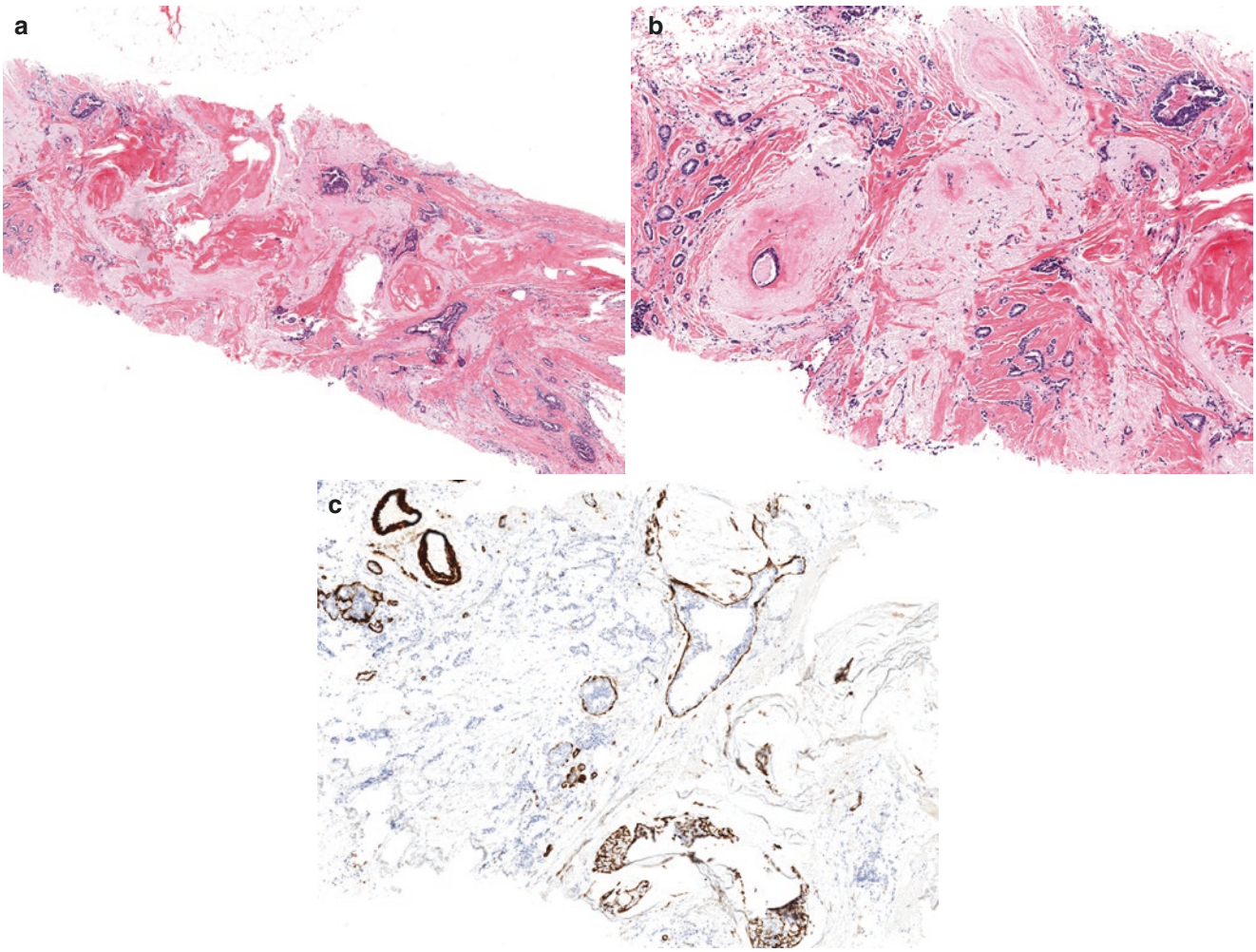

Fig. 10.52 Tubular carcinoma resembling a radial scar. (**a**) Low-power magnification shows extensive elastosis associated with neoplastic glands. (**b**) High-power magnification shows aggregates of angulated glands embedded in the stroma and a rare focus of DCIS (*upper right*). (**c**) SMM immunostain shows lack of myoepithelial staining around invasive neoplastic glands

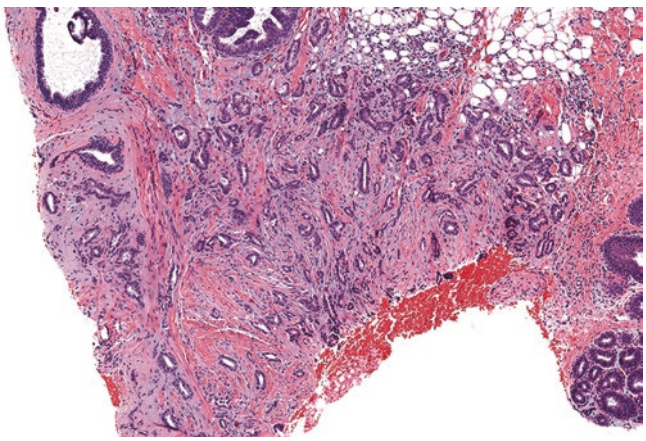

Fig. 10.53 Tubular carcinoma. Numerous angulated glands are embedded in a desmoplastic stroma with coexisting columnar cell lesion (*upper left* and *lower right*)

129, 134, 143]. Pure tubular carcinoma is currently defined as a tumor showing at least 90% tubule formation [145]. Inherently, tubular carcinoma is Nottingham histologic grade 1. In CNB samples, this assessment may not be possible in every case since only portions of the tumor are available for study. Therefore, it is recommended that such cases be reported as "well-differentiated invasive breast carcinoma with (prominent) tubular features" with a comment stating that final classification will be performed on the excisional specimen.

Tubular carcinomas are not uncommonly associated with columnar cell lesions, including FEA, and other low-grade lesions such as ADH, ALH, low-grade DCIS, and classic LCIS. The coexistence of tubular carcinomas, lobular neoplasia, and columnar cell lesions with or without atypia has been described as a "triad" or "Rosen triad" [146–148] (Fig. 10.56). Tubular carcinomas are more frequently associ-

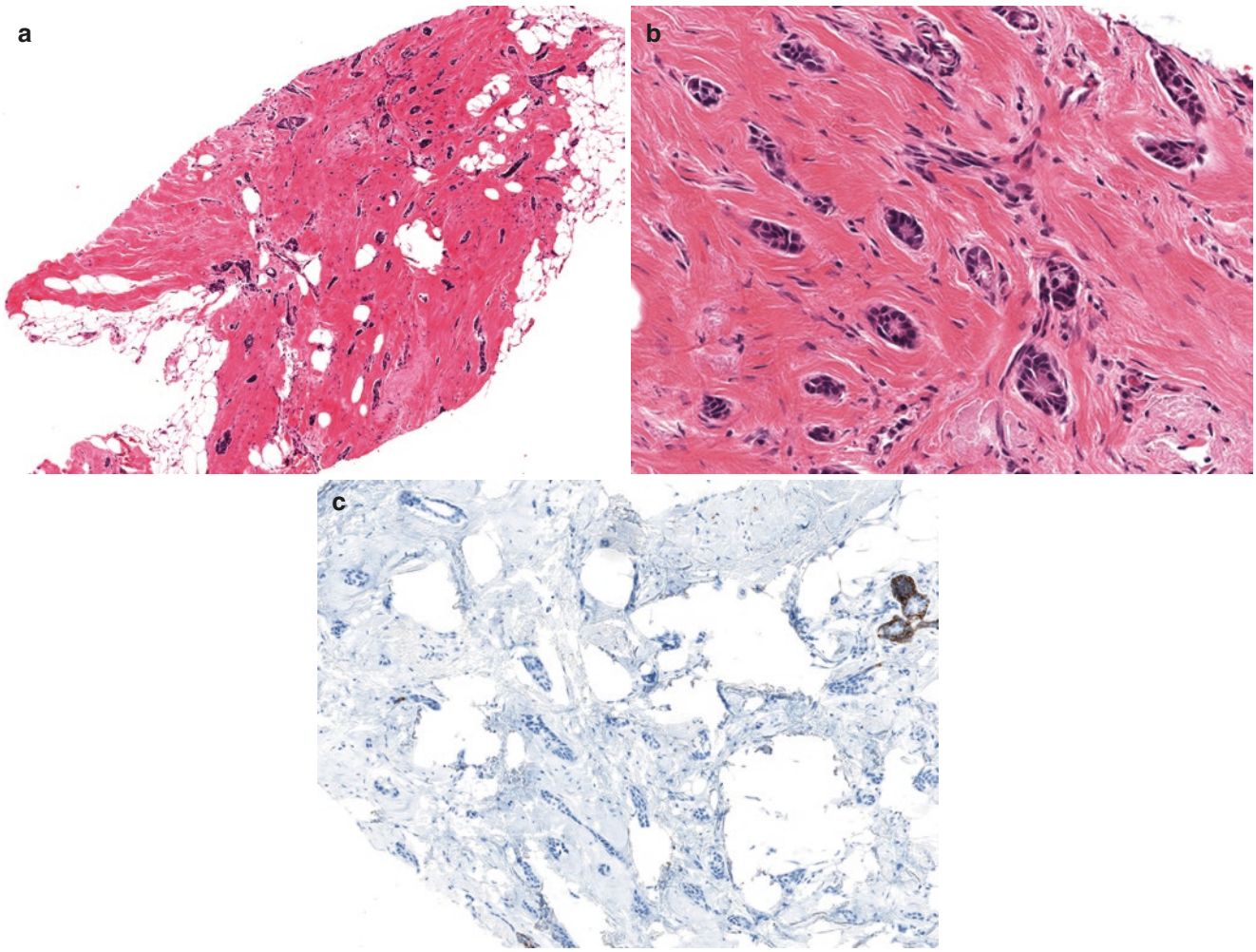

Fig. 10.54 Tubular carcinoma. (**a**) Angulated bland appearing glands of a tubular carcinoma in dense stroma mimics a benign process such as radial scar. (**b**) High-power view shows the low-grade tubular glands, some are compressed. (**c**) SMM immunostain is negative around the neoplastic tubules

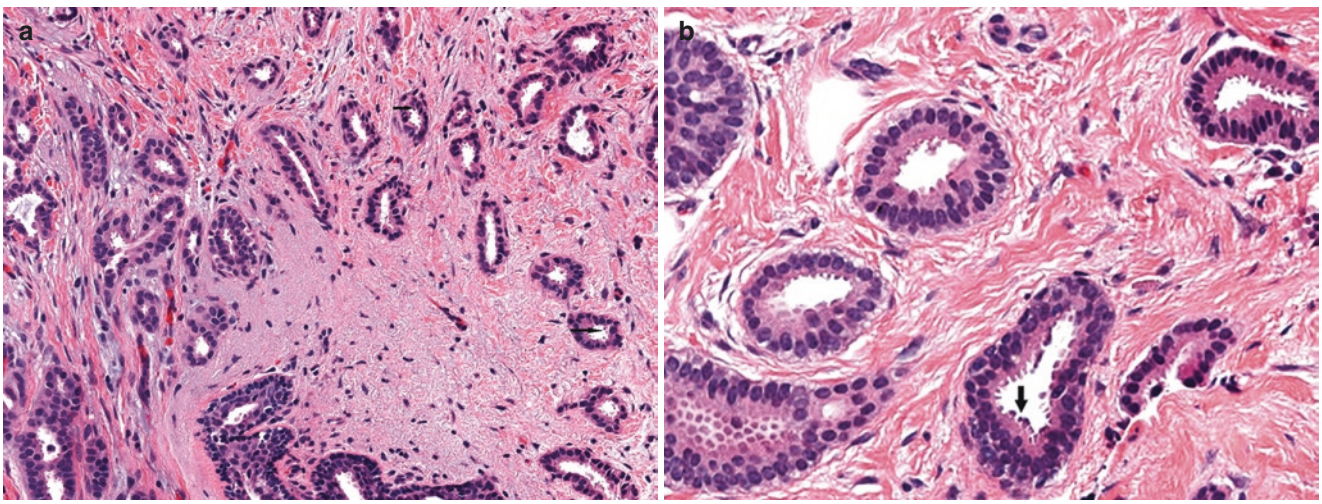

Fig. 10.55 Tubular carcinoma. (**a**) The neoplastic tubules are angular and have open lumens lined by a monolayer of low-grade neoplastic cells. (**b**) High-power view highlights the apical snouts (arrow)

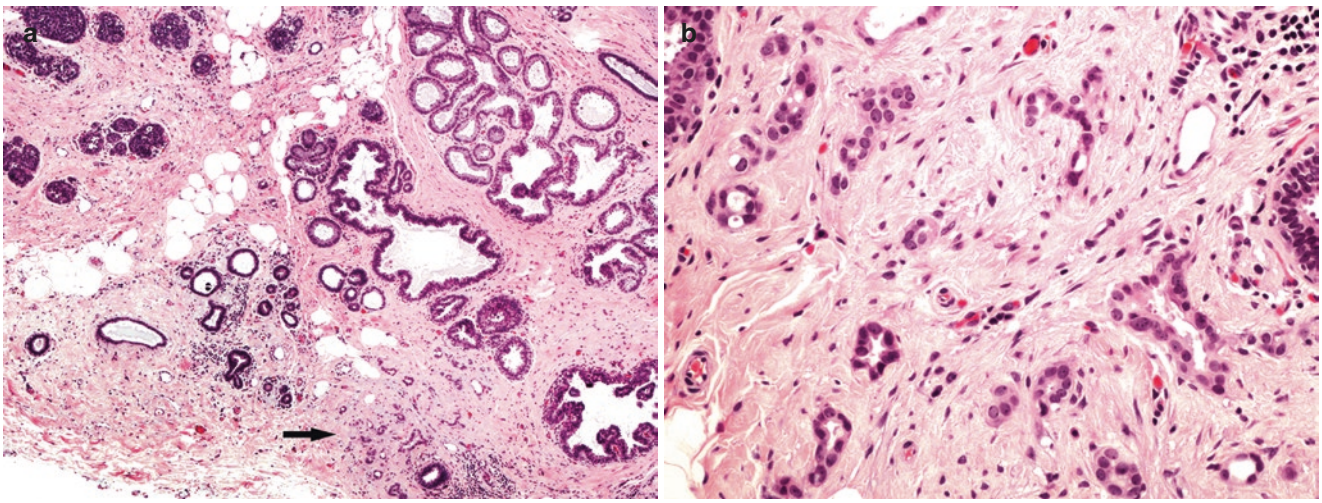

Fig. 10.56 Rosen triad. (**a**) Scanning view of an incidental tubular carcinoma (*arrow*) present in association with lobular neoplasia (*upper left*) and columnar cell lesion. (**b**) High-power magnification shows tubular carcinoma between the ductules with columnar cell change

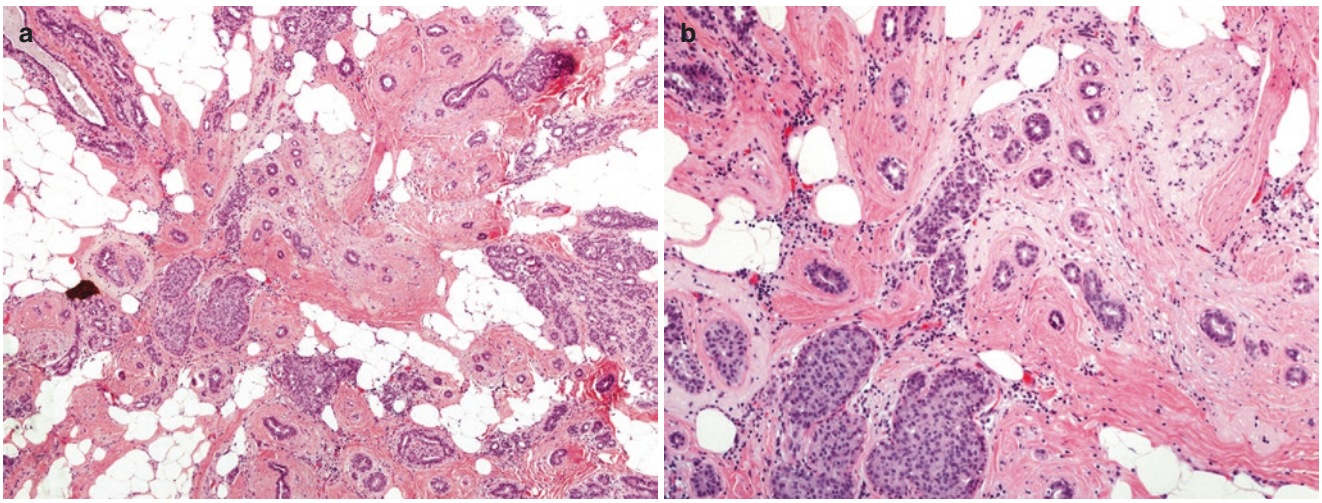

Fig. 10.57 Radial scar. (**a**) Scanning view of radial scar demonstrates a central dense nidus with entrapped glands from which the dilated ducts and ducts with epithelial proliferation radiate. (**b**) High-power magnification of the nidus

ated with columnar cell lesions (93% to almost 100%) than with lobular neoplasia (50%) or usual ductal hyperplasia (18%) [130, 148, 149]. The presence of one or more of these coexisting lesions in CNBs should prompt careful examination by the pathologist to exclude an occult tubular carcinoma.

Differential Diagnosis

The presence of small round to oval glands with bland neoplastic cells makes the diagnosis of tubular carcinoma challenging, especially in a CBN. Because of limited tissue sampling, various benign entities with similar morphologic appearance such as complex sclerosing lesions/radial scar, sclerosing adenosis, tubular adenosis, microglandular adenosis, and syringomatous tumor of the nipple-areolar region may mimic tubular carcinoma.

Complex Sclerosing Lesions/Radial Scar

Large radial scars can mimic invasive carcinoma on imaging studies and on gross examination. In excisional specimens, complex sclerosing lesions/radial scar is easier to recognize as the sclerotic or hyalinized nidus and the dilated and proliferative ducts that radiate from the nidus are seen together (Fig. 10.57). The center or nidus of a radial scar is composed

of dense stroma that often exhibits elastosis and contains entrapped benign glands that are often angulated, closely mimicking tubular carcinoma. Consequently, when the center of a radial scar is sampled in a core biopsy, it can lead to misdiagnosis (Fig. 10.58). Staining for myoepithelial markers generally resolves the dilemma in most cases, as radial scars will show positive staining for myoepithelial cells in the entrapped glands. It is worth noting that in larger or highly sclerotic radial scars, staining for myoepithelium may be absent in a few centrally located tubules but should be intact in the majority of the entrapped glands/tubules. Rarely, tubular carcinoma may involve a preexisting radial scar. One should be careful not to use this rare occurrence to overdiagnose tubular carcinoma when encountering a radial scar (Fig. 10.57).

Tubular Adenosis and Sclerosing Adenosis

The compressed, elongated, and angulated glands embedded in dense sclerotic stroma encountered in sclerosing adenosis may be mistaken for tubular carcinoma, particularly in CNBs. Examination at low-power magnification is extremely helpful as sclerosing adenosis is lobulocentric compared to the infiltrative appearance of tubular carcinoma. At higher magnification, sclerosing adenosis consists of proliferation of compact, swirled glands and tubules, which are compressed and distorted due to dense stromal proliferation, especially in the center of a lobule. At the periphery, glands are usually round and open with scant luminal secretions (Fig. 10.59). Recognizing spindled myoepithelial cells around the tubules may help to avoid misinterpretation. In challenging cases, immunostains for myoepithelial cells such as p63 or SMM can help. Smooth muscle actin (SMA) should be avoided, as it can stain adjacent stromal myofibroblasts in tubular carcinoma, leading to misinterpretation of tubular carcinoma as adenosis. Tubular adenosis is an uncommon benign non-lobulocentric lesion with an infiltrative appearance that may mimic tubular carcinoma. Depending on the plane of section, the glands may appear round or elongated (Fig. 10.60). However, myoepithelial cells and the basement membranes are intact and can be well demonstrated by appropriate IHC stains.

Microglandular Adenosis

Microglandular adenosis is a rare benign lesion composed of small, round, open glands lined by a single layer of epithelial cells without accompanying myoepithelial cells. Certain histological clues can aid in distinguishing between the two lesions. Microglandular adenosis is a diffuse lesion

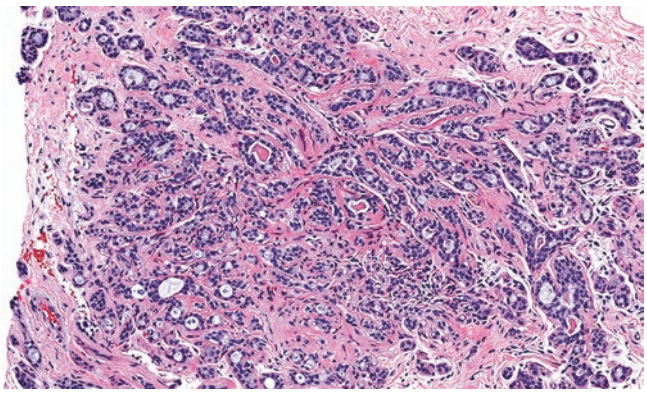

Fig. 10.59 Sclerosing adenosis superficially resembles well-differentiated invasive ductal carcinoma

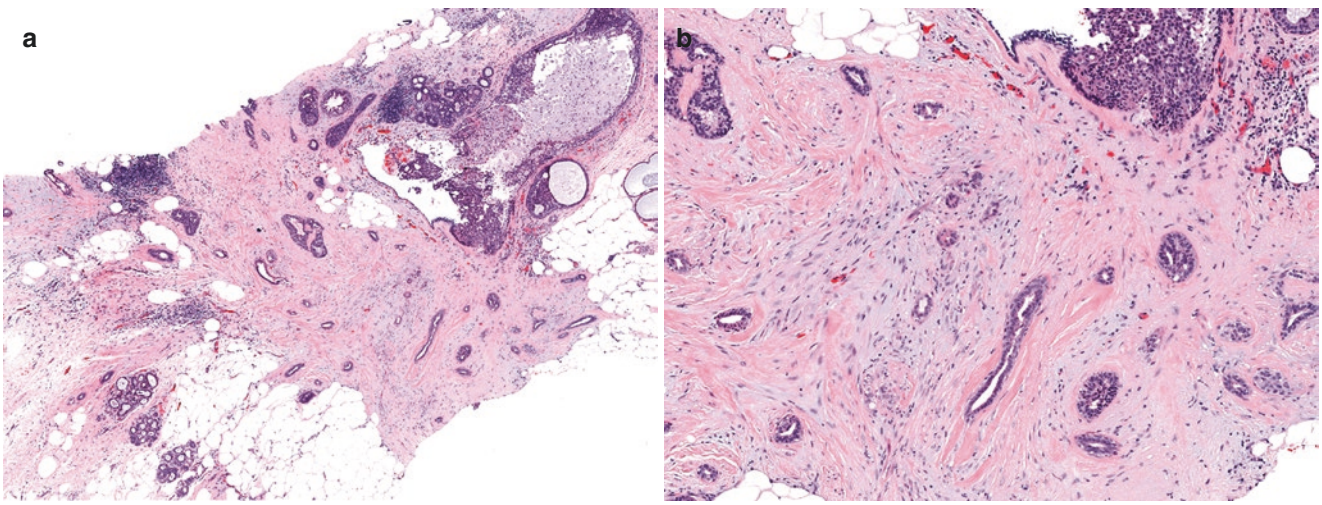

Fig. 10.58 Radial scar. (**a**) The center of a radial scar sampled in a CNB demonstrates sclerotic and elastotic stroma associated with entrapped angulated tubules and (**b**) high-power magnification shows compressed elongated and angulated tubular glands

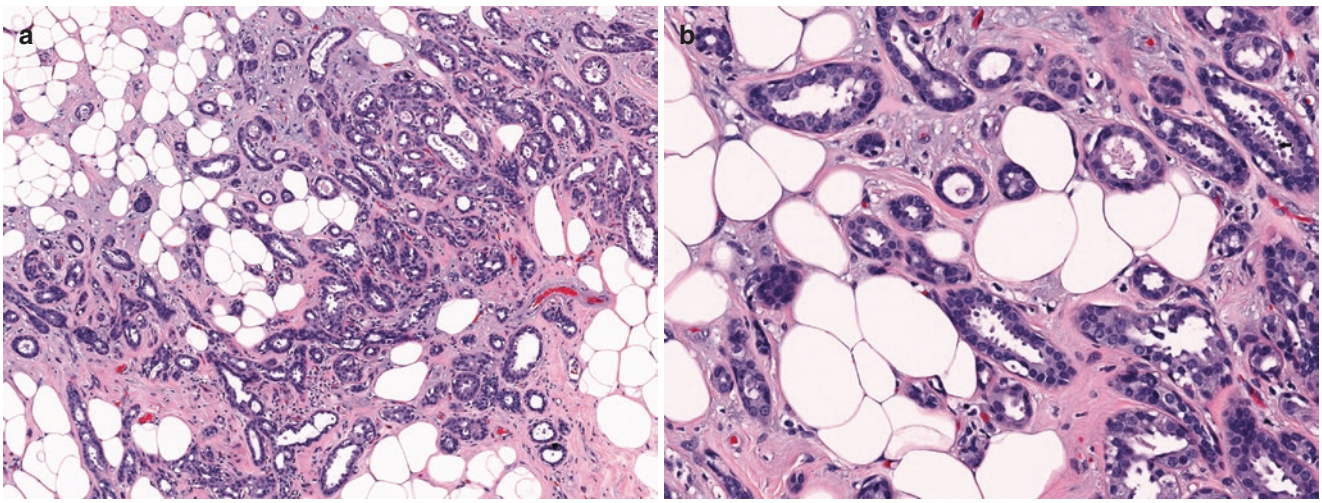

Fig. 10.60 Tubular adenosis. (**a**) Low-power view shows elongated tubular glands embedded in fibromyxoid stroma and (**b**) high-power view shows tubular glands with columnar cell change with apical snouts, myoepithelial cells, and distinct basement membrane around each tubule

with glands infiltrating haphazardly into the fibrous stroma and adipose tissue, whereas tubular carcinoma is more often localized. The neoplastic epithelium of tubular carcinoma has mild nuclear atypia and pleomorphism with apical snouts and tends to have amphophilic or basophilic secretions rather than the dense eosinophilic secretions seen in the round glands of microglandular adenosis [150]. Additionally, the stroma in tubular carcinoma is dense and elastotic whereas in microglandular adenosis the stroma is unaltered. Immunostains can be used to differentiate between these two entities, although myoepithelial stains are unhelpful as both lesions lack myoepithelial cells. The most useful stains are ER and S100 protein as tubular carcinoma is S100 protein negative and ER positive whereas microglandular adenosis shows the opposite pattern of staining. The basement membrane is intact in microglandular adenosis and can be highlighted by either reticulin, periodic acid–Schiff (PAS), or immunostain for collagen type IV or laminin (Fig. 10.61).

Syringomatous Tumor of the Nipple-Areolar Region

Syringomatous tumor is a locally infiltrative, recurring, and non-metastasizing lesion that almost always occurs in the nipple-areolar region (Fig. 10.62). In contrast, tubular carcinoma rarely occurs in the nipple-areolar region. The presence of squamous differentiation or squamous cysts, a characteristic trait of syringomatous tumor, is not seen in tubular carcinoma.

Other carcinomas that should be distinguished from tubular carcinoma are well-differentiated IBC with tubule formation, low-grade adenosquamous carcinoma, and tubulolobular carcinoma.

Well-Differentiated IBC with Tubule Formation

This tumor exhibits greater architectural complexity of its glands including branching or nesting (Fig. 10.63) or higher nuclear grade (Fig. 10.64) than tubular carcinoma.

Low-Grade Adenosquamous Carcinoma

Low-grade adenosquamous carcinoma is a rare type of metaplastic carcinoma with glandular and squamous differentiation typically distributed in a cellular or collagenized stroma. As its name states, it shows low-grade features including well-formed comma-shaped pointed glands, lined by two layers of cells that have low nuclear grade and low mitotic activity as seen in tubular carcinoma or syringomatous tumor. The key to diagnosis is appreciation of squamoid nests and the cellular stroma, particularly around neoplastic glands. Overt keratinization is not a feature. On CNB, the glandular component may predominate and be confused with tubular carcinoma. Immunostains can help, as low-grade adenosquamous carcinomas are HR negative and this lack of expression should make one question a diagnosis of tubular carcinoma. Additionally, immunostain for p63 in low-grade adenosquamous carcinoma shows intact staining around most tubules and positive staining of the squamoid nests and spindle cells (Fig. 10.65).

Tubulolobular Carcinoma

Morphologically tubulolobular carcinomas are low-grade invasive carcinomas that show an admixture of well-formed tubules and single cells arranged in cords as seen in lobular carcinoma in 75% of the tumor [151]. They tend to be HR positive and HER2 negative and are associated with a good prognosis [149, 151–154]. Most but not all examples express membranous E-cadherin, membranous p120 catenin, and

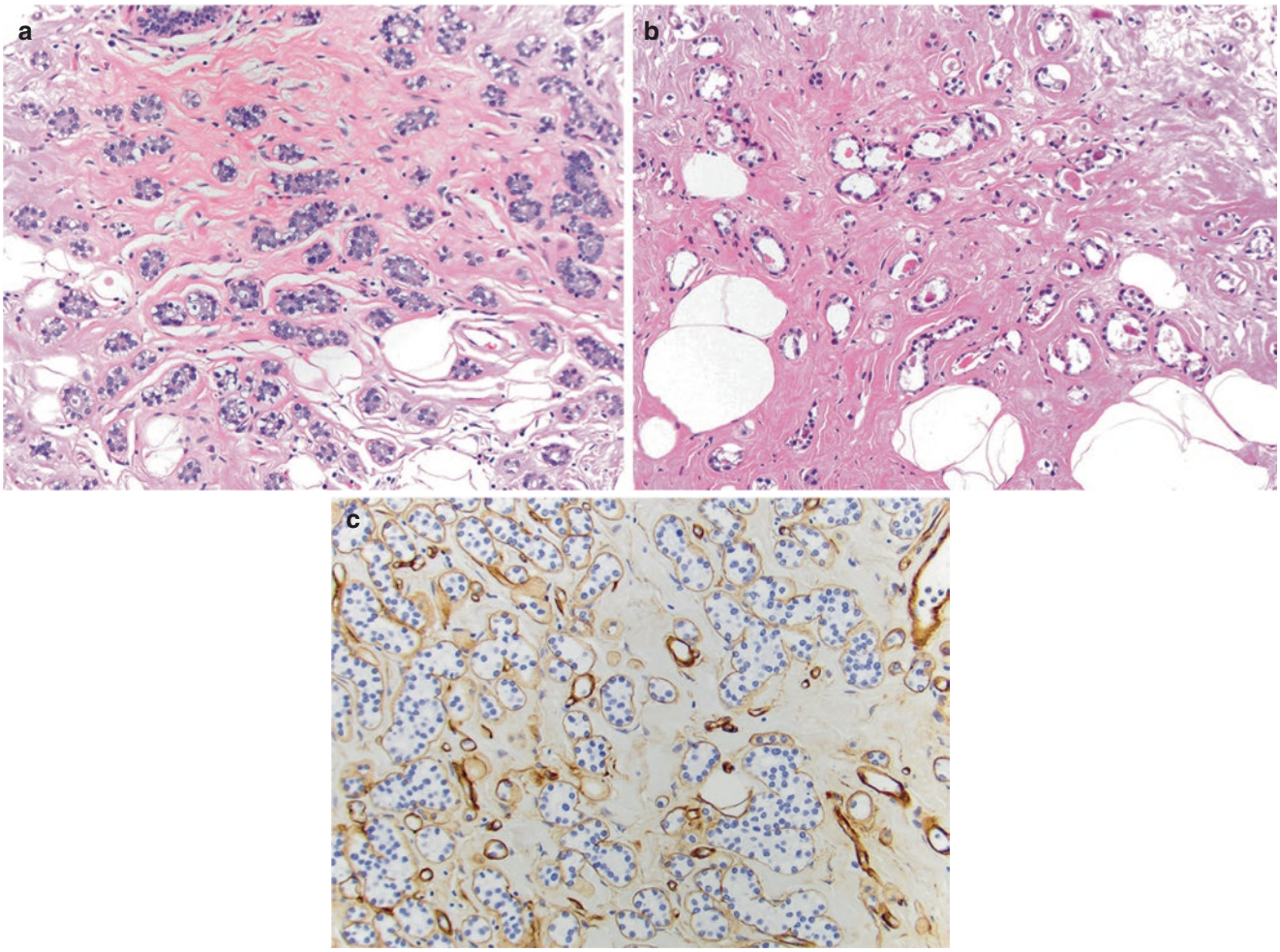

Fig. 10.61 Microglandular adenosis. (**a**, **b**) Small round open glands lined by a single layer of epithelial cells and containing bright eosinophilic secretions are distributed in the breast parenchyma without stromal alteration. (**c**) Collagen type IV immunostain demonstrates intact basement membrane while myoepithelial markers are negative (not shown)

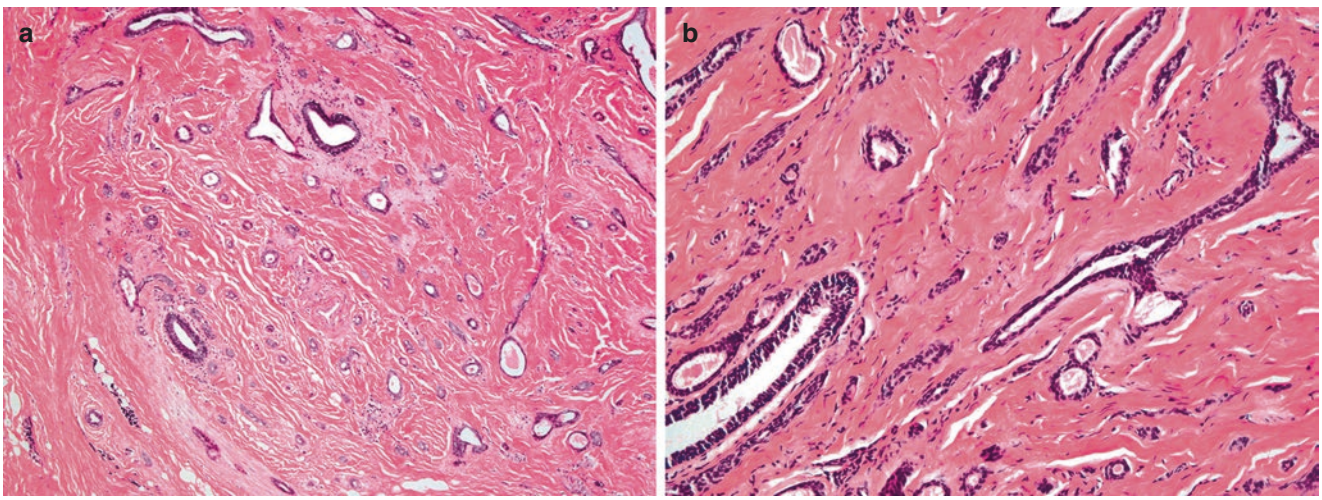

Fig. 10.62 Syringomatous tumor of the nipple. (**a**) Low-power view shows infiltration of the nipple stroma by tubules with pointed ends. (**b**) High-power view shows squamoid cysts characteristic of this entity

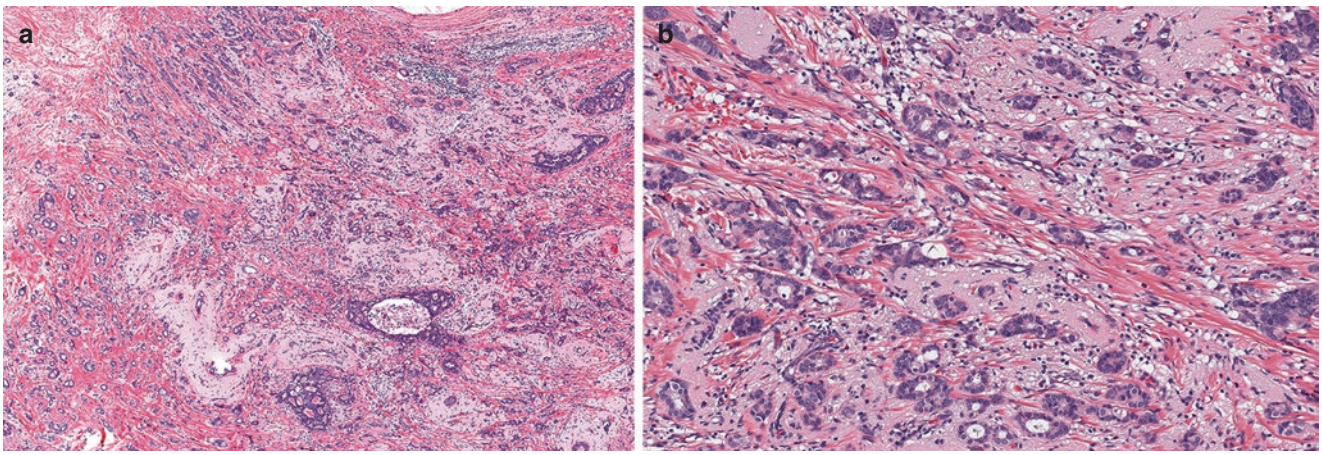

Fig. 10.63 A well-differentiated invasive breast carcinoma NST with predominant tubule formation. (**a**) Low-power and (**b**) high-power magnifications

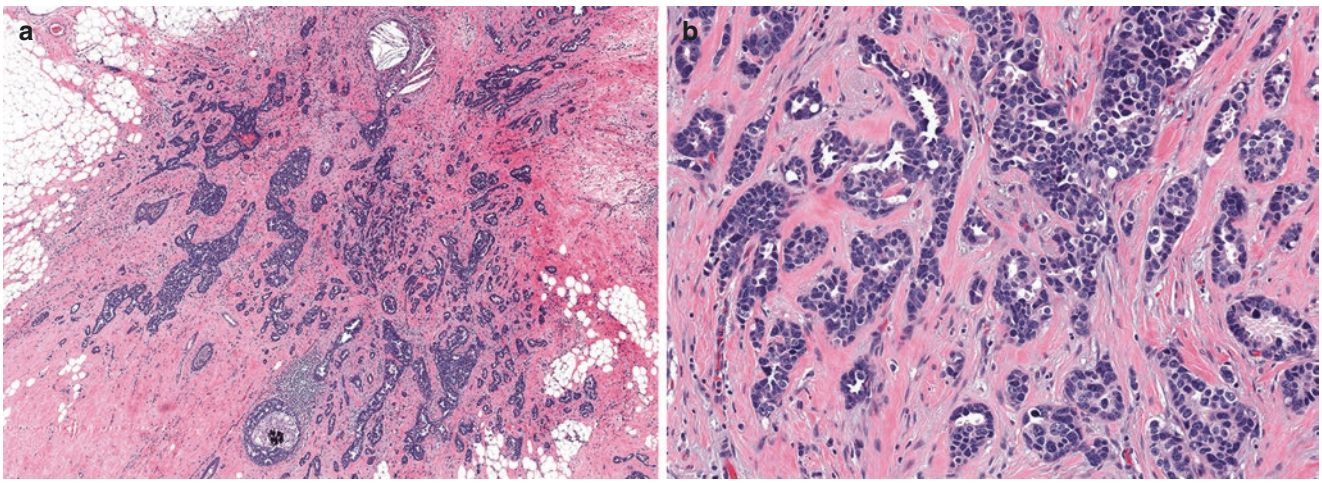

Fig. 10.64 A moderately differentiated invasive breast carcinoma NST. (**a**) Low-power view shows predominant tubule formation with minor component of solid nests of cells but (**b**) high-power view reveals tubular glands with high nuclear grade and focal intraluminal necrosis

beta-catenin staining and accordingly are grouped with ductal rather than lobular carcinomas [151, 152, 155]. Many are seen in association with lobular neoplasia, however, which most likely reflects their origins in the low-grade pathway (discussed previously). This diagnosis may not be highly reproducible as ILC can show some degree of tubule formation (Please see additional discussion of invasive carcinomas with mixed ductal/tubular and lobular morphology in Chap. 15).

Immunohistochemistry

Tubular carcinomas are invariably HR positive and HER2 negative (Fig. 10.66). ER has been reported to be positive in almost all cases, whereas 71–92% of cases have been reported to be PR positive [128–130, 156]. Rare cases of tubular carcinoma have been reported to be HER2 positive [128, 156]. If a tubular carcinoma is ER negative and/or HER2 positive, the diagnosis should be questioned and the case reviewed. The well-differentiated nature of tubular carcinoma is also reflected by a low (<10%) Ki-67 proliferation index and wild-type pattern of p53 expression [157–159].

Pathogenesis

Molecular and genetic studies have found tubular carcinoma to be distinct at the genomic level with a low level of chromosomal alterations compared to IBC-NST in general. However, tubular carcinoma and low-grade breast carcinoma appear more similar to each other than to high-grade carcinomas as both tumors show a higher frequency of 16q loss and 1q gain and lower frequency of 17p loss [160]. By gene expression profiling, the vast majority of tubular carcinomas are classified as luminal A molecular subtype,

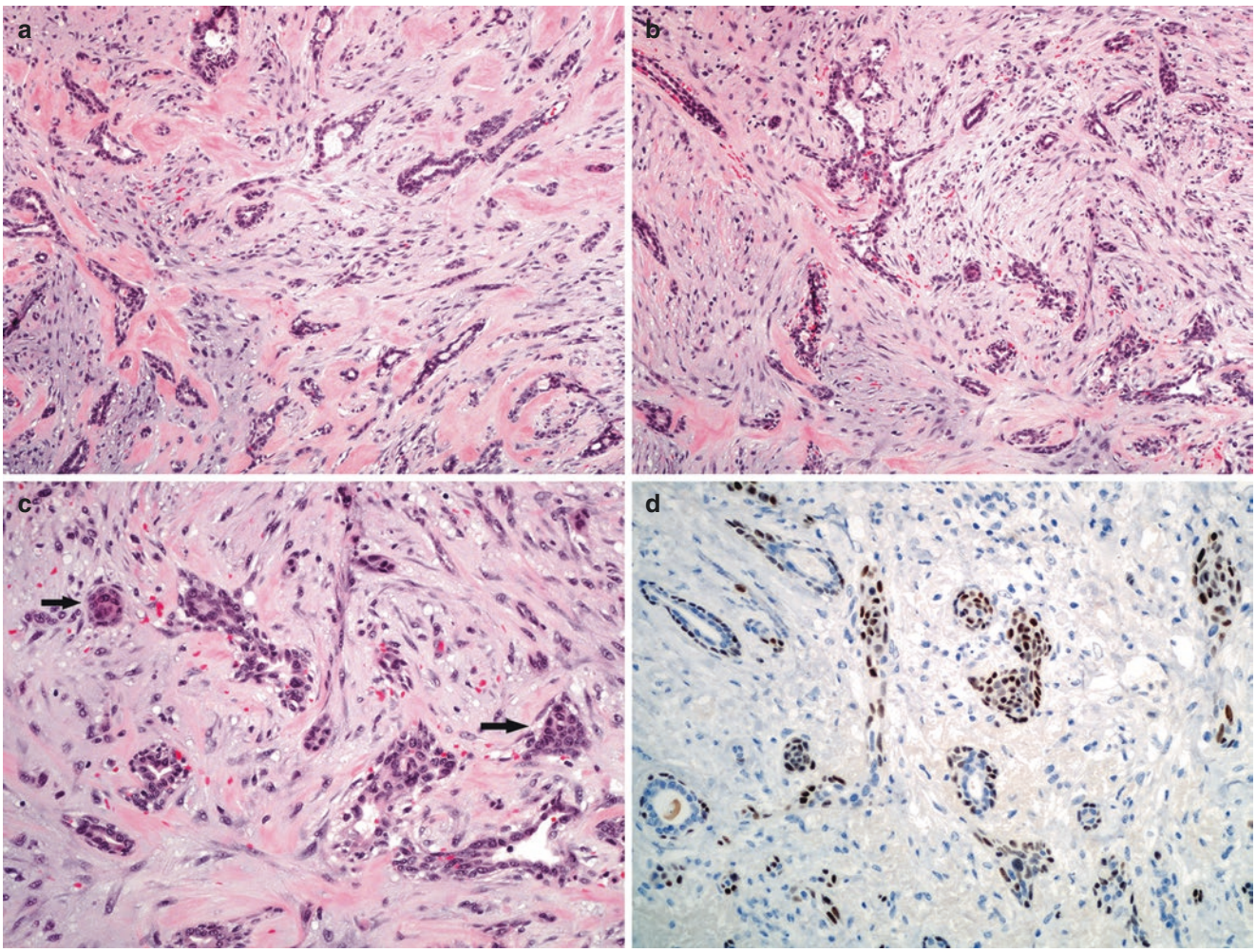

Fig. 10.65 Low-grade adenosquamous carcinoma. (**a**) Open angulated glands embedded in a fibrous cellular stroma showing focal hyalinization. (**b**) Different areas of the tumor show tubular glands and small nests of cells surrounded by cellular stroma. (**c**) High-power view shows squamoid nests with dense eosinophilic cytoplasm (*arrow*). (**d**) Immunostain for p63 reveals nuclear staining in the peripheral cells of the tubules and the squamoid nests. Spindle cells are also positive with CAM5.2 and focally with p63 (not shown)

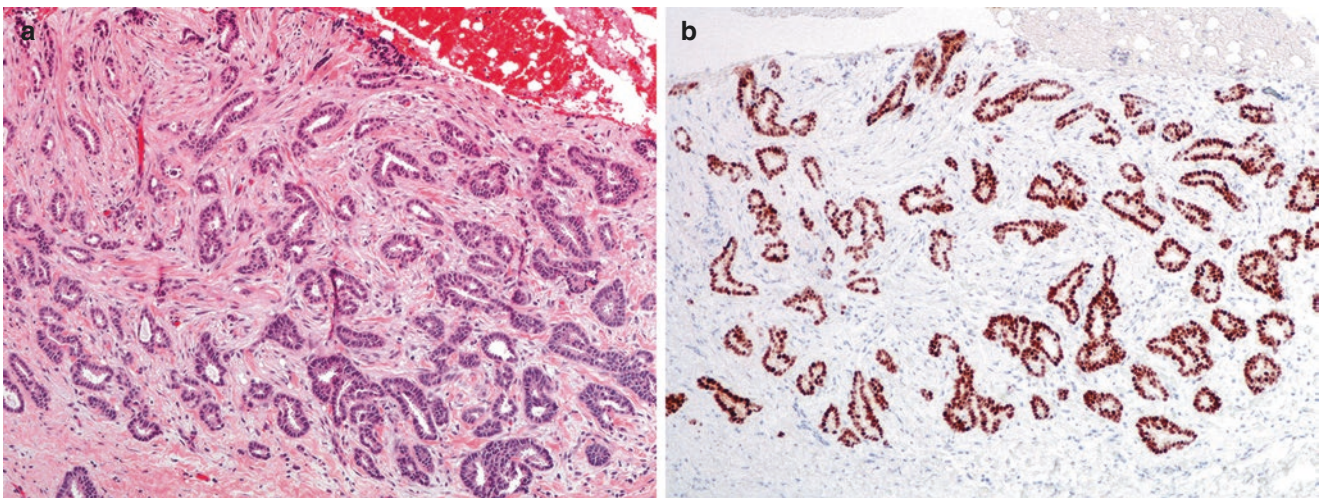

Fig. 10.66 Tubular carcinoma. (**a**) H&E stain and (**b**) strong diffuse nuclear staining for estrogen receptor

similar to low-grade IDC-NST. However, some differences between tubular carcinoma and low-grade IDC-NST have been elucidated by comparative transcriptomic analysis, with upregulation of the ER-driven signaling pathways (ESR1, CREBBP1, and NCOR1 signals) noted in tubular carcinoma [158].

Prognosis

Tubular carcinoma is known for its excellent prognosis. It has a low propensity for lymph node metastases (incidence 2–11%) [129, 130, 134, 143, 161, 162], a low rate of local recurrence (4–7%) [127, 129–131] and distant metastasis, and a high overall survival rate [130, 143, 156, 161]. The 5-year disease-free survival rate is generally more than 90% [129, 156, 161, 163] and the 10-year overall survival rate is comparable to that of the age-matched general population [131, 156, 163]. Due to its excellent prognosis, it is critical to differentiate tubular carcinoma from well-differentiated IBC NST. As mentioned previously, on a core biopsy, depending on the size of the tumor, it may be more appropriate to diagnose the tumor as "IBC with tubular features" and defer the final classification to the excision specimen.

The mainstay of treatment for tubular carcinoma is surgical excision. Due to the extremely favorable prognosis of tubular carcinomas, the impact of endocrine and radiation therapy have been questioned. Current NCCN guidelines state endocrine therapy should be considered but is not clearly recommended for tubular carcinomas less than 3 cm in size and/or in node-negative cases. In patients with macrometastasis in one or more axillary lymph nodes, endocrine therapy is recommended with the option of adjuvant chemotherapy [164]. Neoadjuvant chemotherapy is largely not considered in the treatment of tubular carcinoma [162]. Radiation therapy was found to be a favorable prognostic factor for overall survival in tubular carcinoma patients in a National Cancer Database study [165] while a SEER database study found that radiotherapy improved survival outcomes in patients aged <50 years [166].

While sentinel lymph node biopsy (SLNB) is a fairly standard indication in invasive carcinomas, some studies have questioned its routine use in tubular carcinomas. Few retrospective studies have reported a higher rate of lymph node involvement, mostly because of varying criteria used for this diagnosis [127, 130, 143, 162, 167]. Studies that examined lymph node involvement in "pure" tubular carcinoma, defined as >90% tubule formation with low-grade histology, found 4.6–6.2% cases with lymph node metastasis, including cases with isolated tumor cells [134, 167, 168]. A study by Lea et al. reported 13 patients with lymph node involvement (7 macrometastasis, 5 micrometastasis, and 1 with isolated tumor cells) in their series of 146 "pure" tubular carcinomas (defined as tumors with ≥90% tubule formation). However, in their series, three patients had grade 2 histology and six patients were not graded. Therefore nine cases did not fulfill the criteria for pure tubular histology. In addition, 28 patients in their study did not undergo any axillary lymph node sampling [169]. In a large multi-institutional study by Dejode and colleagues of 234 patients with pure tubular carcinoma, 6 patients (2.5%) had macrometastasis, 15 (6.4%) micrometastasis, and 2 (0.8%) isolated tumor cells. They also reported an overall low rate of non-sentinel lymph node involvement, found only in 3 (1.2%) patients, all of whom had macrometastasis in their sentinel lymph nodes. None of the patients with micrometastasis or isolated tumor cells had metastasis in non-sentinel lymph node on completion of axillary dissection [170].

Fedko and colleagues reported 5 (5.4%) cases with lymph node metastasis and 2 with isolated tumor cells in a study of 105 patients with tubular carcinoma. In their study, the tumor ranged from 0.9 to 1.5 cm in node-positive patients. Despite two node-positive patients with tumors less than 1 cm in size, the authors proposed forgoing axillary staging in patients with tumors measuring less than 1.8 cm [134]. Additionally in the study by Dejode et al., after multivariate analysis, the only parameter significantly linked to lymph node involvement was pathologic tumor size of greater than 10 mm ($p = 0.007$). Of the 122 patients with a pathologic tumor size less than 10 mm, none had macrometastasis, 4 had micrometastasis, and 1 had isolated tumor cells to the sentinel lymph node. They suggested that SLNB could be omitted in patients with tumors less than 10 mm in size, and further postulated that even those patients with metastasis in the sentinel lymph node might not require completion of axillary lymph node dissection [170].

Interestingly, the rate of lymph node involvement in pure tubular carcinoma is comparable to the accepted overall false-negative rate of 5–9.8% reported for sentinel lymph node metastases [171–173]. Long-term data from the prospective National Surgical Adjuvant Breast and Bowel Project (NSABP) B04 trial reported no difference in disease-free survival, relapse-free survival, distant disease-free survival, or overall survival in clinically node-negative women who were randomized to receive radical mastectomy, total mastectomy without axillary dissection but with postoperative radiation, or total mastectomy plus axillary dissection, if their nodes became clinically positive on follow-up [174]. Additionally, univariate analysis using data from the NSABP B06 trial revealed that when comparing node-negative patients ($n = 1090$) to node-positive patients ($n = 651$), those with tumors of favorable histology (including 120 with tubular carcinoma) experienced a significantly greater overall survival at 10 years compared to those without. On multivariate analysis, favorable histology proved to be an independent predictor of survival in node-negative patients [175].

Invasive Cribriform Carcinoma

Overview

Invasive cribriform carcinoma (ICC) is an uncommon morphologic variant of invasive carcinoma comprising less than 1% of all IBC [176, 177]. Page et al. first characterized this entity in 1983 as a well-differentiated carcinoma that often has a tubular component and is associated with a favorable prognosis [176]. The median age is 61 with a wide age range reported (7–91 years) [176, 178–181]. Multifocality has been found in 13.7–20% of cases [176, 180].

Gross and Radiologic Features

The imaging findings of most ICC are similar to other IBC-NST. ICC appears as an irregular high-density spiculated mass with or without associated calcifications on mammogram [179, 181]. One study reported four of eight cases to be mammographically occult [179]. Common features of ICC on ultrasound are irregular shape, hypoechogenicity, and no posterior acoustic shadow [179, 181, 182]. On MRI, most ICC present as an irregularly shaped enhancing mass.

Grossly, ICC appears similar to other mass-forming IBC-NST. The average tumor size ranges from 1.7 to 3.1 cm [176, 178–180].

Microscopic Features

ICC shows a sieve-like pattern or fenestrated appearance in which individual glands are angular or irregular (Fig. 10.67). The cribriform nests may have a round or irregular contour (Fig. 10.68). The neoplastic glands infiltrate between ducts and lobules of normal breast without disturbing their architecture (Fig. 10.69). The lumens may contain bluish mucinous secretions with or without associated microcalcifications [183] (Fig. 10.70). The tumor cells are small with eosinophilic to amphophilic cytoplasm, low-to-intermediate nuclear grade, finely dispersed chromatin, indistinct nucleoli, and infrequent mitoses (Fig. 10.71). The stroma usually shows a desmoplastic response, sometimes associated with inflammatory infiltrates or osteoclastic-like giant cells [160, 184] (Fig. 10.72). It is not uncommon to find neoplastic tubules intermixed with cribriform nests as well as prominent apical snouts in the cribriform nests. In the majority of cases, associated DCIS is seen, usually of cribriform type. ICCs are histologic grade-1 tumors.

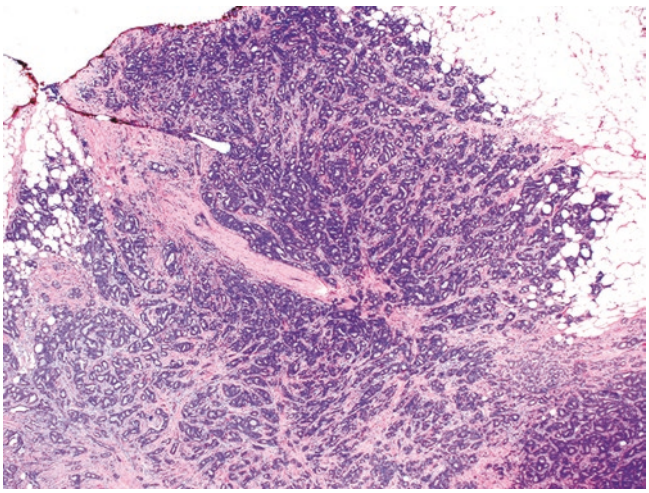

Fig. 10.67 Invasive cribriform carcinoma with sieve-like pattern apparent on scanning view

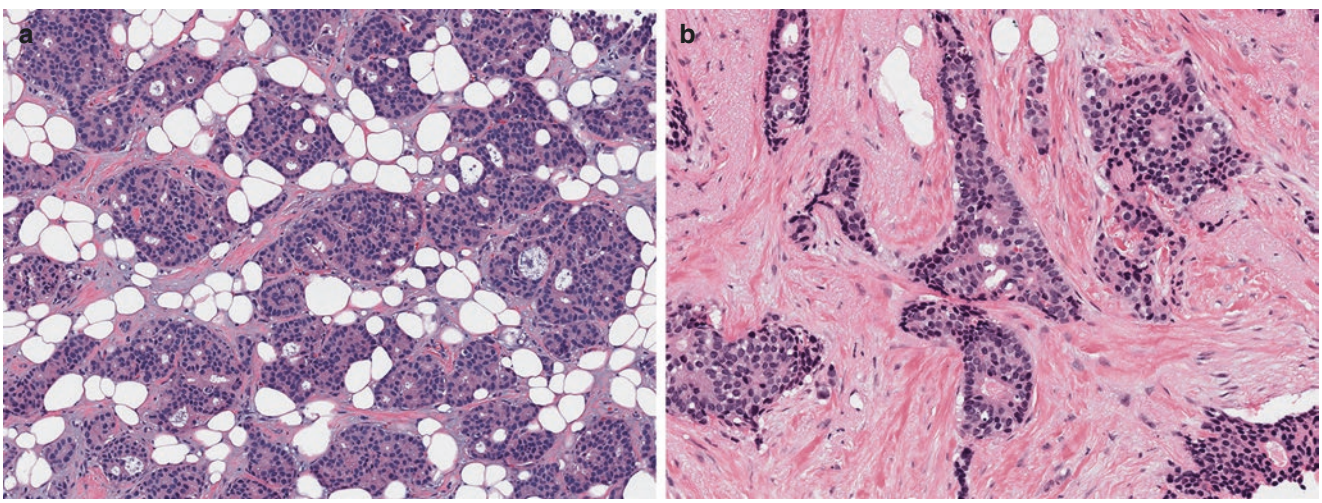

Fig. 10.68 Invasive cribriform carcinoma. (**a**) Individual tumor nests with round-to-oval contour and (**b**) a different case showing tumor nests with irregular and angulated contour

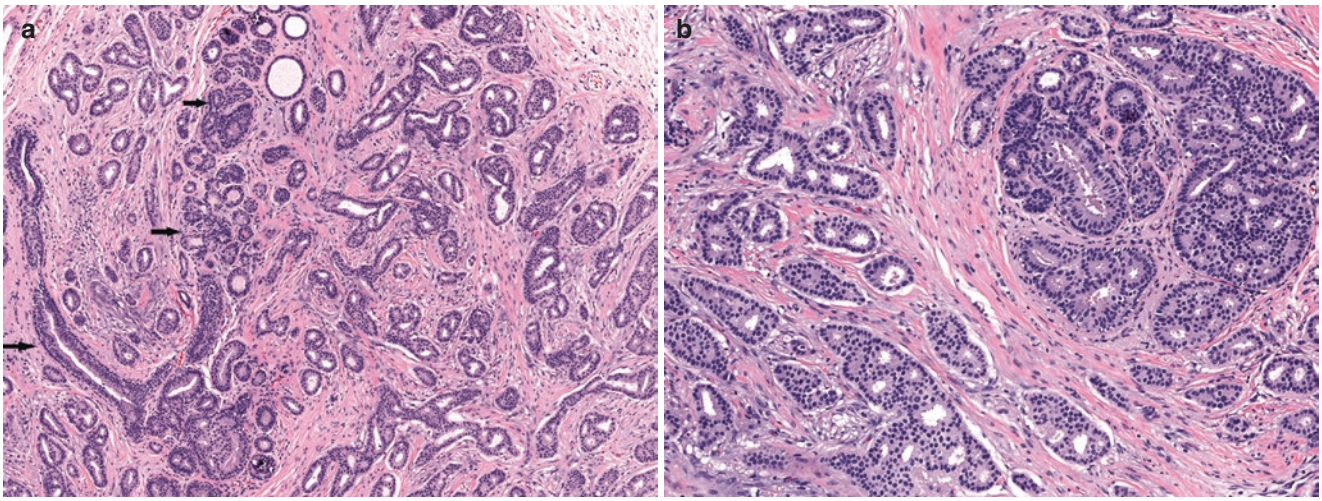

Fig. 10.69 Invasive cribriform carcinoma infiltrates between the normal glandular breast elements (*arrow*), (**a**) low power and (**b**) high power

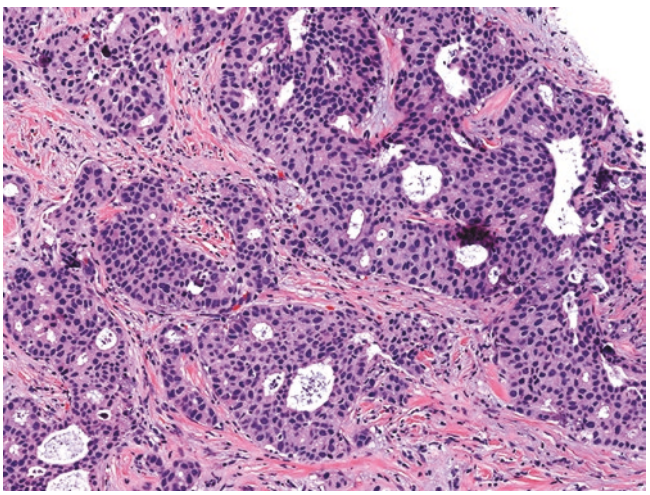

Fig. 10.70 Invasive cribriform carcinoma with basophilic luminal secretions and associated microcalcifications which can superficially resemble adenoid cystic carcinoma

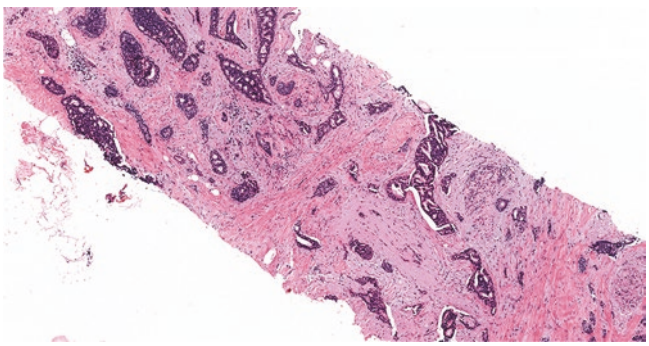

Fig. 10.72 Invasive cribriform carcinoma associated with a marked desmoplastic stromal reaction

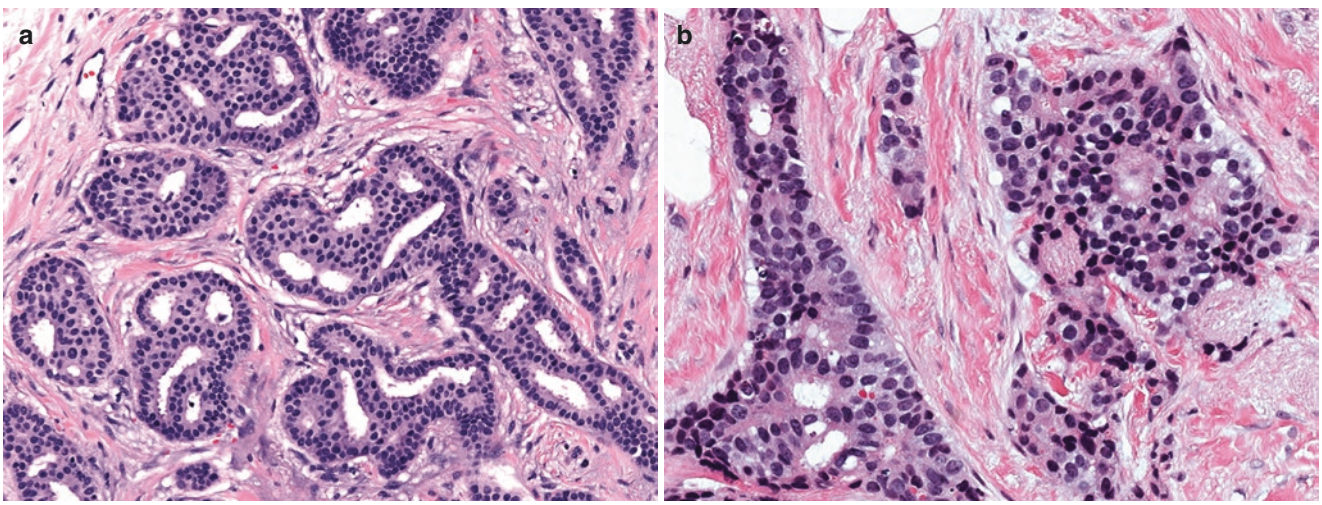

Fig. 10.71 Invasive cribriform carcinoma lined by monotonous low-grade cells with apical snouts and uniform nuclei with fine chromatin (**a**, **b**)

WHO defines pure ICC as tumors showing greater than 90% cribriform architecture. Page et al. originally classified ICC as "classical" or "mixed." Classical ICC was defined as tumors showing at least a 50% cribriform component with the remaining component showing a tubular pattern (Fig. 10.73). Mixed ICC was defined as tumors with at least a 50% cribriform component with any admixed component being non-tubular [176]. ICC should be distinguished from IBC-NST that shows a cribriform pattern but has aggressive characteristics such as high-grade nuclei, increased mitotic activity, or necrosis (Fig. 10.74). These should not be identified as ICC as they are not associated with the favorable prognosis of these tumors.

Differential Diagnosis

The most common differential diagnosis of ICC is cribriform DCIS. Other rare entities such as adenoid cystic carcinoma (AdCC), invasive mammary carcinoma with osteoclast-like giant cells, and collagenous spherulosis may superficially resemble ICC.

Cribriform DCIS

ICC and cribriform DCIS can be mistaken for one another, particularly in a CNB. Cribriform DCIS is often found within ICC, and they must be distinguished from one another in order to obtain an accurate measurement of the invasive

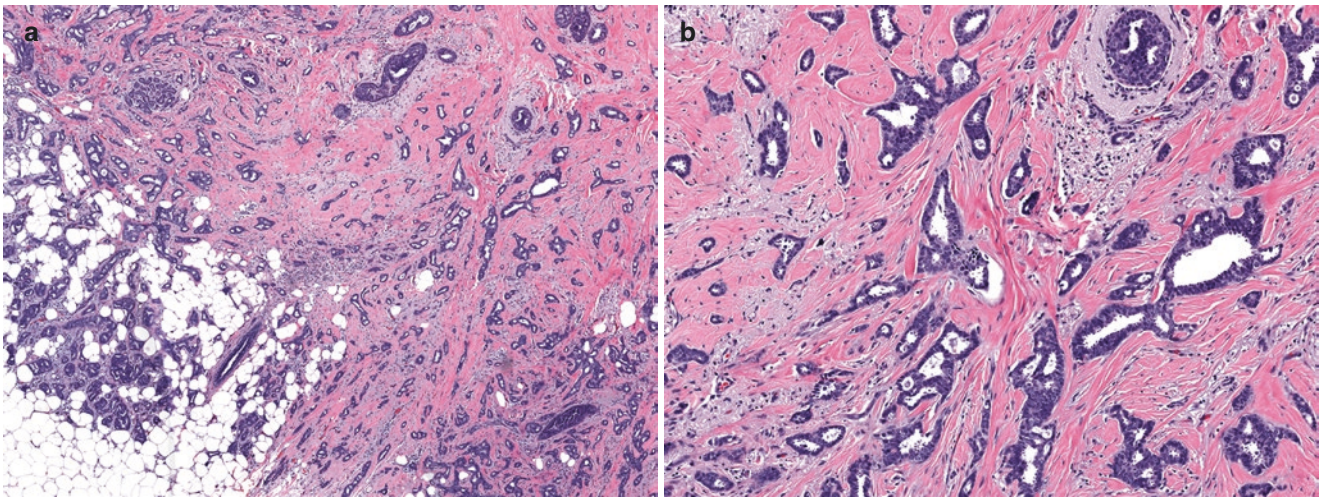

Fig. 10.73 Invasive cribriform carcinoma admixed with tubular carcinoma (**a**) low power and (**b**) high power

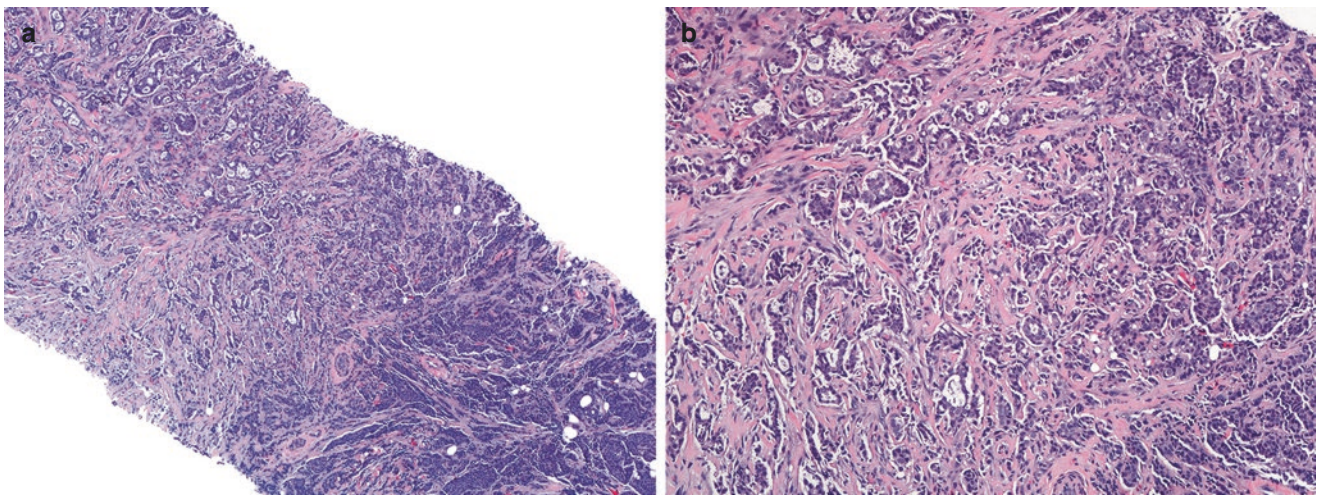

Fig. 10.74 Invasive breast carcinoma NST shows invasive cribriform growth pattern (**a**, **b**)

component for appropriate tumor staging. Cribriform DCIS has smooth round contours as opposed to the angular or irregular contours seen in ICC (Fig. 10.75). Also, cribriform DCIS does not distort the normal breast architecture or induce a desmoplastic reaction. In difficult cases, particularly in core biopsies, immunostains for myoepithelial cells can be invaluable in differentiating the two components (Fig. 10.76).

Adenoid Cystic Carcinoma (AdCC)

Low-grade AdCC can exhibit cribriform architecture resembling ICC (Fig. 10.77). The dual epithelial–myoepithelial cell population and intraluminal basement membrane material present in AdCC are distinguishing features, although ICC can also show intraluminal secre-

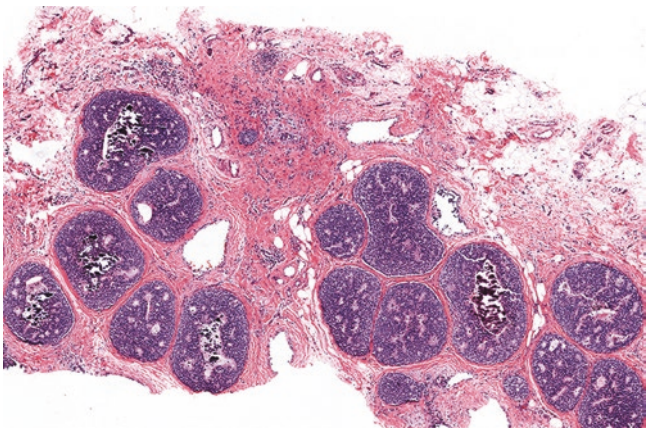

Fig. 10.75 Cribriform DCIS with round contour and normal breast stroma between the nests

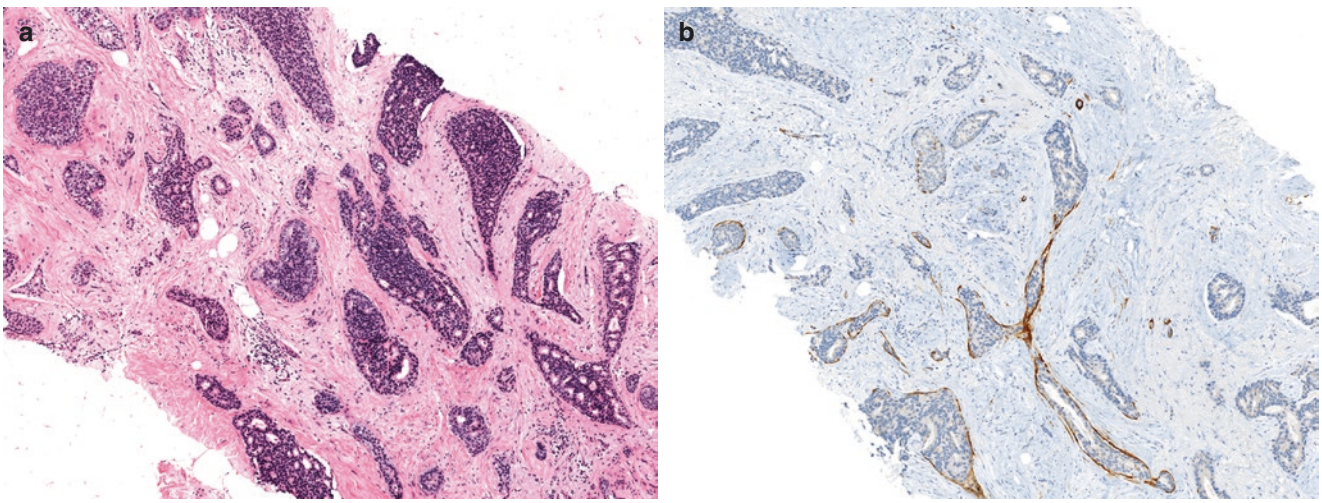

Fig. 10.76 An invasive cribriform carcinoma consisting of cribriform nests with round and irregular contours making it difficult to assess the extent of in situ versus invasive carcinoma, (**a**) H&E stain and (**b**) p63 helps to delineate the in situ and invasive components

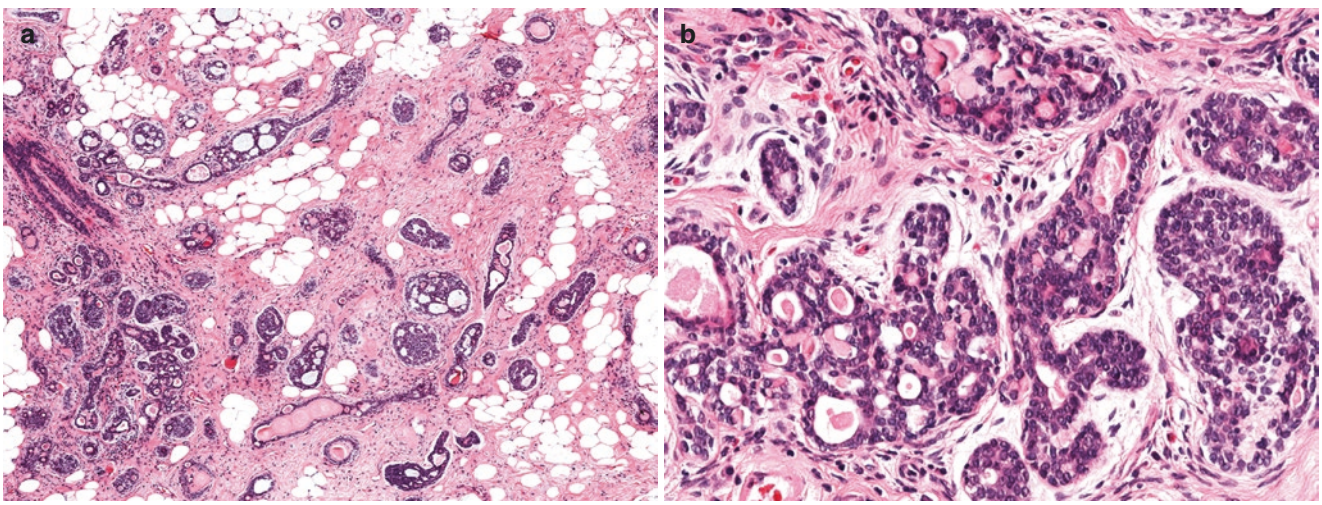

Fig. 10.77 Low-grade adenoid cystic carcinoma of the breast. (**a**) Low power and (**b**) high power shows accumulated basement membrane material (*left*) and the presence of intercalated ducts (*right*)

tions resembling the basement membrane material of AdCC. Immunostains are key as AdCC and ICC show different patterns of expression. One of the most useful stains is ER as AdCC is typically ER negative, whereas ICC expresses ER diffusely in virtually all cases. In addition, AdCC shows p63 expression by its neoplastic myoepithelial component and membranous and cytoplasmic CD117 (c-KIT) staining by its epithelial component while ICC is negative for myoepithelial markers [185] (see Chap. 12 for further discussion of AdCC).

Collagenous Spherulosis

Collagenous spherulosis can be associated with calcifications and hence be the target of CNB (Fig. 10.78). The hallmark of collagenous spherulosis is the presence of amorphous, acellular, dense eosinophilic spherules composed of basement membrane material analogous to the spherules seen in AdCC. Degenerative changes in the spherules may result in empty spaces or a basophilic appearance that can be mistaken for secretions (Fig. 10.79). The ductal cells have a smooth, round appearance with bland cytology. Myoepithelial cells typically surround the spherules and are also present at the periphery of the ductules. Myoepithelial markers such as p63 and SMM demonstrate different patterns of staining in AdCC and collagenous spherulosis, helping to distinguish between the two.

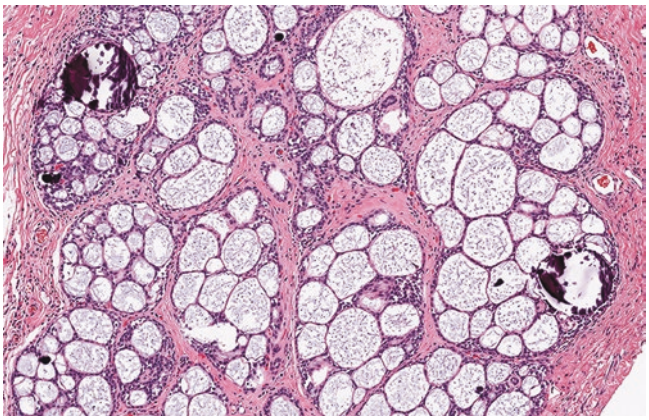

Fig. 10.78 Collagenous spherulosis with associated calcifications. Note the bluish appearing degenerated basement membrane material within the glandular lumens

Invasive Mammary Carcinoma with Osteoclast-Like Giant Cells

This is a rare type of IBC in which the invasive component may exhibit well, moderate-to-poor differentiation with associated cribriform growth pattern or less commonly non-cribriform patterns such as lobular, mucinous, papillary, squamous, or apocrine carcinomas (Fig. 10.80). Distinctive features of this entity include the grossly red–brown appearance of the tumor which microscopically represents numerous red blood cells and hemosiderin-laden macrophages in tumoral stroma, as well as the juxtaposition of numerous osteoclast-like giant cells of histiocytic origin and neoplastic glands. These tumors should be classified and graded according to the morphologic pattern and differentiation.

Immunohistochemistry

ICC is usually HR positive and HER2 negative (Fig. 10.81). Almost all cases are ER positive, and 70–90% are PR positive [178, 180, 181]. The proliferation rate is usually low (<14%) [180].

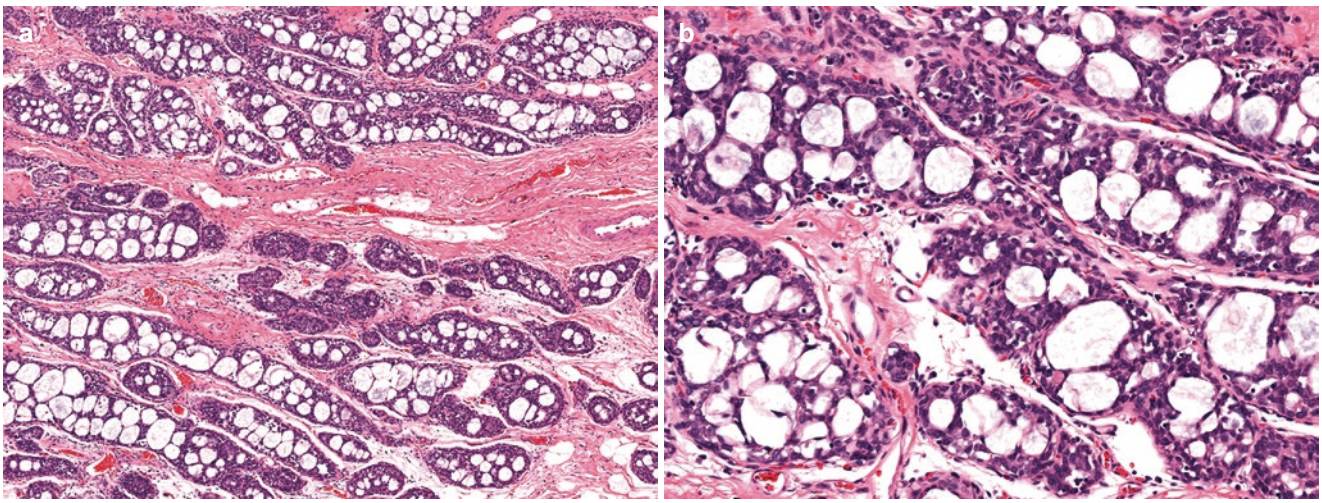

Fig. 10.79 Extensive collagenous spherulosis involved by LCIS. (**a**) Low-power view shows a sieve-like appearance resembling a cribriform growth pattern. (**b**) High-power view shows bluish basement membrane material

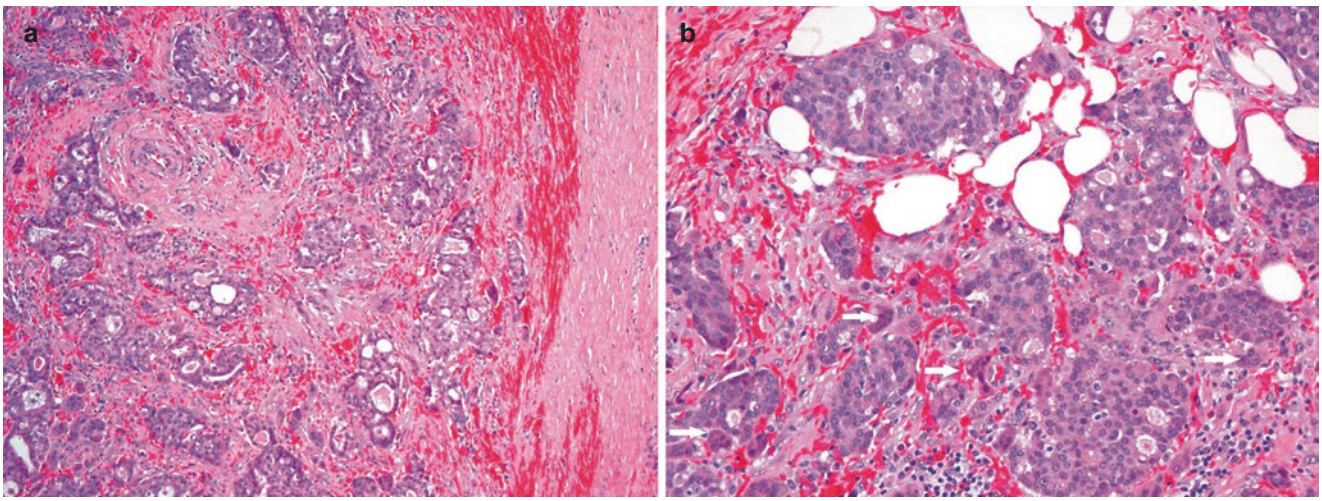

Fig. 10.80 Invasive mammary carcinoma with numerous red blood cells and osteoclast-like giant cells (*arrow*): (**a**) low power and (**b**) high power

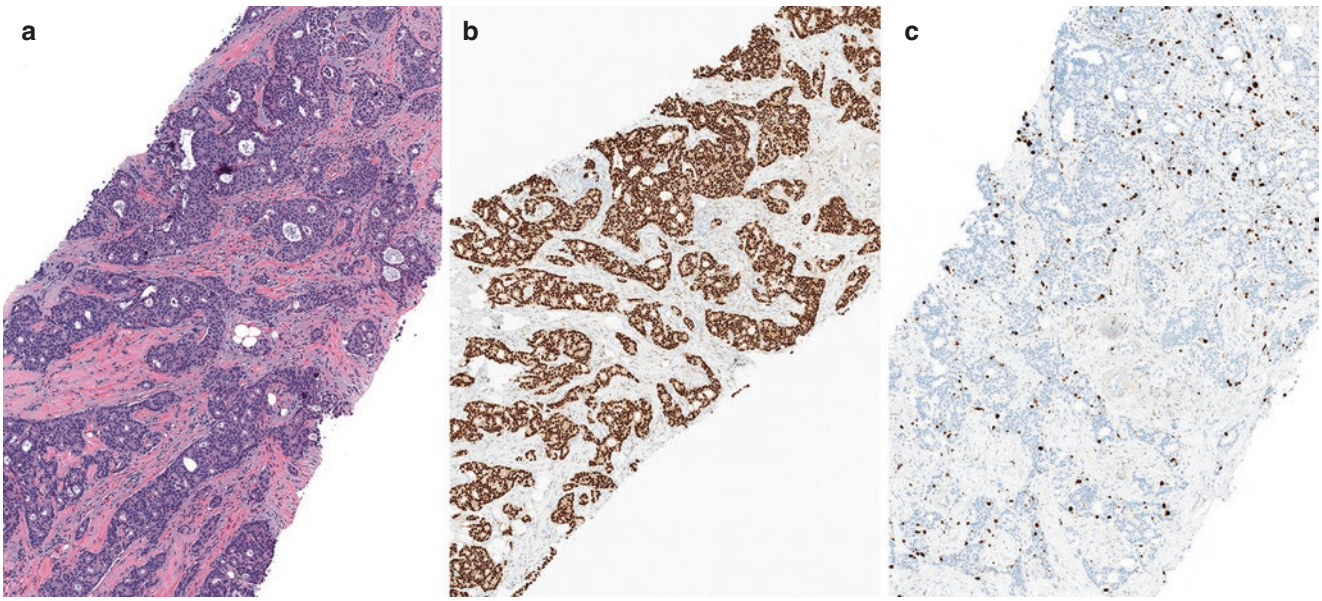

Fig. 10.81 Invasive cribriform carcinoma, (**a**) H&E stain, (**b**) strong and diffuse ER staining, and (**c**) Ki-67 shows low (<10%) proliferation index in tumor cells

Prognosis

Invasive cribriform carcinoma is associated with an excellent prognosis. The largest case series include the study by Page et al. where 51 cases were divided into classical and mixed types as defined above and Venable et al. with 62 cases of "pure" ICC, where essentially the entire tumor exhibited a cribriform pattern, and "mixed" ICC, where tumors displayed cribriform architecture mixed with tubular, papillary, ductal, or lobular patterns [176, 178].

With an average follow-up of 14.5 years, only one patient with classical ICC in Page's study died, but from contralateral breast squamous cell carcinoma [176]. Venable et al. found a 100% 5-year survival rate in those with tumors with ≥50% cribriform pattern [178]. A more recent SEER study found a 90% 5-year survival rate for ICC [177]. Axillary lymph node metastasis in ICC has been reported to range from 14% to 25% [176–178, 180, 181]. ICC is less likely to involve more than three lymph nodes compared to tumors with a smaller (<50%) cribriform component [178]. Interestingly, nodal metastasis from pure ICC maintains a cribriform pattern, whereas metastasis from mixed tumors are more likely to exhibit a non-cribriform component [176, 178]. One case of distant metastasis with ICC has been reported in a patient with untreated tumor for 13 years that eventually ulcerated through the skin. This patient was still alive 7 years after presenting with metastatic disease, demonstrating the indolent nature of this tumor [186].

References

1. Rakha EAAK, Bu H, Ellis IO, Foschini MP, Horii R, Masuda S, Penault-Llorca F, Schnitt SJ, Tsuda H, Vincent-Salomon A, Yang WT. WHO classification of tumours: breast tumours. 5th ed. Lyon: World Health Organization; 2019.
2. Anderson WF, Pfeiffer RM, Dores GM, Sherman ME. Comparison of age distribution patterns for different histopathologic types of breast carcinoma. Cancer Epidemiol Biomark Prev. 2006;15(10):1899–905.
3. Fisher CJ, Egan MK, Smith P, Wicks K, Millis RR, Fentiman IS. Histopathology of breast cancer in relation to age. Br J Cancer. 1997;75(4):593–6.
4. Li CI, Anderson BO, Daling JR, Moe RE. Trends in incidence rates of invasive lobular and ductal breast carcinoma. JAMA. 2003;289(11):1421–4.
5. Ellis IO, Galea M, Broughton N, Locker A, Blamey RW, Elston CW. Pathological prognostic factors in breast cancer. II. Histological type. Relationship with survival in a large study with long-term follow-up. Histopathology. 1992;20(6):479–89.
6. Fisher ER, Gregorio RM, Fisher B, Redmond C, Vellios F, Sommers SC. The pathology of invasive breast cancer. A syllabus derived from findings of the National Surgical Adjuvant Breast Project (protocol no. 4). Cancer. 1975;36(1):1–85.
7. Allred DC, Carlson RW, Berry DA, Burstein HJ, Edge SB, Goldstein LJ, et al. NCCN task force report: estrogen receptor and progesterone receptor testing in breast cancer by immunohistochemistry. J Natl Compr Cancer Network. 2009;7(Suppl 6):S1–21; quiz S2–3.
8. Broberg A, Glas U, Gustafsson SA, Hellstrom L, Somell A. Relationship between mammographic pattern and estrogen receptor content in breast cancer. Breast Cancer Res Treat. 1983;3(2):201–7.
9. Berg WA, Gutierrez L, NessAiver MS, Carter WB, Bhargavan M, Lewis RS, et al. Diagnostic accuracy of mammography, clinical examination, US, and MR imaging in preoperative assessment of breast cancer. Radiology. 2004;233(3):830–49.
10. Moss HA, Britton PD, Flower CD, Freeman AH, Lomas DJ, Warren RM. How reliable is modern breast imaging in differentiating benign from malignant breast lesions in the symptomatic population? Clin Radiol. 1999;54(10):676–82.
11. Sickies EA. Sonographic detectability of breast calcification. Proc SPIE. 1983;419:51–2.
12. Lambie RW, Hodgden D, Herman EM, Kopperman M. Sonomammographic manifestations of mammographically detectable breast microcalcifications. J Ultrasound Med. 1983;2(11):509–14.
13. Stavros AT, Thickman D, Rapp CL, Dennis MA, Parker SH, Sisney GA. Solid breast nodules: use of sonography to distinguish between benign and malignant lesions. Radiology. 1995;196(1):123–34.
14. Fornage BD, Sneige N, Faroux MJ, Andry E. Sonographic appearance and ultrasound-guided fine-needle aspiration biopsy of breast carcinomas smaller than 1 cm3. J Ultrasound Med. 1990;9(10):559–68.
15. Fornage BD, Lorigan JG, Andry E. Fibroadenoma of the breast: sonographic appearance. Radiology. 1989;172(3):671–5.
16. Saslow D, Boetes C, Burke W, Harms S, Leach MO, Lehman CD, et al. American Cancer Society guidelines for breast screening with MRI as an adjunct to mammography. CA Cancer J Clin. 2007;57(2):75–89.
17. Yeh E, Slanetz P, Kopans DB, Rafferty E, Georgian-Smith D, Moy L, et al. Prospective comparison of mammography, sonography, and MRI in patients undergoing neoadjuvant chemotherapy for palpable breast cancer. AJR Am J Roentgenol. 2005;184(3):868–77.
18. Jabbar SB, Lynch B, Seiler S, Hwang H, Sahoo S. Pathologic findings of breast lesions detected on magnetic resonance imaging. Arch Pathol Lab Med. 2017;141(11):1513–22.
19. Choudhery S, Lynch B, Sahoo S, Seiler SJ. Features of non-mass enhancing lesions detected on 1.5 T breast MRI: a radiologic and pathologic analysis. Breast Dis. 2015;35(1):13–7.
20. Schnall MD, Blume J, Bluemke DA, DeAngelis GA, DeBruhl N, Harms S, et al. Diagnostic architectural and dynamic features at breast MR imaging: multicenter study. Radiology. 2006;238(1):42–53.
21. Mandoul C, Verheyden C, Millet I, Orliac C, Pages E, Thomassin I, et al. Breast tomosynthesis: what do we know and where do we stand? Diagn Interv Imaging. 2019;100(10):537–51.
22. van Bogaert LJ, Maldague P. Scirrhous carcinoma of the female breast. Invest Cell Pathol. 1980;3(4):377–82.
23. Arps DP, Healy P, Zhao L, Kleer CG, Pang JC. Invasive ductal carcinoma with lobular features: a comparison study to invasive ductal and invasive lobular carcinomas of the breast. Breast Cancer Res Treat. 2013;138(3):719–26.
24. Galea MH, Blamey RW, Elston CE, Ellis IO. The Nottingham Prognostic Index in primary breast cancer. Breast Cancer Res Treat. 1992;22(3):207–19.
25. Elston CW, Ellis IO. Pathological prognostic factors in breast cancer. I. The value of histological grade in breast cancer: experience from a large study with long-term follow-up. Histopathology. 2002;41(3A):154–61.
26. Elston CW, Ellis IO. Pathological prognostic factors in breast cancer. I. The value of histological grade in breast cancer: experience from a large study with long-term follow-up. Histopathology. 2002;41(3A):151–2; discussion 2–3.
27. Elston CW, Ellis IO. Pathological prognostic factors in breast cancer. I. The value of histological grade in breast cancer: experience from a large study with long-term follow-up. Histopathology. 1991;19(5):403–10.
28. Bloom HJ, Richardson WW. Histological grading and prognosis in breast cancer; a study of 1409 cases of which 359 have been followed for 15 years. Br J Cancer. 1957;11(3):359–77.
29. Patey DH, Scarff RW. The position of histology in the prognosis of carcinoma of the breast. Lancet. 1928;1:801–4.
30. Haybittle JL, Blamey RW, Elston CW, Johnson J, Doyle PJ, Campbell FC, et al. A prognostic index in primary breast cancer. Br J Cancer. 1982;45(3):361–6.
31. Blamey RW, Ellis IO, Pinder SE, Lee AH, Macmillan RD, Morgan DA, et al. Survival of invasive breast cancer according to the Nottingham Prognostic Index in cases diagnosed in 1990-1999. Eur J Cancer. 2007;43(10):1548–55.
32. Cui X, Harada S, Shen D, Siegal GP, Wei S. The utility of phosphohistone H3 in breast cancer grading. Appl Immunohistochem Mol Morphol. 2015;23:689–95.
33. Start RD, Flynn MS, Cross SS, Rogers K, Smith JH. Is the grading of breast carcinomas affected by a delay in fixation? Virchows Arch A Pathol Anat Histopathol. 1991;419(6):475–7.
34. Robbins P, Pinder S, de Klerk N, Dawkins H, Harvey J, Sterrett G, et al. Histological grading of breast carcinomas: a study of interobserver agreement. Hum Pathol. 1995;26(8):873–9.
35. Yildiz-Aktas IZ, Dabbs DJ, Bhargava R. The effect of cold ischemic time on the immunohistochemical evaluation of estrogen receptor, progesterone receptor, and HER2 expression in invasive breast carcinoma. Mod Pathol. 2012;25(8):1098–105.
36. Usami S, Moriya T, Amari M, Suzuki A, Ishida T, Sasano H, et al. Reliability of prognostic factors in breast carcinoma determined by core needle biopsy. Jpn J Clin Oncol. 2007;37(4):250–5.
37. Shannon J, Douglas-Jones AG, Dallimore NS. Conversion to core biopsy in preoperative diagnosis of breast lesions: is it justified by results? J Clin Pathol. 2001;54(10):762–5.

38. McIntosh SA, Panchalingam L, Payne S, Miller ID, Sarkar TK, Hutcheon AW, et al. Freehand core biopsy in breast cancer: an accurate predictor of tumour grade following neoadjuvant chemotherapy? Breast. 2002;11(6):496–500.
39. Andrade VP, Gobbi H. Accuracy of typing and grading invasive mammary carcinomas on core needle biopsy compared with the excisional specimen. Virchows Arch. 2004;445(6):597–602.
40. Monticciolo DL. Histologic grading at breast core needle biopsy: comparison with results from the excised breast specimen. Breast J. 2005;11(1):9–14.
41. Rakha EA, Ellis IO. An overview of assessment of prognostic and predictive factors in breast cancer needle core biopsy specimens. J Clin Pathol. 2007;60(12):1300–6.
42. Denley H, Pinder SE, Elston CW, Lee AH, Ellis IO. Preoperative assessment of prognostic factors in breast cancer. J Clin Pathol. 2001;54(1):20–4.
43. Daveau C, Baulies S, Lalloum M, Bollet M, Sigal-Zafrani B, Sastre X, et al. Histological grade concordance between diagnostic core biopsy and corresponding surgical specimen in HR-positive/HER2-negative breast carcinoma. Br J Cancer. 2014;110(9):2195–200.
44. Kwok TC, Rakha EA, Lee AH, Grainge M, Green AR, Ellis IO, et al. Histological grading of breast cancer on needle core biopsy: the role of immunohistochemical assessment of proliferation. Histopathology. 2010;57(2):212–9.
45. Verkooijen HM, Peeters PH, Buskens E, Koot VC, Borel Rinkes IH, Mali WP, et al. Diagnostic accuracy of large-core needle biopsy for nonpalpable breast disease: a meta-analysis. Br J Cancer. 2000;82(5):1017–21.
46. Verkooijen HM, Core Biopsy After Radiological Localisation Study G. Diagnostic accuracy of stereotactic large-core needle biopsy for nonpalpable breast disease: results of a multicenter prospective study with 95% surgical confirmation. Int J Cancer. 2002;99(6):853–9.
47. Dillon MF, Hill AD, Quinn CM, O'Doherty A, McDermott EW, O'Higgins N. The accuracy of ultrasound, stereotactic, and clinical core biopsies in the diagnosis of breast cancer, with an analysis of false-negative cases. Ann Surg. 2005;242(5):701–7.
48. Ibrahim AE, Bateman AC, Theaker JM, Low JL, Addis B, Tidbury P, et al. The role and histological classification of needle core biopsy in comparison with fine needle aspiration cytology in the preoperative assessment of impalpable breast lesions. J Clin Pathol. 2001;54(2):121–5.
49. Brenner RJ, Fajardo L, Fisher PR, Dershaw DD, Evans WP, Bassett L, et al. Percutaneous core biopsy of the breast: effect of operator experience and number of samples on diagnostic accuracy. AJR Am J Roentgenol. 1996;166(2):341–6.
50. Bassett L, Winchester DP, Caplan RB, Dershaw DD, Dowlatshahi K, Evans WP 3rd, et al. Stereotactic core-needle biopsy of the breast: a report of the Joint Task Force of the American College of Radiology, American College of Surgeons, and College of American Pathologists. CA Cancer J Clin. 1997;47(3):171–90.
51. Rakha EA, Gill MS, El-Sayed ME, Khan MM, Hodi Z, Blamey RW, et al. The biological and clinical characteristics of breast carcinoma with mixed ductal and lobular morphology. Breast Cancer Res Treat. 2009;114(2):243–50.
52. Rakha EA, El-Sayed ME, Powe DG, Green AR, Habashy H, Grainge MJ, et al. Invasive lobular carcinoma of the breast: response to hormonal therapy and outcomes. Eur J Cancer. 2008;44(1):73–83.
53. Wiseman C, Liao KT. Primary lymphoma of the breast. Cancer. 1972;29(6):1705–12.
54. Telesinghe PU, Anthony PP. Primary lymphoma of the breast. Histopathology. 1985;9(3):297–307.
55. Talwalkar SS, Miranda RN, Valbuena JR, Routbort MJ, Martin AW, Medeiros LJ. Lymphomas involving the breast: a study of 106 cases comparing localized and disseminated neoplasms. Am J Surg Pathol. 2008;32(9):1299–309.
56. Ganjoo K, Advani R, Mariappan MR, McMillan A, Horning S. Non-Hodgkin lymphoma of the breast. Cancer. 2007;110(1):25–30.
57. Sauer T. Fine-needle aspiration cytology of extra mammary metastatic lesions in the breast: a retrospective study of 36 cases diagnosed during 18 years. Cytojournal. 2010;7:10.
58. Vaughan A, Dietz JR, Moley JF, Debenedetti MK, Aft RL, Gillanders WE, et al. Metastatic disease to the breast: the Washington University experience. World J Surg Oncol. 2007;5:74.
59. Saluja K, Thakral B, Bit-Ivan E, Kaufman M, Liu L. Fine-needle aspiration of metastatic renal cell carcinoma to a male breast: a rare initial presentation. Cytojournal. 2014;11:8.
60. Nasit JG, Shah B, Shah M. Metastatic hepatocellular carcinoma presenting as gynecomastia in male: a diagnostic dilema in fine needle aspiration cytology. Cytojournal. 2012;9:21.
61. Vassalli L, Ferrari VD, Simoncini E, Rangoni G, Montini E, Marpicati P, et al. Solitary breast metastases from a renal cell carcinoma. Breast Cancer Res Treat. 2001;68(1):29–31.
62. Robens J, Goldstein L, Gown AM, Schnitt SJ. Thyroid transcription factor-1 expression in breast carcinomas. Am J Surg Pathol. 2010;34(12):1881–5.
63. Domfeh AB, Carley AL, Striebel JM, Karabakhtsian RG, Florea AV, McManus K, et al. WT1 immunoreactivity in breast carcinoma: selective expression in pure and mixed mucinous subtypes. Mod Pathol. 2008;21(10):1217–23.
64. Howlader N, Altekruse SF, Li CI, Chen VW, Clarke CA, Ries LA, et al. US incidence of breast cancer subtypes defined by joint hormone receptor and HER2 status. J Natl Cancer Inst. 2014;106(5):dju055.
65. Wick MR, Lillemoe TJ, Copland GT, Swanson PE, Manivel JC, Kiang DT. Gross cystic disease fluid protein-15 as a marker for breast cancer: immunohistochemical analysis of 690 human neoplasms and comparison with alpha-lactalbumin. Hum Pathol. 1989;20(3):281–7.
66. Bhargava R, Beriwal S, Dabbs DJ. Mammaglobin vs GCDFP-15: an immunohistologic validation survey for sensitivity and specificity. Am J Clin Pathol. 2007;127(1):103–13.
67. Han JH, Kang Y, Shin HC, Kim HS, Kang YM, Kim YB, et al. Mammaglobin expression in lymph nodes is an important marker of metastatic breast carcinoma. Arch Pathol Lab Med. 2003;127(10):1330–4.
68. Lewis GH, Subhawong AP, Nassar H, Vang R, Illei PB, Park BH, et al. Relationship between molecular subtype of invasive breast carcinoma and expression of gross cystic disease fluid protein 15 and mammaglobin. Am J Clin Pathol. 2011;135(4):587–91.
69. Dennis JL, Hvidsten TR, Wit EC, Komorowski J, Bell AK, Downie I, et al. Markers of adenocarcinoma characteristic of the site of origin: development of a diagnostic algorithm. Clin Cancer Res. 2005;11(10):3766–72.
70. Mazoujian G, Bodian C, Haagensen DE Jr, Haagensen CD. Expression of GCDFP-15 in breast carcinomas. Relationship to pathologic and clinical factors. Cancer. 1989;63(11):2156–61.
71. Yang M, Nonaka D. A study of immunohistochemical differential expression in pulmonary and mammary carcinomas. Mod Pathol. 2010;23(5):654–61.
72. Miettinen M, McCue PA, Sarlomo-Rikala M, Rys J, Czapiewski P, Wazny K, et al. GATA3: a multispecific but potentially useful marker in surgical pathology: a systematic analysis of 2500 epithelial and nonepithelial tumors. Am J Surg Pathol. 2014;38(1):13–22.
73. Cimino-Mathews A, Subhawong AP, Illei PB, Sharma R, Halushka MK, Vang R, et al. GATA3 expression in breast carcinoma: utility in triple-negative, sarcomatoid, and metastatic carcinomas. Hum Pathol. 2013;44(7):1341–9.

74. Cimino-Mathews A, Subhawong AP, Elwood H, Warzecha HN, Sharma R, Park BH, et al. Neural crest transcription factor Sox10 is preferentially expressed in triple-negative and metaplastic breast carcinomas. Hum Pathol. 2013;44(6):959–65.
75. Wellings SR, Jensen HM, Marcum RG. An atlas of subgross pathology of the human breast with special reference to possible precancerous lesions. J Natl Cancer Inst. 1975;55(2):231–73.
76. Wellings SR, Jensen HM. On the origin and progression of ductal carcinoma in the human breast. J Natl Cancer Inst. 1973;50(5):1111–8.
77. Marshall LM, Hunter DJ, Connolly JL, Schnitt SJ, Byrne C, London SJ, et al. Risk of breast cancer associated with atypical hyperplasia of lobular and ductal types. Cancer Epidemiol Biomark Prev. 1997;6(5):297–301.
78. Lakhani SR, Audretsch W, Cleton-Jensen AM, Cutuli B, Ellis I, Eusebi V, et al. The management of lobular carcinoma in situ (LCIS). Is LCIS the same as ductal carcinoma in situ (DCIS)? Eur J Cancer. 2006;42(14):2205–11.
79. Hanby AM, Hughes TA. In situ and invasive lobular neoplasia of the breast. Histopathology. 2008;52(1):58–66.
80. Oyama T, Iijima K, Takei H, Horiguchi J, Iino Y, Nakajima T, et al. Atypical cystic lobule of the breast: an early stage of low-grade ductal carcinoma in-situ. Breast Cancer. 2000;7(4):326–31.
81. Lerwill MF. Flat epithelial atypia of the breast. Arch Pathol Lab Med. 2008;132(4):615–21.
82. Simpson PT, Reis-Filho JS, Gale T, Lakhani SR. Molecular evolution of breast cancer. J Pathol. 2005;205(2):248–54.
83. Roylance R, Gorman P, Harris W, Liebmann R, Barnes D, Hanby A, et al. Comparative genomic hybridization of breast tumors stratified by histological grade reveals new insights into the biological progression of breast cancer. Cancer Res. 1999;59(7):1433–6.
84. Buerger H, Otterbach F, Simon R, Poremba C, Diallo R, Decker T, et al. Comparative genomic hybridization of ductal carcinoma in situ of the breast-evidence of multiple genetic pathways. J Pathol. 1999;187(4):396–402.
85. O'Connell P, Pekkel V, Fuqua SA, Osborne CK, Clark GM, Allred DC. Analysis of loss of heterozygosity in 399 premalignant breast lesions at 15 genetic loci. J Natl Cancer Inst. 1998;90(9):697–703.
86. Moinfar F, Man YG, Bratthauer GL, Ratschek M, Tavassoli FA. Genetic abnormalities in mammary ductal intraepithelial neoplasia-flat type ("clinging ductal carcinoma in situ"): a simulator of normal mammary epithelium. Cancer. 2000;88(9):2072–81.
87. Tirkkonen M, Tanner M, Karhu R, Kallioniemi A, Isola J, Kallioniemi OP. Molecular cytogenetics of primary breast cancer by CGH. Genes Chromosomes Cancer. 1998;21(3):177–84.
88. Natrajan R, Lambros MB, Geyer FC, Marchio C, Tan DS, Vatcheva R, et al. Loss of 16q in high grade breast cancer is associated with estrogen receptor status: evidence for progression in tumors with a luminal phenotype? Genes Chromosomes Cancer. 2009;48(4):351–65.
89. Allred DC, Wu Y, Mao S, Nagtegaal ID, Lee S, Perou CM, et al. Ductal carcinoma in situ and the emergence of diversity during breast cancer evolution. Clin Cancer Res. 2008;14(2):370–8.
90. Denkert C, von Minckwitz G, Darb-Esfahani S, Lederer B, Heppner BI, Weber KE, et al. Tumour-infiltrating lymphocytes and prognosis in different subtypes of breast cancer: a pooled analysis of 3771 patients treated with neoadjuvant therapy. Lancet Oncol. 2018;19(1):40–50.
91. Amin M, Gress DM, Meyer Vega LR, Edge SB, Greene FL, Byrd DR, Brookland RK, Washington MK, Compton CC. AJCC cancer staging manual. 8th ed. Chicago, IL: Springer; 2017.
92. Veronesi P, Rodriguez-Fernandez J, Intra M. Controversies in the use of sentinel nodes: microinvasion, post surgery and after preoperative systemic treatment. Breast. 2007;16(Suppl 2):S67–70.
93. Hanna MG, Jaffer S, Bleiweiss IJ, Nayak A. Re-evaluating the role of sentinel lymph node biopsy in microinvasive breast carcinoma. Mod Pathol. 2014;27(11):1489–98.
94. Hoda SA, Chiu A, Prasad ML, Giri D, Hoda RS. Are microinvasion and micrometastasis in breast cancer mountains or molehills? Am J Surg. 2000;180(4):305–8.
95. Silverstein MJ, Waisman JR, Gamagami P, Gierson ED, Colburn WJ, Rosser RJ, et al. Intraductal carcinoma of the breast (208 cases). Clinical factors influencing treatment choice. Cancer. 1990;66(1):102–8.
96. Klauber-DeMore N, Tan LK, Liberman L, Kaptain S, Fey J, Borgen P, et al. Sentinel lymph node biopsy: is it indicated in patients with high-risk ductal carcinoma-in-situ and ductal carcinoma-in-situ with microinvasion? Ann Surg Oncol. 2000;7(9):636–42.
97. Schuh ME, Nemoto T, Penetrante RB, Rosner D, Dao TL. Intraductal carcinoma. Analysis of presentation, pathologic findings, and outcome of disease. Arch Surg. 1986;121(11):1303–7.
98. Kinne DW, Petrek JA, Osborne MP, Fracchia AA, DePalo AA, Rosen PP. Breast carcinoma in situ. Arch Surg. 1989;124(1):33–6.
99. Patchefsky AS, Schwartz GF, Finkelstein SD, Prestipino A, Sohn SE, Singer JS, et al. Heterogeneity of intraductal carcinoma of the breast. Cancer. 1989;63(4):731–41.
100. Page DL, Anderson TJ. Diagnostic histopathology of the breast. Edinburgh: Churchill Livingstone; 1987.
101. Solin LJ, Fowble BL, Yeh IT, Kowalyshyn MJ, Schultz DJ, Weiss MC, et al. Microinvasive ductal carcinoma of the breast treated with breast-conserving surgery and definitive irradiation. Int J Radiat Oncol Biol Phys. 1992;23(5):961–8.
102. Silver SA, Tavassoli FA. Mammary ductal carcinoma in situ with microinvasion. Cancer. 1998;82(12):2382–90.
103. National Coordinating Group for Breast Cancer Screening Pathology. Pathology reporting in breast cancer screening. Sheffield: NHSBSP Publications; 1995.
104. Lagios MD, Westdahl PR, Margolin FR, Rose MR. Duct carcinoma in situ. Relationship of extent of noninvasive disease to the frequency of occult invasion, multicentricity, lymph node metastases, and short-term treatment failures. Cancer. 1982;50(7):1309–14.
105. Vieira CC, Mercado CL, Cangiarella JF, Moy L, Toth HK, Guth AA. Microinvasive ductal carcinoma in situ: clinical presentation, imaging features, pathologic findings, and outcome. Eur J Radiol. 2010;73(1):102–7.
106. Sim YT, Litherland J, Lindsay E, Hendry P, Brauer K, Dobson H, et al. Upgrade of ductal carcinoma in situ on core biopsies to invasive disease at final surgery: a retrospective review across the Scottish Breast Screening Programme. Clin Radiol. 2015;70(5):502–6.
107. Dillon MF, McDermott EW, Quinn CM, O'Doherty A, O'Higgins N, Hill AD. Predictors of invasive disease in breast cancer when core biopsy demonstrates DCIS only. J Surg Oncol. 2006;93(7):559–63.
108. Nemoto T, Castillo N, Tsukada Y, Koul A, Eckhert KH Jr, Bauer RL. Lobular carcinoma in situ with microinvasion. J Surg Oncol. 1998;67(1):41–6.
109. Yang M, Moriya T, Oguma M, De La Cruz C, Endoh M, Ishida T, et al. Microinvasive ductal carcinoma (T1mic) of the breast. The clinicopathological profile and immunohistochemical features of 28 cases. Pathol Int. 2003;53(7):422–8.
110. Prasad ML, Osborne MP, Giri DD, Hoda SA. Microinvasive carcinoma (T1mic) of the breast: clinicopathologic profile of 21 cases. Am J Surg Pathol. 2000;24(3):422–8.
111. Diaz NM, Cox CE, Ebert M, Clark JD, Vrcel V, Stowell N, et al. Benign mechanical transport of breast epithelial cells to sentinel lymph nodes. Am J Surg Pathol. 2004;28(12):1641–5.
112. Carter BA, Jensen RA, Simpson JF, Page DL. Benign transport of breast epithelium into axillary lymph nodes after biopsy. Am J Clin Pathol. 2000;113(2):259–65.

113. Schnitt SJ, Collins LC. Microinvasive carcioma. In: Schnitt SJCLC, editor. Biopsy interpretation of the breast. Philadelphia, PA: Lippincott Williams & Wilkins; 2009. p. 236–48.
114. Tunon-de-Lara C, Chauvet MP, Baranzelli MC, Baron M, Piquenot J, Le-Bouedec G, et al. The role of sentinel lymph node biopsy and factors associated with invasion in extensive DCIS of the breast treated by mastectomy: the Cinnamome prospective multicenter study. Ann Surg Oncol. 2015;22(12):3853–60.
115. NHS Breast Screening Programme, Association of Breast Surgery. An audit of screen detected breast cancers for the year of screening April 2012 to March 2013. London: NHS Breast Screening Programme; 2014.
116. Gojon H, Fawunmi D, Valachis A. Sentinel lymph node biopsy in patients with microinvasive breast cancer: a systematic review and meta-analysis. Eur J Surg Oncol. 2014;40(1):5–11.
117. Parikh RR, Haffty BG, Lannin D, Moran MS. Ductal carcinoma in situ with microinvasion: prognostic implications, long-term outcomes, and role of axillary evaluation. Int J Radiat Oncol Biol Phys. 2012;82(1):7–13.
118. Murphy CD, Jones JL, Javid SH, Michaelson JS, Nolan ME, Lipsitz SR, et al. Do sentinel node micrometastases predict recurrence risk in ductal carcinoma in situ and ductal carcinoma in situ with microinvasion? Am J Surg. 2008;196(4):566–8.
119. Shatat L, Gloyeske N, Madan R, O'Neil M, Tawfik O, Fan F. Microinvasive breast carcinoma carries an excellent prognosis regardless of the tumor characteristics. Hum Pathol. 2013;44(12):2684–9.
120. Lyman GH, Temin S, Edge SB, Newman LA, Turner RR, Weaver DL, et al. Sentinel lymph node biopsy for patients with early-stage breast cancer: American Society of Clinical Oncology clinical practice guideline update. J Clin Oncol. 2014;32(13):1365–83.
121. Sopik V, Sun P, Narod SA. Impact of microinvasion on breast cancer mortality in women with ductal carcinoma in situ. Breast Cancer Res Treat. 2018;167(3):787–95.
122. Wang W, Zhu W, Du F, Luo Y, Xu B. The demographic features, clinicopathological characteristics and cancer-specific outcomes for patients with microinvasive breast cancer: a SEER database analysis. Sci Rep. 2017;7:42045.
123. van la Parra RF, Ernst MF, Barneveld PC, Broekman JM, Rutten MJ, Bosscha K. The value of sentinel lymph node biopsy in ductal carcinoma in situ (DCIS) and DCIS with microinvasion of the breast. Eur J Surg Oncol. 2008;34(6):631–5.
124. Dominguez FJ, Golshan M, Black DM, Hughes KS, Gadd MA, Christian R, et al. Sentinel node biopsy is important in mastectomy for ductal carcinoma in situ. Ann Surg Oncol. 2008;15(1):268–73.
125. Cooper HS, Patchefsky AS, Krall RA. Tubular carcinoma of the breast. Cancer. 1978;42(5):2334–42.
126. Carstens PH. Tubular carcinoma of the breast. A study of frequency. Am J Clin Pathol. 1978;70(2):204–10.
127. Kader HA, Jackson J, Mates D, Andersen S, Hayes M, Olivotto IA. Tubular carcinoma of the breast: a population-based study of nodal metastases at presentation and of patterns of relapse. Breast J. 2001;7(1):8–13.
128. Romano AM, Wages N, Smolkin M, Fortune K, Atkins K, Dillon PM. Tubular carcinoma of the breast: institutional and SEER database analysis supporting a unique classification. Breast Dis. 2015;35:103–11.
129. Sullivan T, Raad RA, Goldberg S, Assaad SI, Gadd M, Smith BL, et al. Tubular carcinoma of the breast: a retrospective analysis and review of the literature. Breast Cancer Res Treat. 2005;93(3):199–205.
130. Rakha EA, Lee AH, Evans AJ, Menon S, Assad NY, Hodi Z, et al. Tubular carcinoma of the breast: further evidence to support its excellent prognosis. J Clin Oncol. 2010;28(1):99–104.
131. Cabral AH, Recine M, Paramo JC, McPhee MM, Poppiti R, Mesko TW. Tubular carcinoma of the breast: an institutional experience and review of the literature. Breast J. 2003;9(4):298–301.
132. Li CI. Risk of mortality by histologic type of breast cancer in the United States. Hormones & Cancer. 2010;1(3):156–65.
133. Visfeldt J, Scheike O. Male breast cancer. I. Histologic typing and grading of 187 Danish cases. Cancer. 1973;32(4):985–90.
134. Fedko MG, Scow JS, Shah SS, Reynolds C, Degnim AC, Jakub JW, et al. Pure tubular carcinoma and axillary nodal metastases. Ann Surg Oncol. 2010;17(Suppl 3):338–42.
135. Sheppard DG, Whitman GJ, Huynh PT, Sahin AA, Fornage BD, Stelling CB. Tubular carcinoma of the breast: mammographic and sonographic features. AJR Am J Roentgenol. 2000;174(1):253–7.
136. Elson BC, Helvie MA, Frank TS, Wilson TE, Adler DD. Tubular carcinoma of the breast: mode of presentation, mammographic appearance, and frequency of nodal metastases. AJR Am J Roentgenol. 1993;161(6):1173–6.
137. Vega A, Garijo F. Radial scar and tubular carcinoma. Mammographic and sonographic findings. Acta Radiol. 1993;34(1):43–7.
138. Shin HJ, Kim HH, Kim SM, Kim DB, Lee YR, Kim MJ, et al. Pure and mixed tubular carcinoma of the breast: mammographic and sonographic differential features. Korean J Radiol. 2007;8(2):103–10.
139. Tweedie E, Tonkin K, Kerkvliet N, Doig GS, Sparrow RK, O'Malley FP. Biologic characteristics of breast cancer detected by mammography and by palpation in a screening program: a pilot study. Clin Invest Med. 1997;20(5):300–7.
140. Rajakariar R, Walker RA. Pathological and biological features of mammographically detected invasive breast carcinomas. Br J Cancer. 1995;71(1):150–4.
141. Anderson TJ, Lamb J, Alexander F, Lutz W, Chetty U, Forrest AP, et al. Comparative pathology of prevalent and incident cancers detected by breast screening. Edinburgh Breast Screening Project. Lancet. 1986;1(8480):519–23.
142. Mitnick JS, Gianutsos R, Pollack AH, Susman M, Baskin BL, Ko WD, et al. Tubular carcinoma of the breast: sensitivity of diagnostic techniques and correlation with histopathology. AJR Am J Roentgenol. 1999;172(2):319–23.
143. McDivitt RW, Boyce W, Gersell D. Tubular carcinoma of the breast. Clinical and pathological observations concerning 135 cases. Am J Surg Pathol. 1982;6(5):401–11.
144. Andersen JA, Carter D, Linell F. A symposium on sclerosing duct lesions of the breast. Pathol Annu. 1986;21(Pt 2):145–79.
145. van Deurzen CH, McMillan DC, Purdie CA. WHO classifications of tumours: breast tumours. 5th ed. Lyon: World Health Organization; 2019.
146. Sahoo S, Recant WM. Triad of columnar cell alteration, lobular carcinoma in situ, and tubular carcinoma of the breast. Breast J. 2005;11(2):140–2.
147. Rosen PP. Columnar cell hyperplasia is associated with lobular carcinoma in situ and tubular carcinoma. Am J Surg Pathol. 1999;23(12):1561.
148. Brandt SM, Young GQ, Hoda SA. The "Rosen Triad": tubular carcinoma, lobular carcinoma in situ, and columnar cell lesions. Adv Anat Pathol. 2008;15(3):140–6.
149. Abdel-Fatah TM, Powe DG, Hodi Z, Lee AH, Reis-Filho JS, Ellis IO. High frequency of coexistence of columnar cell lesions, lobular neoplasia, and low grade ductal carcinoma in situ with invasive tubular carcinoma and invasive lobular carcinoma. Am J Surg Pathol. 2007;31(3):417–26.
150. Clement PB, Azzopardi JG, Microglandular adenosis of the breast—a lesion simulating tubular carcinoma. Histopathology. 1983;7(2):169–80.
151. Wheeler DT, Tai LH, Bratthauer GL, Waldner DL, Tavassoli FA. Tubulolobular carcinoma of the breast: an analysis of 27 cases of a tumor with a hybrid morphology and immunoprofile. Am J Surg Pathol. 2004;28(12):1587–93.
152. Esposito NN, Chivukula M, Dabbs DJ. The ductal phenotypic expression of the E-cadherin/catenin complex in tubulolobular

carcinoma of the breast: an immunohistochemical and clinicopathologic study. Mod Pathol. 2007;20(1):130–8.
153. Green I, McCormick B, Cranor M, Rosen PP. A comparative study of pure tubular and tubulolobular carcinoma of the breast. Am J Surg Pathol. 1997;21(6):653–7.
154. Pereira H, Pinder SE, Sibbering DM, Galea MH, Elston CW, Blamey RW, et al. Pathological prognostic factors in breast cancer. IV: should you be a typer or a grader? A comparative study of two histological prognostic features in operable breast carcinoma. Histopathology. 1995;27(3):219–26.
155. Kuroda H, Tamaru J, Takeuchi I, Ohnisi K, Sakamoto G, Adachi A, et al. Expression of E-cadherin, alpha-catenin, and beta-catenin in tubulolobular carcinoma of the breast. Virchows Arch. 2006;448(4):500–5.
156. Diab SG, Clark GM, Osborne CK, Libby A, Allred DC, Elledge RM. Tumor characteristics and clinical outcome of tubular and mucinous breast carcinomas. J Clin Oncol. 1999;17(5):1442–8.
157. Alvarenga CA, Paravidino PI, Alvarenga M, Gomes M, Dufloth R, Zeferino LC, et al. Reappraisal of immunohistochemical profiling of special histological types of breast carcinomas: a study of 121 cases of eight different subtypes. J Clin Pathol. 2012;65(12):1066–71.
158. Lopez-Garcia MA, Geyer FC, Natrajan R, Kreike B, Mackay A, Grigoriadis A, et al. Transcriptomic analysis of tubular carcinomas of the breast reveals similarities and differences with molecular subtype-matched ductal and lobular carcinomas. J Pathol. 2010;222(1):64–75.
159. Rosen PP, Lesser ML, Arroyo CD, Cranor M, Borgen P, Norton L. p53 in node-negative breast carcinoma: an immunohistochemical study of epidemiologic risk factors, histologic features, and prognosis. J Clin Oncol. 1995;13(4):821–30.
160. Waldman FM, Hwang ES, Etzell J, Eng C, DeVries S, Bennington J, et al. Genomic alterations in tubular breast carcinomas. Hum Pathol. 2001;32(2):222–6.
161. Livi L, Paiar F, Meldolesi E, Talamonti C, Simontacchi G, Detti B, et al. Tubular carcinoma of the breast: outcome and loco-regional recurrence in 307 patients. Eur J Surg Oncol. 2005;31(1):9–12.
162. Javid SH, Smith BL, Mayer E, Bellon J, Murphy CD, Lipsitz S, et al. Tubular carcinoma of the breast: results of a large contemporary series. Am J Surg. 2009;197(5):674–7.
163. Min Y, Bae SY, Lee HC, Lee JH, Kim M, Kim J, et al. Tubular carcinoma of the breast: clinicopathologic features and survival outcome compared with ductal carcinoma in situ. J Breast Cancer. 2013;16(4):404–9.
164. National Comprehensive Cancer Network. Clinical practice guidelines in oncology—breast cancer. Version 4.2021; 2021. www.nccn.org
165. Stauber J, Chevli N, Haque W, Messer JA, Farach AM, Schwartz MR, et al. Prognostic impact of radiation therapy in tubular carcinoma of the breast. Radiother Oncol. 2021;159:202–8.
166. Chen JX, Zhang WW, Dong Y, Sun JY, He ZY, Wu SG. The effects of postoperative radiotherapy on survival outcomes in patients under 65 with estrogen receptor positive tubular breast carcinoma. Radiat Oncol. 2018;13(1):226.
167. Deos PH, Norris HJ. Well-differentiated (tubular) carcinoma of the breast. A clinicopathologic study of 145 pure and mixed cases. Am J Clin Pathol. 1982;78(1):1–7.
168. Papadatos G, Rangan AM, Psarianos T, Ung O, Taylor R, Boyages J. Probability of axillary node involvement in patients with tubular carcinoma of the breast. Br J Surg. 2001;88(6):860–4.
169. Lea V, Gluch L, Kennedy CW, Carmalt H, Gillett D. Tubular carcinoma of the breast: axillary involvement and prognostic factors. ANZ J Surg. 2014; https://doi.org/10.1111/ans.12791.
170. Dejode M, Sagan C, Campion L, Houvenaeghel G, Giard S, Rodier JF, et al. Pure tubular carcinoma of the breast and sentinel lymph node biopsy: a retrospective multi-institutional study of 234 cases. Eur J Surg Oncol. 2013;39(3):248–54.
171. Veronesi U, Viale G, Paganelli G, Zurrida S, Luini A, Galimberti V, et al. Sentinel lymph node biopsy in breast cancer: ten-year results of a randomized controlled study. Ann Surg. 2010;251(4):595–600.
172. Krag DN, Anderson SJ, Julian TB, Brown AM, Harlow SP, Ashikaga T, et al. Technical outcomes of sentinel-lymph-node resection and conventional axillary-lymph-node dissection in patients with clinically node-negative breast cancer: results from the NSABP B-32 randomised phase III trial. Lancet Oncol. 2007;8(10):881–8.
173. Goyal A, Newcombe RG, Chhabra A, Mansel RE, Group AT. Factors affecting failed localisation and false-negative rates of sentinel node biopsy in breast cancer—results of the ALMANAC validation phase. Breast Cancer Res Treat. 2006;99(2):203–8.
174. Fisher B, Jeong JH, Anderson S, Bryant J, Fisher ER, Wolmark N. Twenty-five-year follow-up of a randomized trial comparing radical mastectomy, total mastectomy, and total mastectomy followed by irradiation. N Engl J Med. 2002;347(8):567–75.
175. Fisher ER, Anderson S, Redmond C, Fisher B. Pathologic findings from the National Surgical Adjuvant Breast Project protocol B-06. 10-year pathologic and clinical prognostic discriminants. Cancer. 1993;71(8):2507–14.
176. Page DL, Dixon JM, Anderson TJ, Lee D, Stewart HJ. Invasive cribriform carcinoma of the breast. Histopathology. 1983;7(4):525–36.
177. Liu J, Zheng X, Han Z, Lin S, Han H, Xu C. Clinical characteristics and overall survival prognostic nomogram for invasive cribriform carcinoma of breast: a SEER population-based analysis. BMC Cancer. 2021;21(1):168.
178. Venable JG, Schwartz AM, Silverberg SG. Infiltrating cribriform carcinoma of the breast: a distinctive clinicopathologic entity. Hum Pathol. 1990;21(3):333–8.
179. Stutz JA, Evans AJ, Pinder S, Ellis IO, Yeoman LJ, Wilson AR, et al. The radiological appearances of invasive cribriform carcinoma of the breast. Nottingham Breast Team. Clin Radiol. 1994;49(10):693–5.
180. Zhang W, Zhang T, Lin Z, Zhang X, Liu F, Wang Y, et al. Invasive cribriform carcinoma in a Chinese population: comparison with low-grade invasive ductal carcinoma-not otherwise specified. Int J Clin Exp Pathol. 2013;6(3):445–57.
181. Lee YJ, Choi BB, Suh KS. Invasive cribriform carcinoma of the breast: mammographic, sonographic, MRI, and 18 F-FDG PET-CT features. Acta Radiol. 2014; https://doi.org/10.1177/0284185114538425.
182. Lim HS, Jeong SJ, Lee JS, Park MH, Yoon JH, Kim JW, et al. Sonographic findings of invasive cribriform carcinoma of the breast. J Ultrasound Med. 2011;30(5):701–5.
183. Wells CA, Ferguson DJ. Ultrastructural and immunocytochemical study of a case of invasive cribriform breast carcinoma. J Clin Pathol. 1988;41(1):17–20.
184. Saout L, Leduc M, Suy-Beng PT, Meignie P. [A new case of cribriform breast carcinoma associated with histiocytic giant cell reaction]. Arch Anat Cytol Pathol. 1985;33(1):58–61.
185. Rabban JT, Swain RS, Zaloudek CJ, Chase DR, Chen YY. Immunophenotypic overlap between adenoid cystic carcinoma and collagenous spherulosis of the breast: potential diagnostic pitfalls using myoepithelial markers. Mod Pathol. 2006;19(10):1351–7.
186. Zhang W, Lin Z, Zhang T, Liu F, Niu Y. A pure invasive cribriform carcinoma of the breast with bone metastasis if untreated for thirteen years: a case report and literature review. World J Surg Oncol. 2012;10:251.